Investigation of SAP, NPTX1 and their interaction on synaptic function and microglia activity and their possible role in Alzheimer's disease

Tiffanie Benway

UCL

Thesis submitted for partial fulfillment of the degree of Doctor of Philosophy

May 2017

Declaration

I declare that the work presented herein is my own, except where indicated below.

Immunohistochemistry for mouse models was performed in part by Angela Richard-Loendt, and for human tissue was performed in part by Dr. Tammaryn Lashley.

Brain dissections for RNA were performed by Dr. Dervis Salih, and the preparation of organotypic hippocampal slices from GFP-S mice was carried out by Dr. Damian Cummings.

I generated Figures 3.1, 3.5*, 3.7 and 3.8 for my work as part of a previous publication (Cummings, Benway et al., 2017)
*or co-generated with the co-first author of the paper

Acknowledgements

I would first like to thank Dr. Frances Edwards for not only providing me with the opportunity to work in her lab, but also for being such a supportive supervisor who always manages to make time for her students.

A massive thank you to the post docs, Dr. Dervis Salih and Dr. Damian Cummings. In particular, I can't thank you enough Dervis for your resounding patience and for taking the time to teach me so much, despite me probably asking you the same questions hundreds of times.

A big thanks also to current and former lab members, particularly Zelah, Josh and Wenfei, who have helped to make the lab a fun place to work for all the years that I've been there!

Lastly, I want to thank my family and friends, for whom I am immensely grateful to have in my corner. Thank you Sonia for being there, Pips for the countdowns and Heather for all of your help. And especially, thank you Zel, for supporting me through all of it. I'm not sure I would have made it without all the laughs (and the dinners!) that you provided.

Abstract

The pentraxins comprise of a family of proteins that exist in the brain to modulate synaptic formation and plasticity, and in the periphery as part of the immune response. Both the peripheral pentraxin serum amyloid-P component (SAP) and the neuronal pentraxin 1 (NPTX1) have been implicated in Alzheimer's disease (AD) and show up-regulation in AD brains. SAP is always found on amyloid plaques and is linked to amyloid fibril stability, while NPTX1 is present in dystrophic neurons in plaques and can mediate some of the effects of amyloid-beta (Aβ). Under conditions of blood-brain barrier compromise, SAP can also enter the brain and is capable of exerting effects on synaptic transmission.

Results from the current study show that SAP is capable of forming complexes with the neuronal pentraxins. Specifically, SAP can bind with NPTX1, NPTX2 and NPTXR when co-overexpressed in 293T cells. To investigate the effects that this complex may be having in the brain, SAP and NPTX1 were applied separately or simultaneously to primary neurons and to organotypics slices. To evaluate post-synaptic effects, spine density after SAP and/or NPTX1 application was examined. NPTX1 application resulted in decreased spine density, but this effect was prevented by SAP. A similar blocking effect of NPTX1 by SAP was found in the microglia counts from organotypic cultures, where NPTX1 alone resulted in decreased microglia and NPTX1+SAP showed a reduced deficit. Application of both SAP and NPTX1 resulted in a decrease in the proportion of activated microglia, whereas the application of either pentraxin alone was not found to affect levels of activation. Therefore, while SAP alone has no effect, it can block the effect of NPTX1 in decreasing microglial numbers, and contribute to decreased activation levels when co-applied with NPTX1. These results suggest that when SAP enters the brain it may be capable of exerting effects on synaptic transmission and immune response in the CNS via an interaction with the neuronal pentraxins.

Table of Contents

List of Figures

Chapter 1: Introduction

Chapter 3: NPTX1 and SAP colocalize in the brains of mouse models of AD pathology and human AD patients

Chapter 4: Chronic application of NPTX1 decreases spine density in primary cultured neurons

Chapter 5: The effect of NPTX1 and SAP on microglia in organotypic cultures

Chapter 6: The effect of NPTX1 and SAP on microglia in organotypic cultures

Chapter 7: Discussion

List of Tables

Chapter 2: Methods

Chapter 3: Results

Abbreviations

AD	Alzheimer's disease
Aβ	Amyloid-beta protein
BSA	Bovine serum albumin
CA1	Cornu Ammonis region 1
CA2	Cornu Ammonis region 2
CA3	Cornu Ammonis region 3
CA4	Cornu Ammonis region 4
CAA	Cerebral amyloid angiopathy
CNS	Central nervous system
DG	Dentate Gyrus
GFP	Green fluorescent protein
IL	Interleukin
FBS	Fetal bovine serum
LPS	Lipopolysaccharide
LTP	Long-term potentiation
mEPSC	Miniature excitatory postsynaptic current
MHCIIAb	major histocompatibility complex class II A b1
NFT	Neurofibrillary tangle
PBS	Phosphate-buffered saline
PCR	Polymerase chain reaction
qPCR	Quantitative real-time polymerase chain reaction
RT-qPCR	Reverse transcriptase quantitative real-time polymerase chain reaction

SAP (APCS)	Serum Amyloid-P Component
SDS-PAGE	Sodium dodecyl sulfate-polyacrylamide gel electrophoresis
TBS	Tris-buffered saline
WT	Wild-type mice (littermates)

Chapter 1

Introduction

An introduction to the present study

The present study concentrates on two members of the pentraxin family of proteins that have both been implicated in Alzheimer's disease (AD): the neuronal pentraxin NPTX1 and the peripheral pentraxin SAP. While various studies have been performed on either SAP in the context of its interactions in the periphery, or NPTX1 in the context of its interactions in the CNS and/or with other neuronal pentraxins, no studies had previously examined the possible interactions between these two particular pentraxins. This raised the question whether, given the structural homology and the evidence that both pentraxins have been reported to be present on amyloid plaques, SAP and NPTX1 may be capable of interacting or somehow influencing the effects of one another in the CNS, and with focus on their possible roles in AD.

To investigate this question, it was essential for our experiments that we first develop the tools with which to carry out our study most accurately. The reasoning for this was two-fold; 1) there is a significant degree of homology between each of the different pentraxins (Fig. 1.1), and 2) there exists contention in the field over the particular functions of certain pentraxins and the roles they play in pathological processes of the brain. The aim of this thesis is to therefore confirm the localization of SAP and NPTX1 in the brains of AD patients, particularly in relation to one another, and then investigate the effects that each of the two pentraxins may be having in the brain at increased levels, either separately or together.

While some of the evidence presented has recently been published in an article in which I am co-first author (Cummings, Benway et al., 2017), I have performed additional work that expands upon these results, and examines these two pentraxins in the context of AD pathology. To accomplish this, I focused on attributes comprising the hippocampus, as it is the brain structure most significantly affected in AD. The following thesis provides histological and molecular biological characterization in humans and mice, and also assesses the effects of SAP and NPTX1 on features of synaptic plasticity, the immune response, and, for SAP, behavior.

An introduction to the pentraxins

The pentraxins are members of a phylogenically conserved multifunctional superfamily of proteins that are characterized by an evolutionarily conserved 200 amino acid domain in the C-terminus and an eight amino acid long conserved pentraxin signature: HxCxS/TWxS (where x is any amino acid); (Garlanda et al., 2005). This superfamily of proteins is defined by their structural organization of five identical subunits arranged covalently in pentameric radial symmetry (Osmand et al., 1977). The pentraxins share a very high degree of sequence homology (Fig. 1.1), and they are divided into two subdivisions based upon the primary structure of their subunits: the long and the short pentraxins (Garlanda et al., 2005). The short, or classic, pentraxins are produced mostly in the liver and transported through the blood stream to other organs and tissues (Deban et al., 2011), while the long pentraxins are comprised mostly of a subset of neuronal proteins termed the neuronal pentraxins, which are expressed by neurons of the central nervous system (Schlimgen et al., 1995).

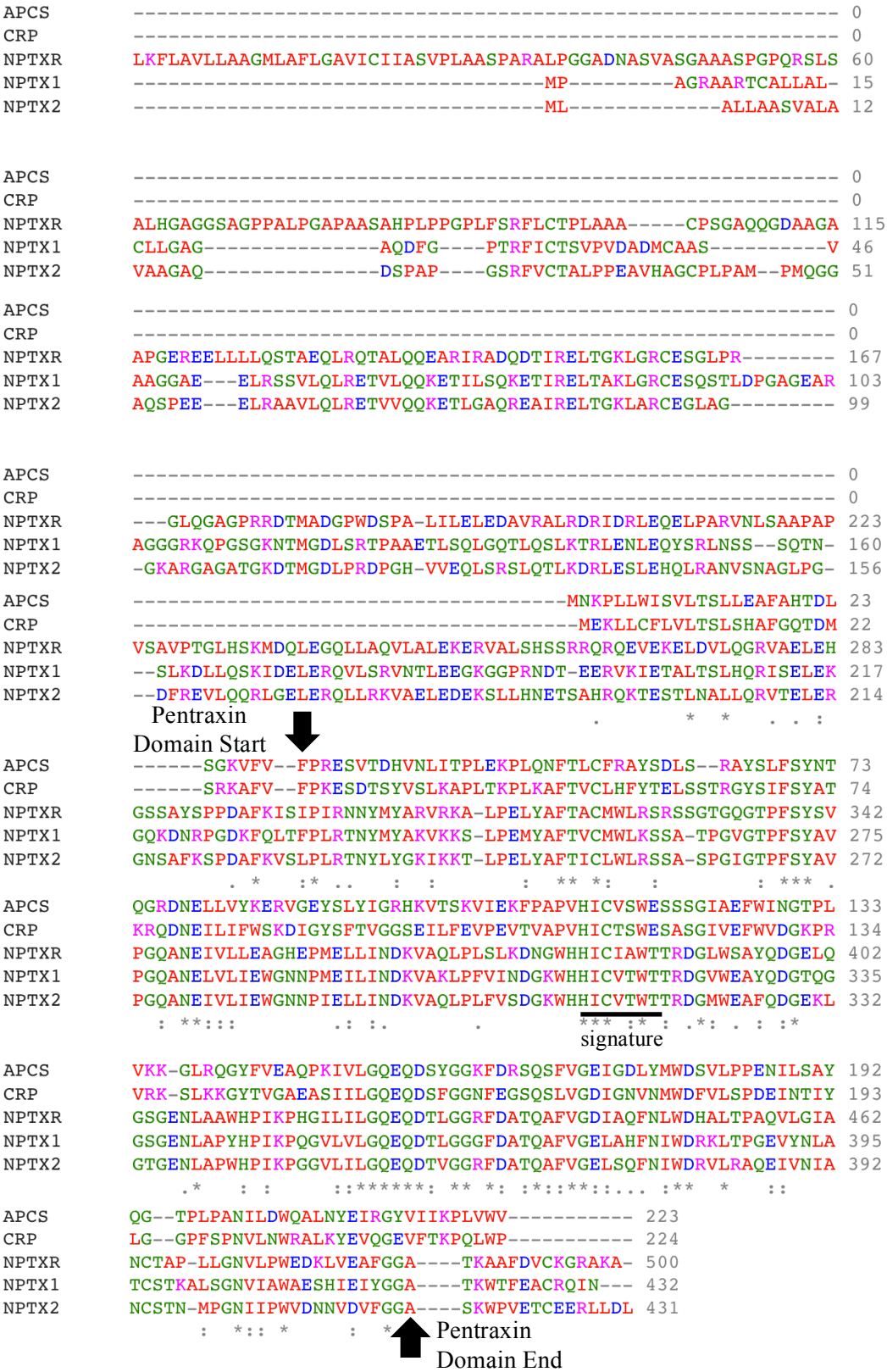

Figure 1.1. The pentraxin share a significant degree of homology. Alignment of the protein sequences for APCS (SAP), CRP, NPTX1, NPTX2 and NPTXR, where asterisks identify the regions shared by the five pentraxins, modified from Clustal Omega.

The short pentraxins

The short (classic) pentraxin arm of the superfamily consists of acute phase C-reactive protein (CRP), the first pentraxin identified in the late 1930s, and serum amyloid P component (SAP). CRP was first discovered in the blood of a patient with *Streptococcus pneumonia*, but could only be detected during the time when the patient was infected. CRP was subsequently found to be at high concentrations in the acute phase sera, where it induced the precipitation of the cell wall of a bacterial cell in the presence of calcium (Tillett and Francis, 1930). The other short and very closely related pentraxin SAP was first discovered by Cathcart et al. (1967) who coined the name P-component after finding a protein constituent of amyloid deposits in the body that was also related to normal plasma protein (Cathcart et al., 1965; Cathcart et al., 1967a; Cathcart et al., 1967b). Using electron microscopy techniques, Bladen et al. (1966) independently discovered SAP in their study on amyloid extracts from the periphery, but misinterpreted the pentagonal molecular structure of SAP as aggregated rods that they believed to be the bulk of amyloid deposits.

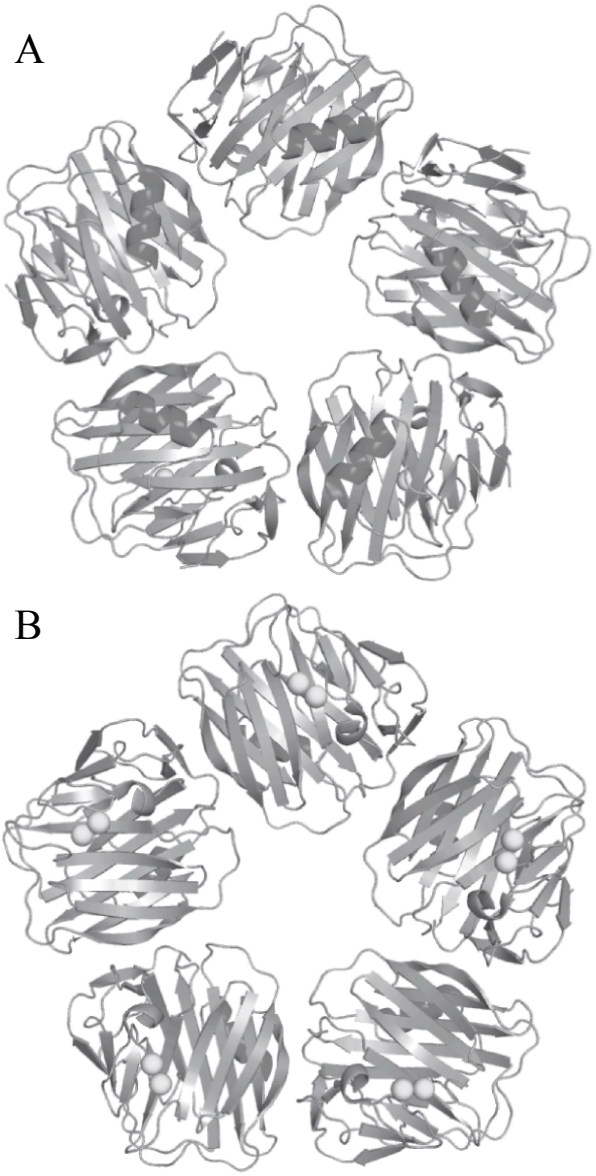

Figure 1.2. The orientations of the five subunits of SAP pentamer: A) the five a-helixes on the A face of the protein, B) the five double calcium binding sites on the B face of the protein (with white calcium atoms). This crystal structure of SAP was solved by Emsley et al. (1994), with the subunits packed into a radially symmetric pentameric disk approximately 100-Å in diameter, 35-Å in depth, and a 20-Å pore in the center. Each subunit consists of 204 amino acids in a single polypeptide chain containing a disulfide bridge that links Cys36 and Cys95. There is also a complex oligosaccharide N-glycosylation site on Asn32, as well as a metal-binding site containing two calcium ions. Adapted from (Kolstoe and Wood, 2010).

SAP was later isolated and independently characterized by Binette et al. (1974), who identified the molecule that the previous studies determined to have both a pentagonal unit (Bladen et al., 1966) and a P-component (Cathcart et al., 1967a).

It has since been found that human SAP and CRP share 51% strict residue sequence identity, or upwards of 66% homology when conservative substitutions are taken into account (Emsley et al., 1994; Srinivasan et al., 1994a). These pentraxins have been conserved throughout vertebrate evolution, with several forms present in species as far back as the arachnid, *Limulus polyphemus* (the horseshoe crab), which has persisted for 250-300 million years (Robey and Liu, 1981). These proteins have retained their ligand specificity and subunit arrangement of five tightly arranged subunits in planar symmetry (Fig. 1.2), in what has been described as a "doughnut-shaped ring" (Osmand et al., 1977), and there remains a significant level of similarity in the sequence of CRP and SAP orthologs among different mammal species (Bottazzi et al., 2010). It has been posited that human CRP and SAP are likely products of gene duplication on 1q23.2, as there is a significant degree of overlap in precise ligand specificity, behavior as acute phase proteins, as well as deposition in amyloid (Srinivasan et al., 1994a). Both short pentraxins have also been found to circulate in the blood as single pentamers (Hutchinson et al., 2000).

Physiological roles of short pentraxins

CRP function was first demonstrated by the injection of typhoid vaccine into rabbit muscle to examine the pattern of its deposition. CRP was found to target dead and damaged cells for processing by the innate immune system (Kushner and Kaplan, 1961). Both short pentraxins have since been found to bind to nuclear antigens released from damaged cells and affect their clearance and antigenic processing, specifically with CRP binding primarily to the small nuclear ribonucleoproteins (snRNPs) (Du Clos, 1989) and SAP binding to chromatin and native DNA (Du Clos, 1996; Pepys and Butler, 1987). These pattern recognition molecules also interact with various ligands: CRP with apoptotic cells, microorganisms and lipoproteins, and SAP also with apoptotic cells, bacteria, lipopolysaccharide (LPS) and amyloid fibrils (Hind et al., 1985; Mulder et al., 2010; Noursadeghi et al., 2000).

Human SAP is produced in the liver at constitutive serum levels reported to average approximately 33 μg/mL in women and 43 μg/mL in men (Pepys et al., 1978). This is consistent with the later measures that reported average serum levels to be at approximately 40 μg/mL (Hicks et al., 1992). SAP is secreted into blood circulation and exhibits a diverse range of functions in mammals (Skinner & Cohen, 1988). Natively, SAP can bind to chromatin, DNA, amyloid fibrils, bacteria, glycosaminoglycans and complement components, polymorphonuclear neutrophil cells, and bacterial lipopolysaccaride. Specifically, human SAP, like CRP, has been shown to clear cellular debris by its high affinity binding to neutrophils, and subsequent degradation by neutrophil enzymes that yields a mixture of small peptides (Landsmann et al., 1994).

As the use of mouse models is common practice in the examination of physiological conditions, and will be discussed later in this introduction, it is important to note that there are some properties of mouse SAP that differ from human SAP. Namely, while SAP is not an acute protein in humans, it is found to be a strong acute phase marker in mice (Pepys et al., 1979), meaning plasma concentrations fluctuate in response to injury or infection (Whicher and Westacott, 1992). Additionally, the affinity with which SAP binds to DNA and to amyloid in mice is reported to be significantly weaker in mice than in humans, with the latter demonstrated by the measurement of injected mouse SAP compared to human SAP that was localized to amyloid fibrils in mice (Gillmore et al., 2004; Hawkins et al., 1988). Among different mouse strains the baseline levels of SAP have been reported to differ considerably (Le et al., 1982), but as an acute phase protein SAP has been shown to be induced by IL-6 (Pepys et al., 1979). However, as in humans, SAP is capable of opsonizing molecules for phagocytosis by binding to FcyRs (Fc receptors that induce phagocytosis of marked microbes), and of activating the complement cascade of the immune system (Lu et al., 2008; Mold et al., 2001).

The physiological protective role of SAP

For the purposes of the current study, focus will be placed upon research performed on SAP, rather than CRP, given the evidence to be provided for its possible role in neurodegenerative disease. However, the similarity in structure of the two short

pentraxins is an important point to consider in the examination of our results. Prior to the examination of SAP's possible role in disease however, it is critical to note that SAP plays a protective role in the homeostatic balance in the periphery, under normal conditions. As such, SAP has been shown to be a constituent of the glomerular basement membrane, which is an extracellular matrix of the selectively permeable glomerular filtration barrier separating the vasculature from the urinary space (Dyck et al., 1980a; Dyck et al., 1980b). *In vivo* studies have demonstrated that SAP can inhibit renal fibrosis by binding to cell debris and causing suppression of inflammatory macrophages through activation of FcγRI and the anti-inflammatory cytokine IL-10 (Castano et al., 2009). Moreover, SAP appears to aid in the protection against different types of infections; SAP knockout mice show higher susceptibility to bacterial infections including *Streptococcus pneumonia* (Noursadeghi et al., 2000), and SAP has also been reported to inhibit the influenza viral infection *in vitro* by disrupting the viral binding to hyaluronic acid (Job et al., 2013). The latter result was consistent with earlier *in vitro* and *in vivo* studies that found SAP to be vital in the inhibition of viral infection (Andersen et al., 1997; Horvath et al., 2001).

The predominant mechanisms by which SAP acts to play a protective role in the periphery are via opsonization of targets for phagocytosis when bound to monocytes and neutrophils (Bharadwaj et al., 2001) or triggering the immune response via the activation of the complement cascade (Hicks et al., 1992; Ying et al., 1992a). While activation of complement is a key feature of the immune response to fight off pathogens and clear debris in the body, recent research has revealed that there are situations in which this protective function can go awry and lead to a disruption of the delicate state of homeostasis in an organism. As SAP has been shown to play a significant role in complement, it is important to consider whether it may also be involved in this disruptive process as well.

SAP and the complement cascade

The classical pathway of the complement system is an integral line of defense comprised of 35 plasma and cell surface proteins that are part of the humoral immune response (Fig. 1.3). Complement plays a major role in immunological and inflammatory processes by monitoring the system and directing the elimination of

foreign intruders, cell debris and apoptotic cells. In addition, this system acts in synaptic maturation and removal, angiogenesis, tissue regeneration and lipid metabolism (Sunyer et al., 1998). This pathway is activated by the versatile pattern recognition molecule (PRM) C1q, which recognizes distinct structures that are on either microbial and apoptotic cells, or via endogenous PRMs such as immunoglobulins and pentraxins (Gaboriaud et al., 2004).

While Ying et al. (1992a) first determined that aggregated SAP could activate complement, Hicks et al. (1992) later demonstrated that chemically aggregated SAP (and CRP) specifically activates the pathway via multivalent interaction with C1q. Interestingly, SAP was found to be able to do so either chemically cross-linked or bound to polyvalent ligands at a concentration of 25μg/mL (100 nM) or greater, which is an amount lower than the physiological concentration of SAP. This activation results from binding of SAP or CRP to an amino-terminal collagen-like region of C1q, within residues 14-26 (ibid). This use of the isolated aggregates allowed for direct comparison of the pentraxin concentration required for activation, without interference of the binding of other ligands that would normally occur under physiological conditions (Gewurz et al., 1995). However, this finding raises the question of how SAP, given its high concentration in the serum, does not then regularly cause complement activation - or at least calls into question the accuracy of the 'normal' plasma SAP concentrations previously measured. However, it is possible that this may be the result of C1q requiring the binding constant to reach a certain threshold. This is supported by evidence that C1q binds a single IgG Fc segment with very low affinity, with a dissociation constant of approximately $K_d \approx 10^{-4}$ M (Kinoshita et al., 1989; Srinivasan et al., 1994a). To activate complement via IgG, physiological C1q binding thus requires an increase in this binding constant, and this can happen in the case of clustering of antigen-driven antibodies which have been shown to allow for multivalent C1q binding (Pepys et al., 1994b).

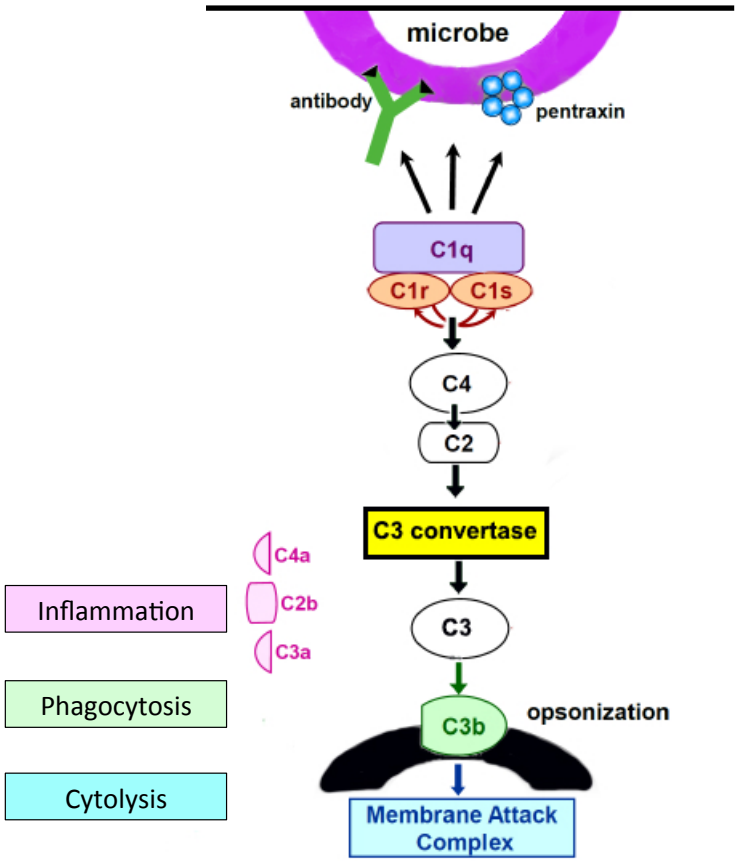

Figure 1.3. SAP can activate the complement cascade by binding to C1q. SAP can interact with C1q via binding to its collagen-like domain, triggering sequential activation of the C1r and C1s proteases associated to the C1q collagen stalks. Activated C1s then cleave C4 and C2, which leads to the assembly of the C3 convertase that cleaves C3 for the opsonization of targets by C3b. Complement activation generates factors involved in inflammation and phagocytosis, and ends in target lysis by the membrane attack complex (which includes complement components C5b, C6, C7, C8 and C9).

SAP in mice

While SAP is an acute phase protein in the mouse that is induced by IL-6 (Pepys et al., 1979), it similarly activates the complement cascade as it does in humans. Also, SAP opsonizes targets for phagocytosis via the binding to FcγRs in the same manner in both species (Lu et al., 2008; Mold et al., 2001), which are receptors expressed by immune effector cells such as monocytes, macrophages, neutrophils, as well as dendritic cells (Nimmerjahn and Ravetch, 2008). However, in the mouse, plasma levels rise following tissue injury and their concentrations fluctuate in accordance to levels of inflammation to induce complement (Bottazzi et al., 2010). (Pilling and Gomer, 2012) investigated the physiological role of SAP in mice by knocking down

SAP and examining the effects. Interestingly, counter to its role in complement activation, they found that SAP promoted the resolution of inflammation induced by bleomycin aspiration, as the knockout mice showed significantly higher numbers of inflammatory macrophages (CD11b+). These data led to the suggestion that, given the inflammatory response was not aberrant in the knockout mice, the lack of endogenous SAP likely allows for the persistence of signals that drive inflammation. It has therefore been posited that the decrease or absence of SAP allows for the persistence of apoptotic cells and debris formed during inflammation that SAP would have normally promoted for phagocytosis. Overall, there is a significant degree of overlap in the functions of mouse and human SAP, but it is important to note that the above-described differences exist and need to be taken into account when considering experimental results using mice.

SAP in Amyloidosis

SAP was named for its physical association with amyloid deposits present in various forms of amyloidosis, a clinical disorder caused by extracellular deposits of insoluble amyloid fibrils in the viscera, connective tissue and/or blood vessels. While the disease is rare, causing about one per thousand deaths in developed countries, it is usually fatal (Pepys, 2006). Organ function progressively becomes impaired as amyloid massively infiltrates the parenchyma (ibid). All abnormal amyloid fibrils reportedly share a common structure with a cross β core and a polypeptide chains running perpendicular to the fibril long axis, whether in the brain or the periphery (Sunde et al., 1997). Electron microscopy studies have shown that amyloid fibrils are approximately 10 nm in diameter, straight, rigid, non-branching and composed of twisted protofibrils (Jaroniec et al., 2004). Common components of amyloid deposits are heparan sulfate and dermatan sulfate proteoglycans and glycosaminoglycan chains, which are typically tightly bound to the fibrils (Nelson et al., 1991a) and aid in fibrillogenesis and stabilization of the structure (Kisilevsky and Fraser, 1996).

It was first claimed that all amyloid deposits also contain SAP by Pepys et al. (1994b). This was based on the finding that SAP undergoes avid (Kd ~1 μmol/l), specific, calcium-dependent, reversible binding to apparently all types of amyloid fibrils. This study also estimated that the concentration of SAP in amyloid deposits

may comprise up to ~15% of their mass (as measured from peripheral deposits). Specifically, it is the glycosaminoglycans and protein ligands on amyloid fibrils that SAP binds to, and it has ben proposed that this binding, which is highly resistant to protease digestion, stabilizes the fibrils and protects them from degradation by proteases and phagocytic cells, as it has been shown *in vitro* (Tennent et al., 1995). This was demonstrated via the binding of SAP to amyloid fibrils from the spleens of patients with different forms of amyloidosis protecting the fibrils from phagocytosis by immune cells and proteolytic enzymes (ibid).

Two studies in 1997 helped to further clarify SAP's role in amyloidosis, using mice with targeted deletion of the SAP gene. Both Botto et al. (1997) and Togashi et al. (1997) independently determined that the deletion of SAP led to delayed amyloidogenesis in a reactive model of systemic amyloidosis. From these results it was hypothesized that SAP likely takes part in amyloidogenesis by accelerating the formation of the amyloid deposits. Interestingly, the mice lacking SAP in these studies did not show any phenotypic abnormalities, though it could be posited that discerning any change would likely require an immune challenge, given mouse SAP is an acute phase protein, as previously discussed.

It is important to note however that amyloid formation does not require SAP. This was shown using the same casein injection method of amyloidosis induction with SAP knockout mice. With a sufficiently powerful stimulus, these mice developed amyloid deposits exactly as the WT controls (Botto et al., 1997). An additional point of consideration is that human SAP reportedly binds much more avidly to amyloid fibrils than mouse SAP does, and is also approximately 30 times more abundant in human amyloid deposits than mouse SAP is in mouse amyloid (Hawkins et al., 1988; Pepys et al., 1997). In taking this point into account with the results of the studies in mice, it could therefore be suggested that human SAP is likely involved more significantly in pathogenesis and/or persistence of human amyloid.

While there is substantial evidence for the role of SAP in amyloid fibril stability in the case of amyloidosis in the periphery, the obvious question raised is whether it may have similar effects with other pathologies involving amyloid deposition. The important point to consider with this question however is that other amyloid

pathologies are in the brain, rather than the periphery. Results of studies examining SAP in the brain have been less clear; assumptions made about the expression of SAP by one group of researchers that SAP is expressed exclusively in the liver (Pepys et al., 1997) was later challenged by another group that reported human neurons also express SAP (Yasojima et al., 2000), thus spurring more questions being raised. It has been claimed that SAP binds avidly but reversibly to all amyloid fibrils, which has been well characterized in systemic amyloidosis (Pepys, 2006) and also shown to occur in cases of sporadic cerebral amyloid angiopathy (CAA)(Charidimou et al., 2012). CAA is an age related cerebral small vessel disease that is characterized by Aβ progressively depositing in the wall of small arteries, arterioles and capillaries of the cerebral cortex and overlying leptomeninges. If SAP is present in small damaged arteries of the cerebral cortex bound to amyloid, this raises the question of whether it could infiltrate the brain and do the same.

In humans, SAP has not been detected in the brain under normal conditions, but it has been immunohistologically associated with the pathology that occurs in Parkinson's, Creutzfeldt-Jakob and Lewy body disorders (Akiyama et al., 1991; Kalaria et al., 1991a), and directly with amyloid deposits in Down's syndrome and hereditary cerebral hemorrhage with amyloidosis (Coria et al., 1988; Iseki et al., 1988; Ogeng'o et al., 1996). Moreover, immunohistochemical studies have revealed widespread immunoreactivity of SAP in the brains of patients with Alzheimer's disease (AD) - the most prominent form of dementia that afflicts 1 out of every 10 people over the age of 65 (Akiyama et al., 1991; Duong et al., 1993; Duong and Gallagher, 1994; Duong et al., 1989; Kalaria et al., 1991c; Kalaria and Grahovac, 1990; Kimura et al., 1994; Perlmutter et al., 1995; Perlmutter et al., 1994).

Alzheimer's disease

One of the most frequent and devastating health problems currently afflicting the elderly is AD, comprising 50-60% of all dementia cases, with no cure or fundamentally effective treatment (Ballard et al., 2011). AD is neuropathologically characterized by the accumulation of extracellular amyloid-β (Aβ) aggregates in the form of plaques and neurofibrillary tau tangles (NFT), as well as significant atrophy

of gray matter (Hyman et al., 2012). The underlying molecular mechanisms for disease development however are yet to be fully understood (Golde et al., 2011).

Accounting for the vast majority of cases, late-onset sporadic AD likely develops as a result of a culmination of multiple factors, including those of aging, environment, and lifestyle, and often presents itself in people over the age of 65. Early-onset familial AD (eFAD) is a rare autosomal dominant disease affecting people well before the age of 65, and sometimes as young as 30, that accounts for approximately 2-3% of all cases of AD (Association, 2017). It is important to note however that AD exists in a continuum, where there can also be early-onset sporadic and late-onset familial cases, and each subtype is not necessarily a pure form unto itself. This is evidenced by research showing that about 25% of families with late-onset AD also have a relative who develops early-onset AD (Brickell et al., 2006). However, the genetic mutations in three genes that can cause eFAD are known: the mutations in the amyloid precursor protein (APP), and the enzymes presenilin 1 (PSEN1) and presenilin 2 (PSEN2) result in the pathological processing of the normal transmembrane protein APP (Blennow et al., 2006). One of the products of the two APP processing pathways (Fig. 1.4), when cleaved by the γ-secretase complex, is the 42 amino acid peptide $A\beta_{1\text{-}42}$, most highly associated with AD pathology (Rovelet-Lecrux et al., 2006).

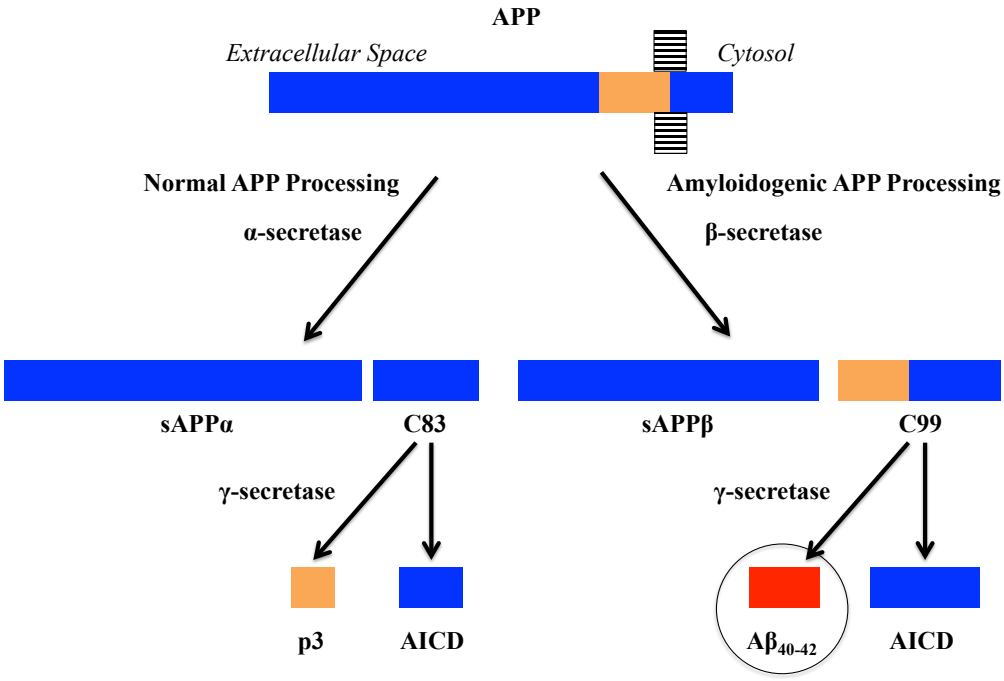

Figure 1.4. The pathways of APP processing. As a transmembrane protein, APP can be processed in a non-amyloidogenic, or 'normal' pathway (left) in which it is cleaved by α-secretase to produce soluble APPα (sAPPα) and C-terminal-83 amino acid fragment (C83), then CTFα is hydrolyzed by γ-secretase to generate APP intracellular domain (AICD) and the p3 fragment. APP can also be processed via the amyloidogenic pathway (right), where it is cleaved by β-secretase resulting in N-terminal soluble APPβ (sAPPβ) leaving the C-terminal 99 amino acid fragment (CTF99) which is hydrolyzed by γ-secretase to yield $A\beta_{40-42}$ and AICD. Presenilin is an aspartyl protease and a subunit of γ-secretase, and PSEN mutation might increase γ-secretase activity to cause plaque formation (Cai et al., 2015).

While the amyloid hypothesis originally proposed Aβ accumulation was the main culprit in the disease, it has since become clear that amyloid deposits are not the direct cause of AD (Jellinger and Attems, 2013), particularly considering that amyloid plaque load is not directly related to cognitive decline (Price et al., 2009). Given the lack of correlation of synaptic and neuronal loss to amyloid plaques, soluble amyloid oligomers rather than insoluble deposits are considered to be largely responsible for the underlying pathology. There is also substantial evidence that increased production of Aβ may be the key to initiating AD and trigger tau pathology, supported by evidence of the co-occurrence of Aβ and tau pathologies in the AD brain, as well as results from genetic, cells and mouse models of AD pathology (Spires-Jones et al., 2017). Considering our relatively limited understanding of the pathological mechanisms all taking place in the lead-up to AD, it is integral that possible contributing factors that have been implicated in AD be thoroughly investigated. The

aim of the thesis is to therefore explore the role of SAP, a protein that has repeatedly been reported in association with key pathological features of AD, particularly given that SAP has not been found in the brain under normal physiological conditions.

SAP in the brain in Alzheimer's disease

It has been proposed that SAP may be a factor in the pathogenesis of AD, given the evidence that it is bound to cerebral and cerebrovascular amyloid deposits as well as neurofibrillary tangles (Coria et al., 1988; Crawford et al., 2012; Duong et al., 1989; Kolstoe et al., 2009). This is also based upon findings that SAP contributes to the pathogenesis of systemic amyloidosis (for review see Pepys, 2006), wherein the extensive nature of peripheral amyloid deposits may reflect the situation present in the AD brain. However, there is also evidence that SAP is located elsewhere in the brain aside from only in the vicinity of Aβ plaques and NFTs, suggesting it may be capable of exerting other effects in the brain as well, in addition to any interaction that it may be having with plaques.

It was first reported by Kalaria and Perry (1993) that SAP was present in the diffuse cerebellar amyloid deposits in AD, in contrast to an earlier study that claimed SAP staining was restricted to only the plaques of AD patients (Rozemuller et al., 1990). However, a key feature that is relied upon for accurate interpretation of these results often fails to be thoroughly assessed; in the case of the study by Rozemuller et al. (1990), no details of the SAP antibody epitope or specificity are provided, whereas the later study by Kalaria et al. (1993) describes the use of two different monoclonal SAP antibodies that were and tested for specificity via immunoblotting in their two previous studies (Kalaria et al., 1991a; Kalaria and Kroon, 1992). However, although the latter study detected bands of the correct size for SAP, they did not report whether there was an assessment of the antibodies binding to other pentraxins. This will be a key point for consideration in the following sections to be discussed within this thesis.

A point of contention currently exists in the field over whether there is local production of SAP in the brain. While it is claimed by some researchers that SAP is synthesized and catabolized only by the liver (Al-Shawi et al., 2016), based upon human and mouse brain transcriptome studies (Hawrylycz et al., 2012; Zhang et al.,

2014), and a study that examined mRNA expression in AD patients (Kalaria et al., 1991c), other studies have shown different results. Points to consider from this evidence are that: i) the transcriptome analysis was based upon the expression levels under normal physiological conditions, and thus may not reflect the changes in expression levels that are likely to occur in a diseased state; and ii) RT-PCR techniques have become more sensitive in their detection capabilities since 1991, and Kalaria et al. (1991c) neglected to include information on the primers used, which may possibly have not been specific or sensitive enough to detect any signal. Opposing RT-PCR findings have since been published that show SAP (and CRP) mRNAs and proteins are generated by pyramidal neurons and markedly upregulated in the brain regions most significantly affected by AD, particularly in the hippocampus and mid temporal gyrus, and in the cerebellum as well (Yasojima et al., 2000). Interestingly, SAP mRNA was also detected in human brain samples that did not show AD pathology (ibid). More specifically, Yasojima et al. (2000) report that the SAP mRNA level was 2.1-fold in the hippocampus, 2.4-fold higher in the midtemporal gyrus, 2.2-fold in both the midfrontal and motor cortices, and 1.7-fold in the cerebellum. With no differences reported between liver values of control and AD cases, it suggests that the upregulation is specific to the brain in the case of AD. Further *in situ* hybridization experiments found SAP mRNA signals for pyramidal neurons in hippocampus CA1 and CA4, dentate granule cells and pyramidal neurons of the temporal cortex. Additionally, SAP mRNA was reportedly found in the lung, heart, arteries, kidney and spleen, indicating macrophages and neurons may likely produce SAP in addition to hepatocytes (ibid). As such findings had not been reported previously, possible factors accounting for the detection include the use of tissue after a very short post-mortem interval that was not frozen, as well as the use of enhancer conditions coupled with higher sensitivity primers.

In examining the evidence for the presence of SAP protein in the brain, extracts from the hippocampus of AD patients and controls showed SAP to be at concentrations of approximately 1μg/mg protein and 0.6μg/mg protein, respectively (Yasojima et al., 2000). These results indicated that SAP mRNAs are translated into their protein products approximately proportional to their relative mRNA levels. In accordance, another more recent study also examined protein levels in AD patients and found SAP levels to be elevated in the hippocampus, as well as in the frontal cortex, compared to

controls. This study reports a four-fold increase to 110 ng of SAP/mg of protein in AD (Crawford et al., 2012), differing from the 1 μg of SAP/mg protein previously reported (Yasojima et al., 2000). However, the authors suggest that the difference is due to the use of total homogenate rather than protein concentrations of supernatants after centrifugation of homogenates. An additional methodological point to consider in the difference between the two aforementioned studies would be that each used a different commercial SAP antibody for detection of protein levels, but neither provides evidence for the specificity of either antibody. Given the significant degree of homology between SAP and CRP, as previously discussed, antibody specificity is imperative in studies examining pentraxins. In addition, the *in situ* studies mentioned above also demonstrated a high degree of similarity in the distribution of the positive signal for both short pentraxins in neurons, and there is immunohistological evidence of SAP and CRP both being associated with Aβ plaques in AD (Yasojima et al., 2000). Therefore, careful interpretation is required with the use of antibodies for these pentraxins.

Studies on SAP concentration in the CSF in AD patients have reported multiple different findings. It is generally accepted that SAP is normally present in the CSF at a concentration of approximately one-thousandth the plasma concentration (Al-Shawi et al., 2016; Hawkins et al., 1994; Nelson et al., 1991b). While detection of SAP in the CSF of AD patients was found to increase in a study by (Hawkins et al., 1994), more recent studies have not been able to confirm this. Mulder et al. (2010), in line with Verwey et al. (2008), found that CSF SAP levels remained the same between AD patients (or MCI patients who progressed to AD) and controls, but suggested that this may be due to high levels of SAP being bound to the significant number of plaques existing in the brains of these patients. Specifically, (Verwey et al., 2008) found decreases in CSF SAP levels in MCI patients who went on to develop AD, proposing SAP as a biomarker. Collectively, these findings pose an important question of what SAP might be doing in the brain in the lead-up to AD if, over a lifetime, SAP infiltrates the brain across its high concentration gradient and/or increases in concentration in the brain.

Initially, the presence of SAP in the brain was thought to indicate a dysfunction or ‘leakage’ of the BBB in multiple different neurodegenerative conditions (Coria et al.,

1988; Duong et al., 1989; Kalaria et al., 1991b; Kalaria and Grahovac, 1990; Shi et al., 1999). Other known risk factors for dementia, including advanced age, cerebral haemorrhage, traumatic brain injury (TBI) and severe or repeated non-penetrating head injury (Association, 2017), all, certainly or probably, increase exposure of the brain to peripheral proteins, which could then contribute to a disruption of brain homeostasis. In old age, it is possible that the increases in SAP that have been observed are simply due to the prolonged duration of exposure to normal CSF SAP concentrations. However, the compromised cerebral vascular integrity present in other pathological conditions may enable plasma, with its 1000-fold higher SAP concentration, to enter the cerebral substance to a much greater extent.

Evidence for the ability of SAP to cross the BBB has been shown under an experimental condition that has been reasonably well established in the field to cause disruption of the BBB and significantly increase its permeability. Administration of lipopolysaccharide (LPS) has been shown to induce inflammation and affect mediators that regulate the BBB permeability to allow for the infiltration of components from the blood (Banks et al., 1998; Minami et al., 1998; Persidsky et al., 1997; Xaio et al., 2001). A study by Veszelka et al. (2013) utilized the administration of LPS to induce a state of inflammation in mice, and first confirmed the migration of SAP across the BBB by comparing the influx rates in mice that received peripheral injections of human SAP. But, the question first needs to be asked about what the BBB is, how it functions and how may it be compromised in neuropathological conditions. In the following section, the possibility of BBB leakage in AD will be discussed, with evidence for its occurrence (or lack thereof) in humans provided. Importantly, as mouse models are often utilized in the examination of neurodegenerative disease, the evidence on BBB function will also be examined in the appropriate models.

Permeability of the blood-brain barrier in AD

The blood-brain barrier (BBB) is a highly selective semipermeable membrane that safeguards the homeostasis of the brain's microenvironment by regulating tight control of the chemical composition crossing from the blood to the CNS (Zlokovic, 2011). This barrier is comprised of cerebral blood vessels, cerebral endothelial cells,

basal lamina, astrocytic foot processes, and pericytes (Iadecola and Nedergaard, 2007), which all function in restricting fluid and entrained molecules from being transported into the brain from the systemic circulation. The initial barrier with the blood is formed of tight junction proteins, such as claudin, occludin, and zona occludin, while the second barrier of the basal lamina contains type IV collagen, fibronectin heparan sulfate, amongst other molecules, which acts as a molecular weight filter (Candelario-Jalil et al., 2009).

It has long been hypothesized that compromises in the BBB may be a major contributing factor in brain diseases, particularly in the cases of cognitive dysfunction associated with aging and AD (Deane et al., 2008). However, it has been difficult to definitively demonstrate whether disruptions of the BBB affect brain regions involved in cognition due to the lack of suitable methods to assess the integrity of the BBB quantitatively and regionally in the human brain *in vivo*. Until recently, the evidence for leakage of the BBB in AD remained unclear; factors that differentiated between different types of dementia failed to be taken into account, along with small sample sizes of AD patients and less advanced technological means of measurement, thus preventing a definitive conclusion from being made. Over the age of approximately 70, there is increasing evidence of vascular disease intersecting with AD (Rosenberg, 2014). Cases of mixed dementias are rising as a large number of normal patients show amyloid and tau deposits and microinfarcts at autopsy (Sonnen et al., 2011). Changes in the vasculature are a normal part of aging, but with increased age there are alterations that occur in the BBB that can contribute to the pathological processes in different types of dementias (Farrall and Wardlaw, 2009). Because of this overlap, careful scrutiny of patients in these studies is crucial, but has not always been performed. In the early stages of AD and vascular dementia, it is generally not possible to separate the different pathophysiologies, or determine whether there may be a mixture of the two (Rosenberg et al., 2014). To best differentiate disease, a combination of advanced imaging techniques with CSF analysis is required, but has not often been fulfilled in most studies examining BBB leakage.

The interpretations of earlier studies examining BBB breakdown are therefore problematic, as more advanced imaging and CSF studies have only recently become available to more accurately separate patients carefully into AD, vascular cognitive

impairment, and mixed. For measuring BBB leakage, previous studies have relied on imaging methods such as positron emission tomography (PET), magnetic resonance imaging (MRI) and computed tomography (CT). One such study claiming to find no evidence of increased BBB permeability in AD used PET imaging with only 5 AD patients and 5 controls (Schlageter et al., 1987) and, along with several other CT and MRI studies with very small subject numbers claiming the same results, little information was available on controls, and it was not specified whether mixed patients were included (Caserta et al., 1998; Starr et al., 2009).

Another method of BBB permeability assessment that is examined either as the sole quantification measure or in combination with an imaging technique is the CSF albumin ratio. Earlier studies have shown increased concentrations of albumin in the CSF with age, indicating that this large protein molecule produced exclusively in the liver and restricted to the blood compartment can be abnormally transported across the cerebral vessels into the CSF (Farrall and Wardlaw, 2009). Results from this method of analysis have been conflicting; while ratios of albumin levels in the CSF to those in the blood are high in patients with vascular causes of dementia (Blennow et al., 1990), some studies report this ratio to be normal in AD (Frolich et al., 1991). These results led to the suggestion that vascular disease was the cause of the increased permeability, and not the pathologies present in AD. However, there are drawbacks to this method of analysis; albumin is a relatively large protein with a molecular weight of 66 kDa, so it cannot be considered as a sensitive measure of permeability. This ratio method also fails to pinpoint the site(s) of BBB disruption. Additionally, this evidence assumes that the CSF reflects concentrations present in the brain, whereas the primary source of protein in the CSF is in fact from the choroid plexus (Wood, 1980). Therefore, CSF protein composition may only have minimal, if any, correlation to the parenchymal changes in the brain (Caserta et al., 1998).

Other studies using protein concentrations to assess permeability of the BBB in aging and dementia have relied on autopsy material. For analysis, extravasation of plasma proteins, such as albumin, or even fibrinogen (of an even greater molecular weight of 340 kDa), has been detected qualitatively in selected brain regions by immunocytochemistry (Zlokovic, 2008). This approach is perhaps even less ideal, given the occurrence of tissue degradation, advanced disease, and coexisting

pathologies that exist in post-mortem brains, which further complicate establishing a cause-effect relationship.

However, a recent study by Montagne et al. (2015) has helped to clarify the matter of BBB leakage in the field of dementia. The aforementioned study has provided the most direct evidence to date of BBB disruption with their finding that compromises are restricted to the hippocampus in aging and in MCI patients who are at increased risk for AD. This examination of 4-times more patients than the previously mentioned PET study (Schlageter et al., 1987) used a multimodal approach of an advanced dynamic contrast-enhanced magnetic resonance imaging (DCE-MRI) with additional analysis of not only CSF biomarkers of BBB breakdown, but also of injury to brain vascular cells, markers for inflammatory response and neuronal injury, tau and pTau levels, and Aβ levels. Moreover, results of this study were strengthened by their capability to perform post-processing analysis with improved spatial and temporal resolutions that allowed for quantification of BBB regional permeability (K_{trans} constant) in the brains of individuals with either no cognitive impairment or MCI. The K_{trans} brain maps were generated from the arterial input function in patients between the ages of 23 to 91, and enabled simultaneous measurement of regional BBB permeability in the grey and while matter, as opposed to previous studies that have only been able to gather measurements of BBB permeability in the white matter (Taheri et al., 2011a; Taheri et al., 2011b; Taheri et al., 2013).

Age-dependent K_{trans} increases were found in the CA1 and DG regions of the hippocampus, but in subjects with MCI, the K_{trans} increases were approximately 60% larger than those observed in cognitively intact age matched controls. This measure in the MCI patients also correlated with findings of injury to BBB-associated pericytes. Interestingly, no changes in hippocampal volume were found in association with increased permeability, suggesting BBB dysfunction precedes hippocampal atrophy. The significantly increased BBB breakdown has raised the possibility that this leakage might therefore contribute to early cognitive impairment, given the vulnerability of this region in AD.

The BBB of the mouse

In contrast to humans, the case of BBB breakdown in mice is considerably less clear. The presence of amyloid has been suggested to be a factor in the opening of the BBB, particularly as Aβ has been shown to activate the pro-inflammatory cyclophilin A-matrix metalloproteinase-9 (MMP-9) pathway in brain pericytes, which in turn results in degradation of the BBB tight junctions and basal lamina proteins (Bell et al., 2012). This MMP-9 pathway induction has been shown in experimental animals and in cell cultures (Deb and Gottschall, 1996), as well as in transgenic mice with APOE4 which, at the age of 18 months, showed significant levels of the endogenous blood-derived IgG accumulation in the brain (Bell et al., 2012). Consistent with an increase in MMP expression and reduction of BBB tight junctions, increased permeability in brain microvessels was also found in nine month old Tg2576 mice which overexpress human amyloid precursor protein (Hartz et al., 2012).

Conversely, other studies in different mouse models of AD pathology report different findings regarding BBB permeability. It has been reported that 27-month old APP_{23} transgenic mice, which overexpress APP_{751} with the Swedish double- mutation under the control of a neuron-specific Thy-1 promoter (Calhoun et al., 1999; Sturchler-Pierrat et al., 1997), display no leakage of the BBB (Winkler et al., 2001). However, there were significant limitations to this study; assessment of BBB leakage was performed using horseradish peroxidase (HRP) and trypan blue, which were found to be associated with amyloid-laden vessels, but not at significantly increased levels in the neuropil (ibid). These methods of BBB permeability assessment were first used as such by (Rossner and Tempel, 1966)trypan blue) and (Brightman and Reese, 1969)HRP), but since the late 1960s technology has come a long way in developing several other far more accurate methods for BBB assessment. Particularly problematic in the case of trypan blue is that its assessment is contingent on it binding to the large protein albumin, for which the drawbacks have already been discussed, and further it actually lacks specific binding to albumin. HRP can cause degranulation of cells and promote the release of neurotransmitters (histamine and serotonin) that can interfere with the integrity of the BBB by affecting vascular permeability and so can give confounding effects if used *in vivo* or live tissue (Majno et al., 1961).

In relating back to our question of whether SAP might be accessing the brain via leakage of the BBB, a study by Shi et al. (1999) directly addressed this question using transgenic mice overexpressing β-protein precursor (βPP). Overexpression of βPP in transgenic mice (by neuron-specific promoters) has been shown to cause AD-type Aβ deposits in the brain (Kalaria, 1996; Nunomura et al., 1999) as Aβ is proteolytically produced from β protein precursor (βPP) (Kalaria and Grahovac, 1990). While the authors claim to find no disruption in the BBB in this model, the only measure examined was immunoreactivity of SAP, which was performed in only three mice, between (a rather large range of) ages 13-25 months old, making the results less than conclusive.

Recently, a more comprehensive study performed by (Bien-Ly et al., 2015) sought to quantitatively measure BBB permeability in multiple different mouse models of AD pathology using an antibody-dosing paradigm and a radiotracer assay with molecular probes of multiple different sizes (dextran: 3 kDa, albumin: 67 kDa, control IgG: 150 kDa). The transgenic models examined were the PS2-APP at the ages of 15–16 months with extensive plaque burden (Grueninger et al., 2010), $TauP^{301L}$ aged 14–18 months with tau aggregation developed by 8 months (Terwel et al., 2005), and Tau^{P301S} aged 8– 10 months that exhibit prominent neurodegeneration by 9 months (Yoshiyama et al., 2007). No passive entry of any radiotracers were observed for any models, and further tests examining endogenous protein showed no differences in albumin or claudin-5 for the PS2-APP mice. While the results of this sensitive assay suggest a lack of BBB in these mice, the findings should still be taken with caution, given the hippocampus (shown to be vulnerable in AD patients, as discussed above) was not independently assessed, and looking only at passive entry fails to account for increases in permeability that may occur from infection over the lifespan, or in advanced age.

Is SAP toxic?

With SAP likely to enter the brain under conditions of compromise and with its 1000-fold higher concentration gradient in the plasma relative to the CSF, or possibly its local production by neurons, the question is raised whether SAP may be exerting

effects on the cells present in the brain. Several *in vitro* studies have investigated the effects of SAP application on primary neurons at levels that have been found to be physiological in the serum. In rat cerebral neurons, significant levels of cell death have been found after 24-hour exposure of SAP at 40 nM concentrations (Urbanyi et al., 1994). In agreement with the former study, (Duong et al., 1998) observed significantly increased levels of neuronal cell death in cultures exposed to SAP at a concentration of ~32 nM for four days, in experiments using postmitotic neurons derived from the human-derived NT2 teratocarcinoma cell line, as opposed to rodent neurons. Compared to the previous study by Urbanyi et al. (1994), a slightly lower concentration of SAP was used; the concentration of only ~32 nM SAP by Duong et al. (1998) was chosen based upon the lowest value in the range of the physiological serum concentration of SAP, as measured in (Pepys, 1992) for the normal range in women (8–55 μg/mL with mean of 24 μg/mL). This demonstrates that even the lowest physiological SAP level is toxic for neuronal cells *in vitro*, however it is important to note that SAP would not be expected to reach these levels in the brain under normal conditions. Moreover, a later study confirmed SAP toxicity *in vitro* examining a significant increase in cell death in rat neuronal cultures after 2 days of incubation with 15 or 30 nM SAP (Pisalyaput and Tenner, 2008). As it has been found that SAP localizes to the nucleus (Du Clos et al., 1990) and binds to chromatin and to nucleoli (Pepys et al., 1994a), it has been hypothesized that these actions then lead to apoptotic cell death (Al-Shawi et al., 2016).

Based upon the results of their previous work, (Urbanyi et al., 2003) went on to explore the possible mechanism of SAP-induced cell death using the concentration of SAP that they found to cause a plateau of maximal cell death, at 40 nM (with 35–40% cell death). Notably, no morphological change or uptake of SAP was observed in astrocytes, even after 80 nM SAP exposure, leading them to suggest that the cellular uptake mechanism may be specific to neuronal cells (Urbanyi et al., 2003). However, only glial fibrillar acidic protein (GFAP), a marker used for astrocytes, was measured, thus excluding the consideration of other cells (i.e. microglia) present in the brain parenchyma. In neuronal cultures, SAP was found to localize in the cytoplasm of neurons that displayed shrunken bodies and dense nuclei, as well as in the membrane-bordered vacuoles and the nuclei, which showed characteristics of apoptosis such as

peripheral chromatin condensation, nuclear fragmentation and reduced cytoplasmic volume. The mRNA expression of Bax and Bcl-2 cells after SAP treatment displayed an increased Bax/Bcl-2 ratio, which is a measure that predicts cell susceptibility to apoptosis (Raisova et al., 2001). In addition, SAP treatment resulted in substantially increased levels of Aβ immunoreactivity, providing further evidence for a possible role of SAP in AD pathology (ibid).

More recent research has found *in vivo* evidence in agreement with the previously mentioned *in vitro* studies that also demonstrates SAP eliciting damage to neurons. In rats (Urbanyi et al., 2007) performed bilateral intrahippocampal injections of 10 μg SAP in both hemispheres to best mimic the physiological hippocampal concentrations previously reported in the AD brain (Yasojima et al., 2000). Their evaluation found significant increases in apoptosis in the hippocampus and cortex after 4 weeks of SAP exposure, where SAP localization in neurons was also confirmed (Urbanyi et al., 2007). These findings therefore support the relevance of increased SAP levels in the brain producing potentially harmful effects.

SAP and amyloid fibrils in the brain

As significant evidence has been shown for the role of SAP in the promotion of amyloid fibril stability in the periphery in the case of amyloidosis (Pepys, 2006), the question is raised whether it does the same with amyloid deposits associated with AD. *In vitro* experiments using physiological concentrations have shown that the aggregation of $A\beta_{1\text{-}40}$ is promoted by SAP, with one study finding an increase in aggregation from 7% to 20% in only 16 hours, with 1nM $A\beta_{1\text{-}40}$ in the presence of 100 nM (25 ug/mL) SAP (Hamazaki et al., 1995). Another similar study took this one step further by examining amyloid fibrils that were isolated from spleens of patients with amyloidosis and *ex vivo* $A\beta_{1\text{-}40}$ fibrils from the cerebrovascular amyloid deposits of AD, as well as synthetic Aβ fibrils (Tennent et al., 1995). In the presence of three different enzymes (pronase, trypsin, and chymotrypsin) that are actually more aggressive than those present *in vivo* (ibid), they found that SAP at concentrations ranging from 10-50ug/mL (40-200 nM) dose-dependently inhibited digestion of all types of amyloid fibrils by each of these enzymes (ibid). Later findings by (Mold et al., 2012) also confirmed the aforementioned findings using under-saturated solutions

of $A\beta_{1-42}$ by again demonstrating the ability of SAP to enhance the stability of amyloid fibrils - particularly those that are the principal species deposited in the brain in AD, as they are more hydrophobic and fibrillogenic (Selkoe, 2001). Overall, these studies demonstrate the importance in considering the effect that SAP may have on both the aggregation and persistence of amyloid fibrils *in situ*. As these data implicate that SAP can contribute to the insolubility of plaques.

With the *in vitro* and *in vivo* evidence for SAP toxicity previously discussed, the question arises whether these effects are relevant and can translate to humans. This was partly examined in a study by (Crawford et al., 2012), where SAP levels in the brain were compared between AD patients, non-demented patients with AD neuropathology (NDAN), and age-matched controls. A key feature of this study was the examination of the NDAN group, as their AD pathology of amyloid plaques and neurofibrillary tangles were comparable to the AD patients who exhibited cognitive impairment. Even though the pathology was similar, the levels of SAP protein and staining around plaques and tangles were significantly different in the hippocampus and frontal cortex; AD patients reportedly had significantly higher SAP levels than both the NDAN and control groups, while no difference in SAP level was detected between the latter two groups (ibid). This therefore raised an important question in the field whether SAP may be a driving force in AD progression that eventually leads to cognitive impairment.

As it has been discussed, SAP is reportedly capable of either entering or possibly being produced in the brain and has been implicated in neuronal toxicity (Urbanyi et al., 1994) and associated with the pathological features of AD (Crawford et al., 2012; Yasojima et al., 2000). However, one critical point that has failed to be taken into account in previous studies examining the effects of SAP in the brain is that other, very closely related and highly homologous pentraxins are also present in the brain. The importance of this consideration is two-fold: i) if prior detection of SAP may have been influenced by the presence of other pentraxins, as many commercial antibodies are often raised against sequences within the pentraxin domain (to be discussed in Chapter 3) and ii) the neuronal pentraxins form complexes with one another via their shared pentraxin domain – a particular sequence of amino acids that SAP possesses as well (Srinivasan et al., 1994b). For consideration of the latter point,

it is therefore integral to understand the role that the neuronal pentraxins play in the brain as well.

The neuronal pentraxins

The pentraxin superfamily includes a subfamily of long pentraxins, which possess the C-terminal pentraxin domain with the pentraxin signature and contain a longer N-terminal domain. A subset of the long pentraxins whose members are particularly expressed by neurons are the soluble secreted neuronal pentraxins (NPTXs) NPTX1 and NPTX2 or NARP, and the transmembrane neuronal pentraxin "receptor" (NPTXR), which is a splice variant of the neuronal pentraxin with chromodomain (NPCD). It is important to note however that NPTXR does not act as a receptor in the classical sense, as it has been found to perform other functions aside from the binding of other NPTXs after being cleaved from the membrane (Cho et al., 2008; Lee et al., 2017). NPTX1, NPTX2 and NPTXR are 50% identical to each other, and the C-terminal amino acids of the NPTXs, which contain the pentraxin domain, are 20-30% identical to SAP and CRP over an approximately 200 amino acid span (Dowton and McGrew, 1990; Rassouli et al., 1992; Tsui et al., 1996).

NPTX1 and NPTX2 each possess an N-terminal half that forms coiled copies and a C-terminal half that encodes the pentraxin domain, while NPTXR has an amino-terminal transmembrane domain. The NPTXs form organized heteromeric complexes stabilized by disulfide bonds, and they localize at excitatory synapses where their C-terminal domains interact with the N-terminal extracellular domains of AMPARs (Dodds et al., 1997; Kirkpatrick et al., 2000). NPTXs have been implicated in synapse formation and remodeling, synaptic plasticity, and clearance of synaptic debris. Specifically, using a coculture system of neurons and nonneuronal cells to create artificial synapses and reconstitute synaptic transmission, it has been found that AMPA receptor subunits GluR2 and GluR4 require the binding of presynaptically-derived NPTXs for trans-synaptic localization (Sia et al., 2007). At the synapse, the presynaptic complex of the linked NPTXs that forms can be cleaved by TACE, relocated to the postsynaptic terminal together with their associated pool of AMPARs, and enter endosomes, thus increasing efficacy of AMPAR endocytosis (Cho et al., 2008). A study by Koch and Ullian (2010) examining visual system development

used NPTX1 and NPTX2 knockout mice to further confirm the role of NPTXs in the establishment of functional synaptic transmission. NPTX1 and NPTX2 knockout mice display disrupted AMPA receptor recruitment necessary for synapse formation.

Knockdown of NPTX1 alone has been shown to induce conditions under which cerebellar granule cell death is reduced in non-depolarizing culture conditions, suggesting its additional role in apoptotic cell death (DeGregorio-Rocasolano et al., 2001). NPTX1 has therefore been ascribed as having a dual function, given the findings of its role in both synapse remodeling and in the gene expression program of cell death occurring from potassium deprivation (ibid).

Given this dual role of NPTX1 in excitatory synaptic remodeling and apoptotic cell death, Abad et al. (2006) investigated the possible link between NPTX1 and AD pathology using Aβ, and found that the treatment of cortical neurons with Aβ (in a time- and concentration-dependent manner, with either 10μM or 20μM, after 24 and 48hrs) resulted in a significant increase in NPTX1, preceding neurotoxicity and subsequent apoptosis. It is important to note however that the concentration of Aβ that was used represents what would likely be around peak levels that would be found endogenously around the synapse or in the vicinity of plaques (though determining Aβ concentrations in post-mortem brain is notoriously difficult due to solution sensitivity and other factors (Bao et al., 2012), making localization and disease progression points to consider for the relevance of this interaction. The knockdown of NPTX1 in the same conditions did however allow for synapse survival and reduced Aβ-mediated apoptosis. Moreover, the overexpression of NPTX1 in cultured neurons without the addition of Aβ appeared to replicate the neurotoxic effects of Aβ.

If NPTX1 is capable of mediating the toxic effects of Aβ, this would then lead to the question of whether there is evidence showing this possibility *in vivo*. Abad et al. (2006) addressed this in their study by examining brain samples from 12-month old transgenic mice expressing human APP/PS1 and sporadic late-onset AD patients. NPTX1 immunoreactivity was seen in the neuritic component of senile plaques, particularly in dystrophic neurites in AD and was found to colocalize with tau deposits in dystrophic neurites of senile plaques, but not in neurons with neurofibrillary tangles. Additionally, increases in NPTX1 protein concentrations were

found in AD patient brains, though this was determined by "markedly augmented" bands recognized by the antibody in tissue from the AD cases, but levels were not quantified. Results of this study therefore suggest that NPTX1 may play an important role in the mechanism that mediates the toxic effects of Aβ in AD. In this regard, another key finding for consideration is that NPTX1 levels significantly increased in primary neurons treated with Aβ at either 10 and 20 μM after 18 hours, which was before any morphological or biochemical signs of apoptosis appeared at 24 hours exposure (ibid). This raises the question of what effect these increased levels of NPTX1 might therefore be having in the buildup to the pathological cascade in AD.

The hippocampus and AD

In looking at the normal distribution of NPTX1 in the brain, high levels have been reported in the hippocampus and entorhinal cortex, particularly in the neuropil, and in AD it has been reported that these levels rise with Aβ and disease progression (Abad et al., 2006; Cho et al., 2008). Concurrently, SAP levels have also been found to be upregulated or even produced in this same brain region, with a greater than 2-fold increase, in cases of AD (Yasojima et al., 2000). Additionally, as previously described, the hippocampus has been shown to have the highest degree of permeability in the BBB, particularly in the CA1 and DG regions of aged and MCI patients (Montagne et al., 2015). These patterns of possible routes of pathogenesis coincide with the hippocampal region of the brain being one of the most significantly affected areas in AD (Braak et al., 1993; Mu and Gage, 2011; Whitwell et al., 2012).

The hippocampus is a relatively conserved area of the brain within mammals, consisting of a unique neuronal network of various subregions. This structure lies deep within the medial temporal lobe of the brain, and includes the hippocampus proper (or CA1, CA2 and CA3), EC, DG, subiculum, presubiculum and parasubiculum. AD pathology often follows a conserved topographical and hierarchical pattern of development and progression that strikes the hippocampus first, and most prominently (Braak and Braak, 1991; Scahill et al., 2002). In AD, significant levels of neuronal loss occur in this area, particularly in the CA1 (West et al., 1994). A reduction in volume occurs from the loss of neurons as well as the neuropil and a large number of synapses. The distribution of AD pathology in the

form of NFTs and amyloid plaques is reflected in the temporal development of cognitive symptoms that are often presented in the course of the disease. One prominent symptom is the loss of memory, which attests to the integral role of the hippocampus in the consolidation and retrieval of new declarative memory – particularly episodic memory, as determined by significant impairment in patients with lesions to this area (Scoville and Milner, 1957).

Given the substantial degree of vulnerability exhibited by this region in AD, it is therefore imperative to understand the molecular mechanisms driving such pathological changes to occur in the lead-up to and progression of the disease. As this introduction has thus far established that there may exist a possible role for the two pentraxins SAP and NPTX1 in AD, particularly given their presence in the hippocampus, it follows to examine what particular features in this structure can be affected, and further investigate the possible mechanisms by which such changes may be occurring.

Examining hippocampal function

The hippocampus is a unique structure that is particularly accessible to electrophysiological study, in that it is comprised of a largely unidirectional circuitry and densely packed cell layers. Recording can be measured over a long time from a population of cells, which enables such mechanisms as LTP, currently considered the best cellular model of learning and memory, to be assessed (Bliss and Gardner-Medwin, 1973; Bliss and Lomo, 1973). Such recordings are commonly used to test the capacity of the circuit for plasticity both *in vivo* and *in vitro*, and various studies have reported that Aβ oligomers inhibit LTP in mouse models of AD pathology (Haass and Selkoe, 2007). Additionally, synaptic transmission can be recorded with patch clamp experiments of single neurons within a network, and these more subtle changes have been found to be one of the first pathological effects that occur in the TASTPM (APP/PSEN1) mouse model of AD pathology (Cummings et al., 2015).

Previous findings from our lab have shown that there is a presynaptic effect of NPTX1 and SAP, recorded under chronic conditions in organotypic slices so as to more closely reflect those *in vivo* (Cummings, Benway et al., 2017). As evidence

shows increased protein levels of both SAP and NPTX1 in the presence of Aβ, paired-pulse ratios were measured in a dose-dependent manner, and significant effects were found at concentrations of SAP at 20 nM and NPTX1 at 60 nM (ibid). The paired-pulse ratios for each pentraxin decreased, which suggests that their chronic application results in an increase in release probability, demonstrating that both SAP and NPTX1 are capable of producing potent presynaptic effects at CA3-CA1 synapses. In addition, and importantly, co-application of both pentraxins produced no additional effect on release probability to that of the application of each pentraxin alone, thus suggesting that they interact with the same targets when applied together, and do not act independently (ibid). The critical implication of these results is that SAP, upon entry or with upregulation in the brain, may be able to interact with the endogenously released NPTX1, either at the level of NPTX1 or at downstream targets.

Ex vivo results from our lab have corroborated those discussed above; patch-clamp recordings from acute hippocampal brain slices of 14-month old transgenic mice expressing human SAP on the human SAP promoter in the liver (Iwanaga et al., 1989) also revealed an increase in glutamate release (Cummings, Benway et al., 2017). Moreover, the magnitude of LTP was found to be significantly decreased in SAP mice (ibid), thus demonstrating that both central transmission and synaptic plasticity are influenced by tonically raised SAP levels (equal to the physiological level in humans) over the course of the life of a mouse, even if only expressed in the liver.

In AD, key locations in the brain where detrimental effects are taking place are at synapses. As discussed previously, both SAP and NPTX1 are capable of influencing synaptic function (Cummings, Benway et al., 2017). The hyperexcitability demonstrated by the application of SAP and NPTX1 parallels the effects found to occur early in AD, with increased release probability being one of the putative physiological effects of released Aβ (Abramov et al., 2009). This type of neuronal hyperactivity has been reported in a multitude of studies examining early changes in AD (Stargardt et al., 2015).

Evidence of increased neuronal hyperactivity have been found in transgenic mice with AD pathology at ages as young as 1-2 months old. (Cummings et al., 2015) reported increases in release probability in the CA1 region in 2-month old TASTPM mice, in accordance with (Busche et al., 2012) who examined 1-2 month old transgenic mice overexpressing both APP_{swe} and $PS1_{G384A}$ in neurons and found dramatic increases in the fraction of hyperactive neurons in the CA1, which is before the onset of plaque pathology at ~3 months of age (Busche et al., 2008). It is also important to note that various studies report that this dysregulation continues with age, with Busche et al. (2012) having also found the same results as mentioned above in mice at 6-7 months of age, and as a recent study found significantly elevated rates and increased incidence of action potential bursts in CA1 neurons in $APP_{swe}/PS1_{M146V}$ mice at ages between 10-14 months (Siskova et al., 2014). These consistent findings of synaptic changes that begin early and persist through the course of the disease in different mouse models of AD pathology strongly suggest that synaptic derailment likely occurs long before the onset of symptoms and prior to plaque deposition. This demonstrates the need for a better understanding of the factors contributing to synaptic dysfunction that occur in the lead-up to the manifestation of AD pathology.

Spine loss in AD and the influence of pentraxins

Excessive release of glutamate has been shown to result in injury of dendrites, in a state referred to as 'dendrotoxicity' (Swann et al., 2000). Consequences of increased amounts of released glutamate and synaptic activation would be expected to produce morphological changes, which have indeed been found and referred to as part of an excitotoxic neurodegenerative process (Isokawa and Levesque, 1991; Scheibel et al., 1974). One such change that can result from neuronal hyperexcitability is the loss of dendritic spines (Swann et al., 2000), which is another key pathological feature of AD. Neurons have been found to adjust their number of synapses with adjacent cells in accordance with neuronal activity levels via structural changes in dendritic spines (Caroni et al., 2012; Holtmaat and Svoboda, 2009). Spine and synapse loss results in the altering of neuronal circuits, as spines are the main postsynaptic targets of excitatory synapses in the cortex and hippocampus of mammals (DeFelipe and Farinas, 1992). The dendritic spines on pyramidal cells are specialized postsynaptic structures that are key features of synaptic transmission (ibid), and the loss of spines

correlates to a decrease in synaptic strength and disruption in homeostatic modulation of the synapse (Matsuzaki et al., 2001). Spines are integral components for the laying down and retrieval of memories, (Hasbani et al., 2001; Parsley et al., 2007; Squire, 1992), and their size changes with plasticity of synaptic transmission (Harris et al., 2003; Honkura et al., 2008; Matsuzaki et al., 2004; Paulin et al., 2016).

Several transgenic mouse models of AD pathology analyzed for dendritic spine anomalies and synaptic loss has provided evidence that these changes occur consistently in an age-dependent manner, despite differences in Aβ accumulation in the various models analyzed (Knobloch and Mansuy, 2008). In the examination of hippocampal spines, decreases in spine density in the outer molecular layer of the DG were found at 4 months of age in the Tg2576 mouse model (Jacobsen et al., 2006), with supporting evidence found by (Wu et al., 2004) in 3-month old PDAPP transgenic mice with significant reductions in the granule cells of the posterior region of the DG (Wu et al., 2004). In accordance, (Lanz et al., 2003) evaluated spine density of both models in the CA1 and found significant reductions in the Tg2576 and PDAPP models at 4.5 months and 2 months, respectively. Collectively these results suggest that spine density is reduced prior to Aβ plaque deposition.

There are also consistent reports of synapse and spine loss found in tissue samples from patients with AD, specifically in the hippocampus and throughout the cortex, the areas most significantly affected in the disease (DeKosky and Scheff, 1990; Selkoe, 2002; Walsh and Selkoe, 2004). A greater extent of spine loss has been found to be associated with low mental status (DeKosky and Scheff, 1990; Selkoe, 1989), with MCI patients less affected AD patients, but still higher than in controls (Arendt, 2009). These findings from humans and mouse studies suggest that synapse and spine loss occur early in the development of AD (particularly in relation to diagnosis) and increase as the disease advances, thus providing good indication of disease progression. However, the question remains whether there are other factors, alongside the likely candidate of soluble amyloid, that may be contributing these changes.

Recently, a study by (Figueiro-Silva et al., 2015) presented evidence for NPTX1 being a negative regulator of excitatory synapse density, which was in line with previous research that found NPTX1 in dystrophic neurites in the brains of AD

patients (Abad et al., 2006). Specifically, they found that knockdown of NPTX1 increased the number of dendritic protrusions and excitatory synapses, along with neuronal excitability, in cultured rat cortical neurons. This was further supported by *in vivo* evidence that showed an enhancement in excitatory drive and long-term potentiation in the hippocampus of behaving mice with NPTX1 knockdown (Figueiro-Silva et al., 2015). These results therefore pose the question whether increased concentrations of NPTX1, as reported to occur in AD patients, produce a decrease in spine density. Additionally, as SAP colocalizes in similar regions surrounding plaques, it should be considered whether the two pentraxins may be capable of producing an augmented effect on the synapses during the progression of AD in areas of the brain either already burdened with, or prior to the deposition of, Aβ.

Role of the immune system in AD and possible effects of pentraxins

Recent evidence has shown that the resident microglia of the brain can play a vital role in the pathological progression of AD, particularly involving the mediation of synapse loss (Hong et al., 2016). In a normal state, the CNS modulates its own immune system comprised primarily of astrocytes and microglia to protect against pathogens and ensure homeostasis. It has been reported that microglia make up to 5-20% of all cells in the CNS (Li et al., 2014). Microglia remain in a state of quiescence under normal conditions of health, with ramified projections scanning the local environment (Town et al., 2005) so as to maintain tissue homeostasis or quickly react to pathogen invasion or injury (Davalos et al., 2005; Nimmerjahn et al., 2005).

Upon microglial activation, such as during times of infection, their phagocytic potential greatly enhances (Blander and Medzhitov, 2004), and they display an increase in soma size and rescinded projections back toward the cell body. Activated microglia display increased motility, increased proliferative abilities and upregulation of the production of inflammatory cytokines and chemokines involved in the rapid acute immune response (Frank-Cannon et al., 2009; Mosher and Wyss-Coray, 2014). Importantly, this microglial response is usually self-limiting and discontinues once the insult has been resolved. However, chronic states of neuroinflammation have been associated with neurodegenerative diseases including AD, in which it is proposed that

inflammation crosses a tipping point from being beneficial to harmful and likely aid in disease progression (Streit, 2006).

There is substantial evidence for neuroinflammation being a key feature of the pathology of AD, with post-mortem tissue from AD patients showing markers of inflammation enriched in the hippocampus and frontal cortex with AD pathology, in positron emission tomography studies showing an inverse correlation between microglia and cognitive status (Edison et al., 2008), and genome-wide microarray studies of gene expression finding significant correlations between microglia gene expression changes and Aβ plaque development (Matarin et al., 2015). However, in the past few years the role that inflammation plays in the progression of AD has come into question. The branding of microglia as 'dangerous' immune effector cells was derived from cell culture studies that found endotoxic-treated microglia producing potential neurotoxins that led to neuronal death *in vitro*, dismissing the integral protective functions of microglia with assumptions made based upon a limited experimental scope (Giulian, 1987). While many researchers in the field had supported the initial hypothesis that inflammatory cytokines may be the forces driving pathology (Akiyama et al., 2000; Rubio-Perez and Morillas-Ruiz, 2012), which early studies with non-steroidal anti-inflammatory drugs (NSAIDs) in AD patients supported (Breitner et al., 1994), subsequent large randomized trials failed to produce any beneficial effect on the etiology of AD (Aisen et al., 2003; Soininen et al., 2007). Surprisingly, NSAIDs were even found to lead to increased incidence of AD in patients with MCI (Thal et al., 2005), clearly necessitating the need for a reassessment of the hypothesis.

A common hypothesis from more recent research is that neuroinflammation is beneficial, and that it is when other factors impede the inflammatory process that the neuroprotective capabilities of microglia diminish. One major factor is age, which is also the top risk factor for neurodegenerative diseases. Under normal physiological conditions, it has been shown that the microglia population maintains itself throughout adult life through mitosis of resident microglia (Graeber et al., 1988). While there is evidence that microglia progenitors from the bloodstream can infiltrate the CNS to contribute to immune defense, it is likely that this only occurs at times of dysfunction in the BBB with injury or inflammation (Ajami et al., 2007). Therefore,

the endogenous microglia must show resilience to a multitude of insults over the course of a lifespan, enduring repeated cycles of cell division, thus prompting the question of what their limit might be before they start to experience telomere shortening and eventually a state of senescence.

Morphological and behavioral changes in microglia that occur with age have been implicated in the pathological process of neurodegenerative disease (see review by Conde & Streit, 2006). With age, it has been found microglia take on more 'reactive' morphology via an upregulation of proinflammatory cytokines (Koenigsknecht-Talboo et al., 2008; Perry et al., 1993; Sierra et al., 2007), and also have been found to display reduced motility (Orre et al., 2014). A study by Hefendehl et al. (2014) confirmed these findings with their analysis of the morphology and behavior of microglia *in vivo* in three difference age groups of mice, with young (3-month old), adult (11-12-month old) and aged (26-27-month old) using 2-photon microscopy. Additionally, this study found that microglia displayed an increased soma volume, a shortening of process length, and a disruption of homogenous tissue distribution with the advancement of age (ibid). This evidence, taken together with findings that aged microglia demonstrate an extended and enhanced pro-inflammatory activation state (Njie et al., 2012; Sierra et al., 2007), strongly suggest that there is likely to be a dyregulation in the microglial response with age. The implication of such dysfunction is that the brain is therefore more susceptible to the pathologies of AD, given that, with the onset of microglia senescence, healthy microglia become exhausted and the remaining dysfunctional aged cells cannot offer the level of protection required. It is therefore possible that in the case of AD, microglia activate and clear the toxic species that are being produced, but can only do so up until a 'tipping point' is reached, where the aged microglia can no longer maintain homeostasis, and the inflammation produced from higher levels of activation switches from being beneficial to detrimental.

Aside from being incapable of sufficient clearance of toxic species in AD, microglia have also been found to play an active role in neurodegeneration via the re-initiation of one of the processes that they are involved in during development, involving synaptic pruning via the classical complement pathway. During development, a great excess of synapses are generated in the brain, and so to prevent metabolic waste,

microglia take on the role of mediating synaptic pruning, as has been confirmed in studies that have disrupted microglial detection capabilities and found excesses of immature synapses (Paolicelli et al., 2011; Paolicelli and Gross, 2011). While normally this function ceases after development, recent studies suggest that this process becomes re-activated in AD (Hong et al., 2016; Vasek et al., 2016), particularly involving the pattern recognition molecule C1q, which is the initiator of the complement cascade. This pathway normally plays a key role in the inflammatory response with the elimination of foreign intruders, debris and apoptotic cells (Ricklin et al., 2010), but can also play a detrimental role at the synapse with exposure to soluble Aβ oligomers in AD, as reported by Hong et al. (2016). In the aforementioned study, use of the J20 mouse model of AD pathology (overexpressing human APP) revealed elevation of C1q particularly in the hippocampus and frontal cortex, which has also been reported in the APP/PS1 mouse model (Jankowsky et al., 2004). Importantly, elevated levels were reported as early as 1-month of age, prior to synapse loss, and coincided with punctate Aβ deposition in the hippocampus. During development, C1q promotes the activation of C3, a downstream factor that opsonizes synapses for elimination via phagocytic microglia engulfment (Stevens et al., 2007). Using a series of KO experiments, Hong et al. (2016) found this mechanism to be induced by oligomeric Aβ, in a region-specific manner that resulted in significant synaptic loss.

While microglia have been shown to bind and clear amyloid in several models of AD pathology (Koenigsknecht et al., 2004; Koenigsknecht-Talboo et al., 2005; Mandrekar et al., 2009; Bamberger et al., 2003), from the evidence discussed above it is highly likely that this protective mechanism becomes impaired with the progression of AD. With the findings from these aforementioned studies taken together, the re-expression of complement receptors that microglia exhibit with exposure to Aβ that lead to synapse engulfment may in large part be due to dysfunction as a result of aging. If it is indeed a delicate homeostatic balance that gets tipped during AD to produce such detrimental effects, then it is imperative to determine the contributing factors that may be pushing cells towards the direction of a tipping point.

Pentraxins and microglia

Both SAP and NPTX1 have been found at higher concentrations in the AD brain, and associated with Aβ plaques and neurofibrillary tangles (Abad et al., 2006; Duong et al., 1997). Moreover, both pentraxins have also been show to bind to C1q (Stevens et al., 2007; Ying et al., 1992b). SAP, aggregated or attached to most of its ligands, was first found to bind to the collagen-like domain of C1q and cause activation of the complement cascade by (Ying et al., 1992b). This result was confirmed by (Hicks et al., 1992) who additionally found that chemically aggregated SAP was able to activate the complement system at a concentration of 100 nM and over. However, this result should be considered with caution, as 100 nM is nearly half the concentration of physiological levels reported Pepys et al. (1978), and the authors report that complement was activated by cross-linked SAP, which consisted of dimers and insoluble aggregates, whereas native SAP protein did not cause activation at the same concentration (Hicks et al., 1992). Veerhuis et al. (2003) later observed the co-localization of SAP and C1q in fibrillar Aβ plaques, which were associated with the accumulation of activated microglia in the temporal cortex of post-mortem AD brain tissue. Also, using human microglia isolated from post-mortem brain specimens, they found that co-application of SAP at a physiological concentration of 85 nM, Aβ at 10 μM and C1q at 5 nM significantly increase the $A\beta_{1-42}$-induced secretion of the pro-inflammatory cytokines IL-6 and TNF-α by microglia *in vitro*, indicating that SAP may be capable of attracting and activating microglia synergistically with Aβ and C1q (ibid).

The possible interaction of NPTX1 and microglia has been explored very little. While Stevens et al. (2007) raise the possibility of NPTX1 being involved in synapse elimination based on the evidence of NPTX1 binding to C1q, no studies have confirmed this, or any interaction of NPTX1 with microglia. However, when NPTX1 is not in a complex with other pentraxins, studies have found that it is capable of exerting very different effects involving cell death and mediating the effect of Aβ (Abad et al., 2006; DeGregorio-Rocasolano et al., 2001), raising the question of whether it may be involved in the immune response during AD as well.

SAP and behavior

With the evidence discussed thus far of the vulnerability of the hippocampus in AD, coupled with the findings that SAP is either generated in neurons or crosses the BBB and co-localizes with Aβ plaques in this same region, our next aim was to determine whether high expression of this normally peripheral protein might produce detectable cognitive impairment in mice with AD pathology. With the evidence from Crawford et al. (2012) of higher levels of SAP in the hippocampus and the localization of SAP around plaques in AD, but not in NDAN patients, the question is raised whether SAP may be playing a role in the advancement of AD pathology that leads to cognitive impairment. Recent research has shed light onto what may be one of the earliest detectable signs of cognitive impairment in patients who are at risk for developing AD later in life. Ritchie et al. (2017) used a battery of computerized cognitive tests with over 200 middle age adults with a family history of dementia and were reportedly able to detect changes in visuospatial functions, which was associated with lower brain hippocampal volume. In contrast to previous cognitive testing that has detected alterations in function at much later stages (Salmon, 2012; Twamley et al., 2006), this study aimed to detect the underlying neuropathological changes that might be occurring in the preclinical stage of dementia, rather than in the prodromal period. These results indicate that tests in spatial navigation and spatial memory that are specifically reliant on hippocampal function are more sensitive measures of the cognitive changes occurring in AD, prior to the onset of symptoms (Ritchie et al., 2017).

Mouse models and behavior assessment

For analysis of hippocampal function in rodents, various tests have been developed to assess spatial memory. These tests often rely on the use of different mazes in which the animal is trained on and requires them to remember a particular location (i.e. the location of a platform in the Morris water maze), or the location it has previously visited to alter its response accordingly, such as in the T-maze or Y-maze (Stewart et al., 2011). The T-maze forced alternation task has previously been shown as one of the most sensitive tests to detect hippocampal dysfunction (Dudchenko, 2001), and corresponds to the type of cognitive test that was found to be a more sensitive

preclinical measure of impairment in humans, as discussed above. This task has been reported to show high sensitivity to the phenotype of the Tg2576 mouse model of AD (Stewart et al., 2011) despite its relative simplicity. Previous work from our lab has used the T-maze to assess cognitive impairment in the TASTPM mouse model of AD, and has shown no detectable changes in spatial memory in mice up to the age of 9 months, though higher anxiety levels were found (Benway MSc, 2011).

Given the evidence discussed previously, the question is raised whether SAP could possibly be contributing to cognitive dysfunction in the case of AD, and if such changes can be detected through the use of hippocampal-dependent tasks and mouse models of AD pathology. In order to examine the effects of SAP in relation to AD pathology, a mouse model was recently generated using TASTPM mice that express physiological levels of human SAP in the liver (Al-Shawi et al., 2016), but no behavioral tests on these mice have been performed. TASTPM mice are double transgenic models carrying two mutations associated with early onset AD: the Swedish mutation in APP and the M146V mutation in PSEN1. Amyloid-β deposits can be seen as early as 3 months of age, and extracellular, fibrillar Aβ plaques are observed around six months (Howlett et al., 2004). As discussed previously, our lab has also reported increases in release probability in the CA1 region in 2-month old TASTPM mice (Cummings et al., 2015).

While the characterization of mouse models such as the TASTPM mice has provided advantages in the investigation of AD pathology, it is important that the limitations of these models also be considered when relating back to diseases that affect humans. The ability to genetically modify mice with relative ease has greatly enhanced our understanding of the etiology and mechanisms of many disorders. However, to make such transgenic models often requires the use of 'artifical' promoters that do not reflect complete endogenous expression of a protein, such as with the overexpression of APP using the Thy-1 promoter that gives expression only in neurons (Andra et al., 1996). Additionally, a major criticism with the use of transgenic models is that they are based on genetic mutations that are associated with rare familial AD genes, and do not reflect the changes that occur in humans over the course of decades. With mice, only a 2-2.5 year window exists in which the disease can be replicated, meaning that the slow initiation of the disease process cannot be fully examined. Even with such

limitations, mouse models currently provide one of the most useful tools for examining different features of disease development and progression, particularly as mice possess sufficient genetic and neuroanatomical similarity to humans.

Summary

Much is yet to be determined in the field of AD research as to what factors contribute to the buildup and progression of the disease pathology. While possible roles of the pentraxins, specifically NPTX1 and SAP, have begun to be established, further elucidation of the other effects they may be influencing in the brain in relation to AD are required. Herein I consider the effects of SAP and NPTX1 and their interplay, given the ability of the pentraxin family members to interact with one another, and use multiple techniques to explore what this may affect, in relation to AD.

Using and histological molecular biology techniques, I provide evidence confirming the presence of SAP protein in the brain of AD patients and also demonstrate its ability to cross the BBB in the mouse models used. I also show that NPTX1 and SAP colocalize around Aβ plaques in both humans and mice.

Considerable evidence has so far been directed towards the synapse being the site of the initial dysfunction occurring in AD (Oddo et al., 2003; Scheff et al., 2006). Therefore, to address what increased concentrations of both these proteins may be having on synapses in the brain, cell culture work was performed to assess spine density with the application of SAP and NPTX1, alone and together, at concentrations reported to first cause changes in synaptic transmission (Cummings, Benway et al., 2017).

Given the significant role of the immune system in AD, I also broaden the experimental scope and examine the effect of SAP and NPTX1 on microglia in organotypic cultures so as to more closely mimic physiological conditions. Additionally, with the evidence confirming the presence of SAP in the brain, and evidence suggesting it may play a role in cognitive decline (Crawford et al., 2012), it follows that behavioral tests be performed in order to examine whether human SAP may be capable of enhancing the pathological features present in the TASTPM mouse

model in a way that produces cognitive effects. Overall, new insight with be provided into the effects that both SAP and NPTX1 can have in the brain, importantly focusing on their possible interaction with each other, and in relation to the progression of AD.

Chapter 2

Materials and Methods

Molecular biology

Mouse brain dissections

All experiments were conducted according to UK Home Office regulations under the Animals (Scientific Procedures) Act 1986 and in agreement with the GlaxoSmithKline statement on the use of animals, as well as UCL local ethical guidelines.

For obtaining brain samples, mice were decapitated and brains were swiftly removed and dissected on ice. Following the isolation of cortex or hippocampus, tissue for protein and RNA analysis was immediately snap frozen on dry ice and stored at -80^{o}C until required.

Brain tissue homogenization for protein and gene expression analysis

Mouse cortex or hippocampus were sonicated (Branson sonifier, 450) for 30s at 9W in ice cold RIPA buffer (1% Triton X-100, 1% sodium deoxycholate, 0.1% SDS, 0.15M NaCl, 20mM Tris.HCl (pH 7.4), 2mM EDTA (pH 8.0), 50mM sodium fluoride, 40mM β-glycerophosphate, 1mM EGTA (pH 8.0), 2mM sodium orthovanadate, 1mM PMSF, protease inhibitor tablet (Roche), 0.055 units aprotinin (Gunter et al.), 1% phosphatase inhibitor cocktail (Gunter et al.)). Samples were centrifuged at 13,000RPM for 10 minutes twice, with supernatants kept each time and insoluble pellets disposed of. Half the volume of the resulting homogenate was separated and diluted with half the volume of 3X Laemmli buffer (188 mM Tris-Cl [pH 6.8], 3% SDS, 30% glycerol, 0.01% bromophenol blue, 15% β-mercaptoethanol) and boiled for 3 minutes before being stored at -20^{o}C until required. Non-laemmli diluted homogenate was used for protein concentration quantification for each homogenate using the Bio-Rad Bradford protein assay by comparison to a standard curve generated from serial dilutions of bovine serum albumin.

For gene expression analysis, mouse cortex and hippocampus samples were homogenized using a homogenizer for 30 seconds on ice using RNA lysis buffer (QIAGEN). Following homogenization samples were aliquoted and stored at -80^{o}C.

Quantitative real-time PCR

Quantitative real-time PCR (qRT-PCR) primers were designed to span exon boundaries to distinguish between the PCR amplification from cDNA versus contaminating genomic DNA. Primer3-BLAST software (NCBI) was used to help determine primer specificity against all transcripts from the genome. *Apcs* (*SAP*) primer sequences (Eurofins MWG Operon):

Forward: 5' GTTCCACACCCAAGTAACAGC 3';
Reverse: 5' TTCAGATTCTCTGGGGAACAC 3'.

Specificity of the *Apcs* primers was tested using cDNA from the liver of 4 months old WT mice C57BL/6. Forward and reverse primers were incubated with cDNA samples, 0.25 μM of each primer and KAPA2G PCR ReadyMix (Anachem) and resolved using a 3% agarose gel with ethidium bromide and visualised using Bio-Rad Chemi-Doc MP imaging system. Cycling conditions: 95°C for 5 min, (95°C for 15 s, 58°C for 15 s, 72°C for 20 s)x30 cycles, then 72°C for 5 min. A single band of the predicted product size (155 bp) was observed for the *Apcs* primer pair, with no band observed in the control lanes (cDNA synthesis reaction lacking reverse transcriptase), or in the cDNA from the cortex. To independently assess the specificity of these primers, a melt curve analysis was performed following PCR of liver cDNA on a CFX96 system (Bio-Rad) and by incubating PCR products containing SYBR green PCR mix (Bio-Rad) from 60°C to 95°C in 0.5°C increments every 5 s. A single peak corresponding to one product size was observed for the *Apcs* primers. To assess the efficiency of the primers a dilution series of the liver cDNA was tested by PCR using the SYBR green PCR mix in triplicate and the data was plotted for DNA dilution versus Cq with a line of best fit. The efficiency value for the primer pair was 0.976 with an r2 value of 0.99, demonstrating the primer pair efficiency was close to 100% with low technical variation.

Molecular cloning: Generation of pentraxin overexpression constructs

Total RNA was extracted from hippocampal tissue of 4-month old male C57BL/6 mice using the miRNeasy protocol (Qiagen). The synthesis of cDNA was performed using 2 µg total RNA with the high-capacity cDNA reverse transcription kit (Thermofisher). The entire cDNA sequence for *Apcs*, *Nptx1, Nptx2* and *Nptxr* was amplified by high-fidelity PCR (Platinum Pfx, Invitrogen) using the primers listed in Table 1 and then subcloned into the pEGFP-N1 expression vector (Clontech) using the EcoR1 and BamH1 restriction sites upstream of GFP to create a pentraxin-GFP fusion.

Table 2.1. Primer sequences to clone the cDNA of the pentraxin family

Gene	Upstream Restriction Enzyme	Forward Primer Sequence (5'->3')	Downstream Restriction Enzyme	Reverse Primer Sequence (5'->3')
Apcs (SAP)	EcoR1	CGGAATTCAGCATGG ACAAGCTACTGCTTT GGATGTTTGTC	BamH1	CGCGGATCCCGATCC CAGACACGGGGCCT GATGACTAC
Nptx1	EcoR1	CGGAATTCGCCATGC TGGCCGGCCGCGCCG CACGCACC	BamH1	CGCGGATCCCGGTTG ATCTGGCGACAAGCC TCGAATGTCC
Nptx2	EcoR1	CGGAATTCGAGATGC TGGCGCTGCTGACCG TCGGC	BamH1	CGCGGATCCCGCAA GTCCAGGAGCCGCTC TTCACAGG
Nptxr	EcoR1	CGGAATTCAGCATGC TGGCGTTCCTCGGTGC CGTCATCTG	BamH1	CGCGGATCCCGTGCC TTTGCCCTCCCCTTG CACACATC

HEK293T cell transfection

Human embryonic kidney (Stewart et al.) cells were cultured in DMEM high-glucose supplemented with 10% fetal bovine serum (Gibco), 1%

penicillin/streptomycin/glutamine (Invitrogen) at 37°C in 5% CO2 and 95% humidity. Cells were cultured in 35 mm dishes (300,000 cells per dish). After 24 hrs, at approximately 30% confluence, each plate of cells was transfected using the calcium phosphate method with 20μg of pEGFP-NPTX1, -NPTX2, -NPTXR, -SAP or empty pEGFP. For the calcium phosphate transfection, to plasmid DNA, 125 mM CaCl and 2x HBS (274 mM NaCl, 42 mM HEPES, 15 mM D-glucose, 10 mM KCl, 1.4 mM Na_2HPO_4; pH 7.05) were added. After 5 min this mixture was administered dropwise to the cells. The cells were incubated for 4 hr, then the transfection media was rinsed off and replaced with fresh fetal bovine serum media. The cells were incubated for 48 hr prior to collection.

Pentraxin antibody specificity

In the current study, it was imperative to determine antibody specificity given the significant degree of homology between the pentraxins. To achieve this, the protein sequences for mouse SAP, NPTX1, NPTX2 and NPTXR were aligned in order to find regions that were not conserved amongst the pentraxin family (Fig. 1.1). Commercial antibodies were chosen if they were against these regions. However, it is important to note that most did not fit this criterion, which made extensive specificity testing critical.

Antibody specificity was tested by Western immunoblotting using lysates from HEK293T cells overexpressing each of the pentraxin family members individually (Fig. 3.1 A, B). Antibodies demonstrated to be specific were: NPTX1 monoclonal antibody (raised against rat NPTX1, 137- 312 aa); NPTX2 polyclonal antibody (against recombinant human NPTX2, N-term-350 aa); NPTXR antibody (against recombinant human full length NPTXR, 1-489 aa); and SAP polyclonal antibody (against recombinant mouse SAP, 21-224 aa). The antibodies in Table 2.2 were demonstrated to be specific for the pentraxin each was raised against.

Table 2.2. Specific pentraxin antibodies

Antibody	Species	Company	Catalog Number	RRID
Anti-SAP	Sheep; polyclonal	R&D	AF2558	AB_2236171
Anti-NPTX1	Mouse; monoclonal	BD Biosciences	610369	AB_397755
Anti-NPTX2	Rabbit; polyclonal	Proteintech	10889-1-AP	AB_2153875
Anti-NPTXR	Mouse; polyclonal	Abcam	AB168254	AB_2572281
Anti-GFP	Chicken; polyclonal	Abcam	AB13970	AB_300798

Western immunoblotting

Protein samples were Bradford assay-corrected and resolved by sodium dodecyl sulfate-polyacrylamide gel electrophoresis (SDS-PAGE) using 10% polyacrylamide gels, and transferred to nitrocellulose membranes (0.45 μm Bio Rad). A molecular weight standard (BioRad, #161-0374) was used to verify protein molecular weights. Proteins were transferred via electrophoresis (30V, overnight), washed in Tris-buffered saline with 0.1% Tween-20 (TBST) and blocked to prevent non-specific antibody binding in 5% milk/TBST for 1 hour at room temperature. Membranes were incubated in the appropriate concentration of primary antibody (see Table 2) in 5% milk/TBST overnight at 4°C. Following overnight incubation, membranes were washed in TBST for 5 changes of 7 minutes each at room temperature and again blocked for 10 minutes in 5% milk/TSBT. Incubation with the appropriate horseradish peroxidase-conjugated secondary antibody specific to the species of the primary antibody (1:10,000; Jackson ImmunoResearch) was performed in 5% milk/TBST for 1 hour at room temperature, then again washed as before, with a final wash of TBS. An enhanced chemiluminescence detection kit (ECL, Amersham) was used to reveal peroxidase activity. ImageLab software (v4.1, BioRad) was used for image acquisition and densitometric analysis, as described (Taylor et al., 2013). Image acquisition and densitometric analysis was performed using ImageLab (v5.2, BioRad) and statistical analyses were performed using Prism6 (GraphPad Software).

Co-immunoprecipitation

HEK293T cell lines were transfected as previously described, with 20 μg of pEGFP-NPTX1, -NPTX2, -NPTXR, -SAP or empty pEGFP, or a combination of two. After a 48 hr incubation, cells were washed and scraped into 400 μl immunoprecipitation (IP) buffer (10 mM NaH_2PO_4, 100 mM NaCl, 10 mM $Na_4P_2O_7$, 1 mM Na_3V0_4, 1 mM PMSF (phenylmethane sulfonyl fluoride) and 1% Triton X-100). The co-immunoprecipitation procedure was adapted from that of (O'Brien et al., 1999). Briefly, Protein-G and L agarose beads (Gunter et al.) were washed in IP buffer three times. The beads (50 μl/sample) were then coupled to 6 μg of the appropriate antibody (see Table 2) in 60 μl PBS solution and the mixture was incubated at 4°C for 2 hr. Following incubation, the beads were washed again in IP buffer. The collected cells were sonicated for 10 s, then centrifuged at 5,000 rpm for 20 min at 4°C. The supernatant was added to the coupled beads and incubated overnight at 4°C with rotation. Following incubation, the mixture was spun at 13,000 rpm for 2 min at 4°C, and supernatant was collected and frozen. The coupled beads were then washed with 1 ml IP buffer three times, IP buffer without Triton-X 100 three times, IP buffer with 500 mM NaCl and then PBS alone (twice), all at 4°C. Protein samples were collected by boiling in 3x Laemmli buffer before being frozen for storage. They were subsequently diluted to 1x Laemmli for loading. Image acquisition was performed using ImageLab (v5.2, BioRad).

Purified Native and Recombinant Pentraxin proteins

Recombinant human neuronal pentraxin 1 was obtained from R&D Systems: rhNPTX1 (-NP), and human native purified SAP from Abcam (#ab96056). Pentraxin concentrations were calculated and re-suspended according to the molecular weight of the monomeric structure for each type of pentraxin used. Stock vials of pentraxins were maintained at -80ºC for long-term storage, or -20ºC for short-term use. Serial dilutions were made to obtain working concentrations in culture medium, which was stored at +4ºC for a maximum of 7 days. All solutions were made under sterile conditions. As the human purified SAP contained sodium azide and EDTA, in order to avoid any off-target effects, the SAP was desalted by buffer exchange as described

by (Pilling and Gomer, 2012). Briefly, an Amicon Ultra 0.5 ml centrifugal filter unit with an Ultracel 10 kDa membrane cut-off (Merck Millipore) was used to reduce the buffer in which the SAP was re-suspended. The SAP solution was then diluted with 20 mM sodium phosphate buffer (pH 7.4) four times sequentially with 80% of the original volume of the SAP solution, and centrifuged after each dilution step. The final concentrated SAP solution was recovered and diluted to 80% of the original starting volume with 20 mM sodium phosphate buffer (pH 7.4). The SAP solution was sterilized using a 0.22 μm Millex GV filter (Merck Millipore). The integrity, purity and concentration of the desalted SAP and neuronal pentraxins were confirmed using non-denaturing and denaturing PAGE (Fig. 3.1 Ci, Cii) alongside a BSA standard. Given the pentraxins normally form pentamers containing one or more type of pentraxin, the presence of pentamers was verified using non-denaturing PAGE. Image acquisition was performed using ImageLab (v5.2, BioRad)

Non-denaturing and denaturing PAGE

Non-denatured samples were mixed 1:1 with 2x Tris/glycerol sample buffer: 125 mM Tris-HCl (pH 6.8), 20% glycerol and bromophenol blue (10 μg/ml) as described in Cummings, Benway et al. (2017). Samples were resolved on a 10% acrylamide gel, with 375 mM Tris-HCl (pH 8.8), 0.06% TEMED and 0.05% APS, and electrophoresed in buffer with: 25 mM Tris base and 192 mM glycine. Samples to be denatured were mixed with 3x Laemmli buffer and boiled for 2 min. Denatured samples were resolved using 10% SDS-PAGE, with 375 mM Tris-HCl (pH 8.8), 0.1% SDS, 0.06% TEMED and 0.05% APS. The electrophoresis buffer contained: 25 mM Tris base, 192 mM glycine, and 0.1% SDS. Image acquisition was performed using ImageLab (v5.2, BioRad).

Experimental animals

For analysis, four lines of transgenic mice were used in our study:

- TASTPM mice were transgenic for $APP_{swe+}PSEN1_{M146V}$ on the Thy-1 promotor and generated as previously described (Cummings et al., 2015, Matarin et al., 2015).
- TgSAP mice were transgenic for the human APCS (SAP) gene, including 5′ and 3′ flanking sequences, with a steady state SAP plasma concentrations within the human range (Iwanaga et al., 1989).
- $TgSAP_{Line38}$ ($TgSAP_{L38}$) mice were transgenic for the human APCS (SAP) gene and had >2-fold higher human SAP expression than TgSAP mice and developed by UCL (Al-Shawi et al., 2016).
- 3xTg mice were transgenic for $APP_{swe+}PSEN1_{M146V}$ on the Thy-1 promoter, and crossed with $TgSAP_{L38}$ mice.

The TASTPM mouse model was chosen as the model of AD pathology for the present study for a multitude of reasons. Previous studies have revealed that TASTPM mice develop amyloid plaques as early as 3 months of age, and extracellular, fibrillar Aβ plaques have been observed at approximately six months (Howlett et al., 2004) and, given the previous research showing the association of SAP and NPTX1 with Aβ, this feature was integral to have for our investigation of the pentraxins. As discussed previously, our lab has also reported increases in release probability in the CA1 region in 2-month old TASTPM mice, and has characterized the first electrophysiological changes that occur in this mouse model (Cummings et al., 2015). Moreover, our lab has generated microarray data that show the expression levels of genes in this mouse model and the changes in expression with age, and have found correlations in this data with human AD data, particularly in immune genes. The TASTPM model was therefore chosen based upon the substantial amount of characterization already performed by our lab and others in order to provide a basis from which to compare other pathological features.

WT animals used for the experiments were from C57BL/6J colonies. All other strains were on a C57BL/6J background. Male mice were bred in UCL Biological Services

Unit or the Royal Free Hospital, and generated as previously described (Pardon et al., 2009). Mice were housed in groups of 2-5 from weaning and, for behavioral testing, singly housed for only a brief 1-2 hour period daily during testing to allow for individual feeding. Mice were otherwise kept under standard housing condition in 12-hour light dark cycles, and allowed *ad libitum* access to food and water. All mice used were male.

LPS and SAP treatment in vivo

To test the ability of SAP to cross a compromised blood-brain barrier a protocol modified from Veszelka et al. (2013) and Bien-Ly et al. (2015) was used. Briefly, 4- to 6- month-old male C57BL/6 mice were given two intraperitoneal injections of lipopolysaccharide (LPS, from Escherichia coli 0111:B4; Sigma-Aldrich; 100 μg per injection per mouse dissolved in phosphate-buffered saline) or vehicle at 0 and 6 hours. Mice then received a further injection of either 250 μg purified native human SAP (Abcam) in 20 mM phosphate buffer or vehicle at 22 hours. Mice were perfused with phosphate-buffered saline at 24 hours and the brain dissected and snap frozen for Western blot analysis. Image acquisition and densitometric analysis was performed using ImageLab (v5.2, BioRad) and statistical analyses were performed using Prism6 (GraphPad Software).

Spine density analysis

Primary cultures of hippocampal neurons were prepared with a modified protocol (Beaudoin et al., 2012; Salih et al., 2012) from P0 to P1 mice expressing green fluorescent protein (GFP) on the Thy1 promoter, line S (Feng et al., 2000), resulting in a subset of their glutamatergic neurons being fluorescent. Following decapitation, the brains were quickly removed and placed in ice-cold dissection media (160mM NaCl, 5mM KCl, 1mM $MgSO_4$, 4mM $CaCl_2$, 5mM, HEPES, 5.5 mM glucose, 5μM phenol red, pH 7.4). The cortices and hippocampi were then dissected under a light microscope in dissection media, and kept on ice in fresh dissection media. When all brains had been dissected, cortices and hippocampi were removed from dissection media, diced, and incubated at 37ºC for 30 minutes in enzymatic digestion media

(dissection media, 1.5mM L-cysteine, 0.5mM EDTA, 5mM $CaCl_2$, 30mM NaOH, 100V papain, 1% DNaseI), with occasional agitation. Digested tissue was allowed to settle, digestion media removed, and inactivation media added (serum media: MEM w/Earle's w/o l-glutamine, 5% FBS, 0.4g/l glucose, 0.25%w/v BSA), for 2 minutes before removal, and then serum media was added. Cells were liberated from digested tissue via trituration, with the resulting cell suspension pipetted off from settled debris, pelleted at 1,000RPM for 5 minutes at room temperature, and then the pellet re-suspended, and plated at a density of 130,000 cells/cm^2 in poly-d-lysine coated 24 well plates, in neuron media (Neurobasal Media, 4% B27 with vitamin A, 1% Glutamax-I).

One-half the media volume was replaced with Neurobasal/B27 media 24-hrs after plating, and then once a week after that. After 4 days, 10μM FUDR was added to the media to inhibit non-neuronal cell growth. Neurons were maintained for 14 days, and for neurons treated with pentraxins, purified native human SAP or recombinant human NPTX1 was dissolved in the culture medium at the specified concentration and applied for 7 days starting at 7 DIV. Neurons were fixed at day 14 in 2% (w/v) PFA in in PBS for 10 minutes, then washed once in PBS for 10 minutes. Coverslips were then washed 3 times in 0.125% Trition X/PBS solution and blocked in 8% horse serum in 0.125% Trition X/PBS for 40 minutes at room temperature. Neurons were then incubated with primary antibody anti-GFP (1:300) in 8% horse serum in 0.125% Trition X/PBS solution at 4°C overnight. On the following day neurons were washed 3 times for 10 minutes each in PBS, then incubated in 8% horse serum in 0.125% Trition X/PBS with the secondary antibody: Alexa Fluor 488 goat anti-chicken IgG (H+L) (Abcam) at 1:600 dilution. Neurons were then washed as before in PBS and also stained with DAPI (1:10,000 in PBS) for 5 minutes to identify cell nuclei, then washed again, as before. Coverslips were mounted onto SuperFrost® Plus glass slides (VWX International) with Fluoromount G (SoutherBiotech) mounting media and sealed with nail varnish.

Spine imaging and analysis

To image dendritic spines, dendrites were chosen at random and scanned (confocal microscope: Olympus Fluoview 300; Olympus 60x oil immersion objective, with 3x

zoom. Images taken were in a z-stack formation at 0.2μm steps through the neuron over a depth of 2.4 μm, with 12 z-stack images were taken per image. Spine density was quantified by counting the number of spines in approximately 100um-long sections of either primary, secondary or tertiary dendrites, for 2 dendrites per neurons, 5 neurons per coverslip, and 12-18 coverslips per prep, in a blinded manner. Counts were taken from 3 independent preparations, with 2-3 mice used per preparation. All sample sizes for spine density analysis are expressed as number of coverslips. ImageJ was used to trace and determine the length of dendrites and to count spines, using NeuronJ add-on. Spines were counted manually by scrolling through image stacks, and the density was calculated by dividing by the dendrite length.

In order to assess the impact of treatment on spine density, two-way ANOVAs with multiple comparisons were conducted. As experiments were designed such that control experiments were interleaved between the different pentraxin treatments, the control group is common to all experiments. Where appropriate, post-hoc comparisons were conducted, adjusted with the Sidak correction for multiple comparisons. All statistical analyses were performed using Microsoft Excel and Prism6 (GraphPad Software).

Organotypic hippocampal slices

Organotypic slices were prepared under sterile conditions from 5-7 day old C57BL/6J mouse pups of either sex using standard methods (De Simoni and Yu, 2006; Stoppini et al., 1991; Paulin et al., 2016). Briefly, mice were killed by decapitation and the brain rapidly removed and placed immediately in ice-cold dissection artificial cerebrospinal fluid (artificial CSF, containing (in mM): 125 NaCl, 2.4 KCl, 26 $NaHCO_3$, 1.4 NaH_2PO_4, 20 D-glucose, 3 MgCl, 0.5 CaCl, pH 7.4, ~315 mOsm/l). The forebrain was hemisected and a segment cut away from the dorsal aspect of each hemisphere, at an angle of approximately 15° off parasagittal. Slices were cut at 300 μM using this angled cut as it is optimal for maintaining the viability of CA1 neurons. Slices were incubated at 37ºC at the interface between a 5% CO2/air and 1 ml culture medium (50% Modified Eagle Medium plus Glutamax, 25% horse serum, 23% Earl's balanced salt solution, 36.1 mM glucose, 50 units/ml

penicillin/streptomycin, 6.25 units/ml nystatin, pH 7.25, ~315 mOsm/l). Hippocampal slices were placed on small hydrophilic membrane discs (confetti; Millipore, cat. no. FHLC01300) on the bottom of the insert rather than directly onto the insert. Plating the slice on the confetti membrane piece enabled the slice to develop normally in culture by providing a surface for adherence and growth. The medium was replaced 3 times a week. For slices treated with pentraxins, purified native human SAP or recombinant human NPTX1 was dissolved in the culture medium at the specified concentration and applied for 7 days starting at 13–15 DIV. Both control and treated sliced were taken for experimentation at 20–22 DIV, at the same time point that was used for our previous electrophysiological studies, after providing optimal time for the slices to recover and receive exposure to treatment conditions.

Organotypic slices were fixed and stained using a modified protocol from (Gogolla et al., 2006). Briefly, slices were treated with 2% PFA in PBS for 30 minutes, then washed once in PBS for 10 minutes. Permeabilization of the slices was performed overnight, in 0.5% Trition X/PBS solution, at 4°C. The following day, slices were blocked in 20% BSA in 0.5% Trition X/PBS solution, for 4 hours at room temperature. Slices were then incubated with primary antibodies anti-IBA1 (Rabbit, Wako Pure Chemical Industries, LTD 019-19741, 1:250) and anti-CD68 (Rat, AbD Serotec, MCA 1957T, 1:250) in 5% BSA in 0.5% Trition X/PBS solution at 4°C overnight. Slices were then washed 3 times for 10 minutes each in 0.5% Trition X/PBS, then incubated in 5% BSA in 0.5% Trition X/PBS with the appropriate secondary antibody: Alexa Fluor 488 donkey anti-rabbit IgG (H+L) (Invitrogen), at 1:500, and Alexa Fluor 594 donkey anti-rat IgG (H+L) (Jackson ImmunoResearch Laboratories) at 1:500. Incubation was for 4 hours at room temperature in dim light, then slices were washed 3 times for 10 minutes in PBS. Slices were treated with 4',6-diamindino-2-phenylindole (Pereira et al.) (1:10,000) to identify cell nuclei for 5 minutes, then washed again with PBS. Slices were mounted onto SuperFrost® Plus glass slides (VWR International) and Fluoromount-G (SouthernBiotech) mounting media was added before applying the coverslip and sealing with nail varnish. Slices were mounted with the membrane because the slices become firmly attached to the membrane substrates over time in the culture, making it difficult to separate the slice from the membrane without causing damage.

Organotypic slice imaging and analysis

Slices were imaged for quantification using an Olympus Fluoview confocal microscope using excitation wavelengths at 568 and 488. For microglia counts, 3 areas of 62,500 μm^2 from the CA1 and DG were imaged from each slice using a 40x water objective. Images taken were in a z-stack formation at 1.0μm steps through the organotypic slice, with 10 z-stack images taken per image within the region of interest covering a 10μm depth of the slice. Quantification was performed using ImageJ to make compositions of the 2 channels, and the manual count function was used to determine number of microglia within the defined area, with cells identified by their morphology. Microglia were counted as IBA1-positive cells, and only counted if their cell body was present. Activated microglia were classified based upon morphology and high-intensity CD68 staining. In order to avoid imaging through the glial scar of hypertrophic astrocytes that forms on the top layer (approximately the top 3-5μm) of the hippocampal organotypic slice (del Rio et al., 1991), all images were obtained from below this depth of the cell surface.

For analysis of cell counts, each slice is considered as independent, despite originating from the same pup and, therefore, sample sizes represent the number of slices from which counts were taken. However, data for each group were obtained from a maximum of three slices prepared from any single animal. A minimum of three independent organotypic preparations was used to calculate the means for each treatment.

In order to assess the impact of treatment on microglia numbers and activation levels, two-way ANOVAs with multiple comparisons were conducted. As experiments were designed such that control experiments were interleaved between the different pentraxin treatments, the control group is common to all experiments. Where appropriate, post-hoc comparisons were conducted, adjusted with the Sidak correction for multiple comparisons. All statistical analyses were performed using Microsoft Excel and Prism6 (GraphPad Software).

Immunohistochemistry for human samples

Human AD samples were processed and then obtained by collaborators at the Queen Square Brain Bank. Tissue sections (7 μm thick) were cut from wax embedded hippocampi of four sporadic Alzheimer's disease cases (Table 3.1) donated to the Queen Square Brain Bank for Neurological Disorders, Institute of Neurology, University College London. Ethical approval for the study was obtained from the National Hospital for Neurology and Neurosurgery Local Research Ethics Committee. Sections were deparaffinised in xylene and rehydrated using graded alcohols. Immunohistochemistry against NPTX1 and SAP required antigen retrieval with a pressure cooker for 10 min in citrate buffer (pH 6.0). Endogenous peroxidase activity was blocked (0.3% H_20_2 in methanol, 10 min) and non-specific binding with 10% dried milk solution for 1 hour. Tissue sections were incubated with the primary antibodies (1:100 anti-NPTX1 and 1:100 anti-SAP, Table 2.2) overnight at 4°C, followed by biotinylated anti-mouse IgG and biotinylated anti-goat respectively (1:200, 30 min; DAKO) and ABC complex (30 min; DAKO). Color was developed with diaminobenzidine/H202 (Lashley et al., 2011) and counterstained with haematoxylin. For mouse brains, immunoperoxidase histochemistry was performed on a Ventana Discovery XT staining platform using the Ventana DAB Map Kit. Wax sections of formalin fixed tissue were pretreated with Ventana Protease 3 (for SAP staining) or sCC1 (for NPTX1) and blocked for 8 min using Superblock (Medite). The primary antibodies used were: an in-house monospecific polyclonal rabbit antiserum was used to detect human SAP (1:200 for 4 hrs), anti-NPTX1 (Table 2.2; 1:200, 1 hr), and Amyloid beta 6F3D Dako (Invitrogen, 1:50, 1 hr). Sections were counterstained with haematoxylin.

Behavioral Assessments

Mice were food deprived to 90% free feeding weight from 2 days before the start (habituation) of the T-maze experiment. *Ad libitum* access to water was provided. The holding room was maintained on a reversed 12 hr. light and 12 hr. dark cycle with lights off at 7 am, and temperature was controlled at 21 ± 2C. All mouse cages consisted of sawdust, nesting material, and play tubes from the age of weaning. All procedures were carried out in accordance with the UK animals Scientific Procedures

Act.

T-maze spatial alternation task

Mice were handled at the start of food deprivation and throughout T-maze habituation period for 15 minutes per animal per weekday. Mice were tested in 4 batches, with n=16-18/batch. Hippocampal function was assessed using a standard forced choice T-maze paradigm (Dudchenko, 2001; Stewart et al., 2011).

The room within which the T-maze was performed contained visible landmark cues on each of the 4 walls. This was done to aid the mice in making the correct choice using non-egocentric cues outside of the maze (Dudchenko, 2001). The T-maze was constructed from three arms, each arm measuring 50 x 8 x 10 cm. The maze was placed on a table in a room with numerous distal visual cues, such as black and white posters on the walls. The maze had clear Perspex walls and a grey floor. Black wooden blocks were used to block the start and goal arms. Mice ran for a drop of reward (Nestlé Carnation Condensed Milk) that was placed in a food cup at the end of each goal arm.

All mice received 4 days of habituation to the maze, during which mice were placed in the maze for 5 minutes with all arms open and allowed to explore. Drops of reward were scattered in day 1 and 2 of habituation along the floor and in food wells to encourage exploratory behavior, then restricted to only the food wells at the ends of the goal arms in days 3 and 4. The behavioral regime consisted of 3 weeks, with 5 days of training per week (from Monday-Friday). Each day animals received 6 trials, and each trial consisted of a sample and choice run. In the sample run, the mouse was placed at the starting point at the base of the T, a block was raised and the mouse was allowed to go to the available arm and eat a drop of reward from the food well (entrance to the other arm was blocked by a barrier) (Fig. 6.1 A). On the second run (choice run), the mouse was returned to the starting point, and the barrier in the previously blocked arm was removed. The starting block was then raised and the animal was allowed to choose between the two arms, but only rewarded if it chose the previously unvisited arm (Fig. 6.1 B). Thus, a correct choice was made when the mouse selected the arm not visited in the sample run. After the choice run mouse was

removed to its holding box from the maze. The location of the sample arm (left or right) was varied pseudorandomly across the session. Mice received three left and three right presentations, with no more than two consecutive trials with the same sample location. Response time was measured as the time from when the mouse was placed in the maze and start block removed until all four feet were over a specified line at the entry point to each goal arm. Because prolonged response times for choice runs effectively introduce a delay to the trial by increasing the amount of time the mouse must remember its previous choice, a time limit was placed. Mice were allowed five minutes to make a choice to enter a goal arm in both runs before a trial was aborted and 20 seconds to consume the reward after entering a goal arm. If the incorrect arm was chosen during the choice run the mouse was confined in the arm for 20 s and then removed from the maze. Arms were cleaned with 70% ethanol between runs and animals. During the first 2 weeks of training the choice run followed immediately after the sample run (there was a delay of approximately 15 s between runs). To prevent the mice from determining the arm with reward using scent cues, the reward station at the end of each arm contained a cap filled with approximately 2mL reward, on top of which was a paper barrier where the drop of reward was placed.

In the 3rd week, four days of test delays were introduced between the sample and choice run. During the specified interval, each animal was placed in a separate holding box. Each mouse received 2 of each of the delay lengths per day varied pseudorandomly across days. Delay times were 2.5, 5 and 10 minutes.

Data presented from the training are means blocked across 2 days for each animal. Response time and performance were analyzed by repeated measures ANOVA with effect of training block measured within-subjects and the effect of genotype and treatment between groups. Data was analyzed using Microsoft Excel and Prism6 (GraphPad Software).

Elevated plus maze (1 trial only test)

The plus-maze was constructed from 2 enclosed arms (30 cm x 5 cm x 20 cm) and 2 open arms (30 cm x 5 cm x 0.8 cm) connected by a small central platform (5 x 6 cm).

The maze was elevated 30 cm above a table. Mice were placed in the center of the plus maze facing an open arm and allowed to freely explore the maze for a 6 minute trial. The time spent on each arm (open vs. closed) was recorded, as well as the number of entries into the arms (an entry into an arm was defined as all 4 paws resting on a given arm). Data was analyzed using Microsoft Excel and Prism6 (GraphPad Software).

Open field (1 trial only test)

The open field consisted of a white plastic cylinder (diameter: 47.5 cm, height 36 cm) with a white plastic floor. Mice were put into the open field periphery and allowed to explore freely for 15 min. The path of each mouse was recorded using an hp 1080p Autofocus f2.0 camera. The open field was divided into a central circle and a peripheral ring with the area of center equal to area of periphery. Mice were tracked within a defined area of interest (optical division of equal areas consisting of the central circle vs. peripheral ring) using Image Pro (v7.0). Analysis of data was completed using custom functions created using R statistical programming (v2.14.1). Statistical analyses were performed using Microsoft Excel and Prism6 (GraphPad Software).

Chapter 3

NPTX1 and SAP colocalize in the brains of mouse models of AD pathology and human AD patients

Introduction

SAP and NPTX1 localization in the brain

A four-fold increase in SAP levels has been reported in the hippocampus and cortex of AD patients compared to controls, to an average of 110ng SAP/mg protein when total homogenate is examined (Crawford et al., 2012). However, additional members of the pentraxin family are expressed by neurons, share a significant degree of homology to SAP (Fig. 1.1), and have been shown to localize to amyloid deposits in the brain as well (Abad et al., 2006). It is therefore important to note that studies investigating SAP levels in the brain have failed to simultaneously evaluate those of the other neuronal pentraxins, and that the specificity of the antibodies used in some studies has not been definitively demonstrated. Therefore, the first goal of this chapter is to thoroughly verify antibody specificity, along with their affinity to intended targets. Considering that both NPTX1 and SAP have been reported to be associated with neuritic plaques in post-mortem brain tissue of people with AD (Abad et al., 2006; Duong et al., 1989; Kalaria et al., 1991a), I went on to compare the localization of these pentraxins in post-mortem brains from AD patients using the antibodies that I had determined to be specific for each pentraxin. Determining the specific localization of SAP in the brains of AD patients can help to determine whether it may be capable of interacting with NPTX1 or of enhancing plaque stability as it does in the periphery (Pepys, 2006).

While in humans SAP remains at a relatively stable circulating plasma concentration of ~10–100 μg/mL (~0.4–4 μM, based on 25 kDa monomer; Pepys et al., 1978), in mice, SAP acts as an acute-phase response protein (Pepys and Hirschfield, 2003). While there has been no published evidence for SAP production or infiltration into the brains of mice either under normal conditions or with transgenes for AD pathology, is it important to consider whether this may be possible, particularly given the

widespread use of mouse models in the field of AD. I therefore sought to determine, with the independently validated primers and antibodies, whether SAP could be detected in mouse models of AD pathology. Moreover, I also asked the question of whether higher levels of SAP in the periphery can results in infiltration into the brain, using mouse models transgenic for human SAP, with and without human transgenes for AD. To best address these questions, two different transgenic lines that express human SAP on the human SAP promoter in the liver were used in our study: TgSAP mice that have a steady state SAP plasma concentrations within the human range (Iwanaga et al. 1989), and $TgSAP_{L38}$ mice that have a human SAP concentration in sera of over twice the amount that is within the human range (with a mean concentration of 216.9±154.9 mg/L), as determined by Al-Shawi et al. (2016). To address this question in terms of AD, this study then examined the effect of crossing the high-SAP expressing mice with the TASTPM mouse model, as it possesses AD transgenes that encode pathogenic variants of human APP and human presenilin-1. The TASTPM mice were transgenic for $APP_{swe+}PSEN1_{M146V}$ on the Thy-1 promotor (Cummings et al., 2015, Matarin et al., 2015).

How might SAP get into the brain? What effect could this have?

In humans, under normal physiological conditions, penetration of SAP through the BBB is poor, as only low nanomolar concentrations of SAP have been found in the brain, with previous findings of concentrations in older adults averaging approximately 28ng SAP/mg protein in the hippocampus (Crawford et al., 2012) and 8.5ng/mL in the CSF (Hawkins et al., 1994). However, SAP has consistently been found at higher concentrations in the brains of AD patients (Crawford et al., 2012; Yasojima et al., 2000) and bound to Aβ plaques (Duong et al., 1989; Kalaria et al., 1991a). It has therefore been proposed that SAP likely crosses into the brain due to dysfunction of the BBB (Kalaria et al., 1991b), albeit there is also evidence for its upregulation by neurons in brains from AD patients (Yasojima et al., 2000). It is important also to consider the substantial concentration gradient that is likely to allow for such penetrance (Pepys et al., 1978), along with the considerable amount of evidence for BBB breakdown occurring in many cases of AD (Blennow et al., 1990; Montagne et al., 2015).

With the findings stated above that the peripheral pentraxin SAP is present in the brain at increased levels in AD, it is thus important to consider what possible effects it may therefore be capable of invoking, and how it may be doing so. NPTX1, NPTX2, and NPTXR can all form heteropentamers via the pentraxin domain, and function in developmental and activity-dependent synaptic plasticity (Kirkpatrick et al., 2000; Xu et al., 2003). Given the structural similarity of SAP to the NPTXs, particularly in the pentraxin domain, the question arises whether infiltrating SAP could mimic or otherwise directly interact with the NPTXs, possibly modulating synaptic transmission in the CNS. This study therefore explored whether this could be the case in a series of coimmunoprecipitation experiments with our specificity-tested antibodies.

In the following results section, the RT-PCR, antibody specificity, coimmunoprecipitation, western blot and lps experiments were performed by myself, and the staining of human and mouse tissue was performed by our collaborators at the Queen Square Brain Bank and by the lab of Professor Sebastian Brandner, respectively. All necessary controls were carried out and were all negative and validated by pathologists at the Queen Square Brain Bank or the UCL Institute of Neurology.

Aims

The aim of this chapter is to first determine whether the peripheral pentraxin SAP can be detected in a mouse model of AD pathology and in patients with AD using independently validated and specific antibodies. Secondly, we test whether SAP can permeate the BBB under a condition of BBB breakdown and lastly to investigate whether SAP can interact with its similarly structured family members of the brain - the neuronal pentraxins.

Results

Determination of antibody specificity

Reliable detection of the different members of the pentraxin family was integral to our experiments. The significant levels of homology between each pentraxin could easily allow for misidentification and, generally, commercial antibodies for SAP were raised against the conserved pentraxin region of SAP. This was also the case for many antibodies available for NPTX1. Therefore, given the significant overlap of this region among pentraxin family members, it was necessary to determine antibody specificity using molecular biology cloning techniques.

In order to ensure antibody specificity, the protein sequences for mouse SAP, CRP, NPTX1, NPTX2 and NPTXR were aligned, and we attempted to choose commercial antibodies that were against the regions of SAP and the neuronal pentraxins that were not conserved amongst the pentraxin family. However, most antibodies commercially available did not generally fit this approach, and thus extensive practical specificity testing was required.

Specificity of each pentraxin antibody used in this study was tested by overexpressing each individual pentraxin in HEK293T cells and subsequently running Western immunoblots (Fig. 3.1 A, B) to test that signal would not be detected for the incorrect, or for multiple, pentraxin proteins. I thus identified a highly specific antibody for SAP, NPTX1, NPTX2 and NPTXR after testing ten commercial antibodies. Moreover, serial dilutions of purified/recombinant pentraxin proteins were used, with concentrations of all the purified/recombinant pentraxins independently verified to determine the relative affinity of each of these specific pentraxin antibodies to its respective target (Fig. 3.1 D). The formation of pentamers, size and integrity verification of proteins was also verified. Here, our results show that the SAP antibody showed higher affinity than the NPTX1 antibody (Fig. 3.1 D), which is an important point to consider for the experiments that followed.

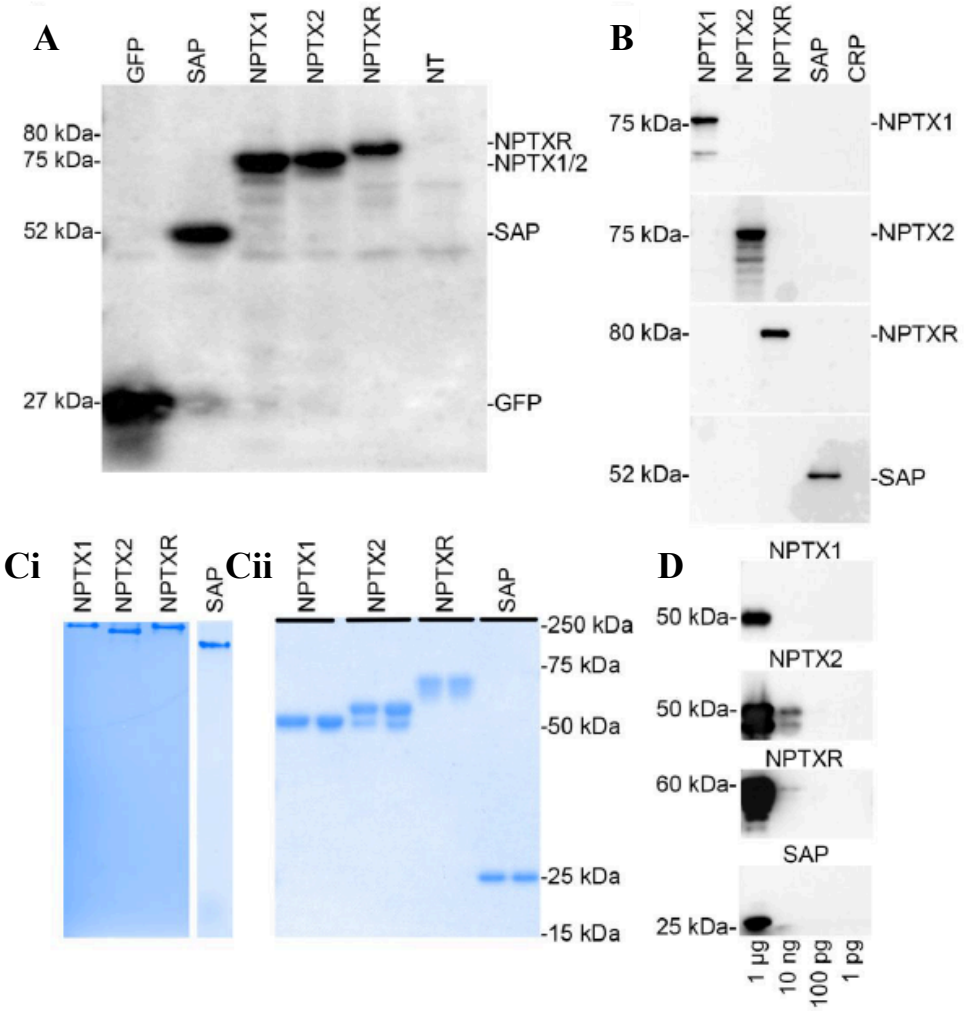

Figure 3.1. Pentraxin antibodies used are highly specific. A) HEK293T cells were transfected with constructs expressing each murine pentraxin fused to GFP individually to confirm their expression. After 48 hours, lysates were collected and 25µg protein was resolved using a 10% SDS-PAGE gel. Western blotting was performed using a GFP antibody to confirm the expression and molecular weight of each NPTX-GFP protein. All bands corresponded to the predicted molecular weight of each GFP-fused pentraxin, with GFP:27kDa, SAP:25kDa, NPTX1:47kDa, NPTX2:47kDa, NPTXR:65kDa. NT: Non-transfected. B) We identified antibodies that were specific for each pentraxin. HEK293T cells overexpressing each pentraxin were probed with the specified pentraxin antibody. Only specific bands for each antibody were detected on each blot, with lysates loaded from HEK293T cells overexpressing each of the pentraxins loaded (labeled above each lane). Note, the specific antibodies are also specific over the pentraxin C-reactive protein (CRP). C) Recombinant human neuronal pentraxins and native purified human SAP proteins form homopentamers. Ci) Pentameric structure verification of each non-denatured pentraxin protein, 2µg protein resolved per well on a non-denaturing PAGE gel. Bands correspond to pentameric forms of the proteins at their expected high molecular masses. Cii) Denatured human pentraxin protein resolved in duplicate lanes for verifying concentration, size and integrity. D) Affinity test of the specific pentraxin antibodies. A dilution series of each recombinant pentraxin protein in a set of 100-fold decreasing concentrations shows NPTX2 has higher affinity than other pentraxin antibodies, with band detection capable at a concentration of 10ng protein loaded. Faint bands for NPTXR and SAP at 10ng indicate higher affinity than the NPTX1 antibody. Figure adapted from Cummings, Benway et al. (2017).

Can SAP be detected in the brains of mouse models of AD pathology?

We next sought to independently determine whether SAP could be detected in the brains of the TASTPM (homozygous) mouse model of AD pathology. As these mice develop fibrillar Aβ plaque deposits by four months of age, we examined whether the expression of SAP in the brain could be detected or possibly upregulated in mice with the pathology associated with such changes in expression in human patients with AD (Crawford et al., 2012; Duong et al., 1989). To best detect any evidence for upregulation, we tested for SAP mRNA expression at the ages of 4 and 18 months with APCS (SAP) primers we developed and verified to be specific (Chapter 2).

Using our primers, we detected no expression of SAP at the mRNA level in the cortex of 4, or 18-month old WT, or 18-month old homozygous TASTPM mice using RT-qPCR (Fig. 3.2 A, B). In accordance, no expression of SAP was detected using microarray analysis of hippocampus, cortex or cerebellum of WT mice or mice transgenic for genes for familial AD at 2, 4, 8 and 18 months of age (www.mouseac.org; see Matarin et al., 2015). With SAP being an acute-phase protein in mice, its expression levels in the brain were not expected to be high, but it would be possible for levels to rise in these mice given that inflammation is increased in TASTPM mice (ibid). Given the discrepancies in the evidence for SAP expression in the brain (Al-Shawi et al., 2016; Hawrylycz et al., 2012; Yasojima et al., 2000), it was necessary to confirm whether this could have been the case by using our specific tools and models. However, we detected no SAP in whole-brain lysates from 20-month old TASTPM and WT mice, suggesting that SAP does not cross the BBB in this mouse model of AD pathology.

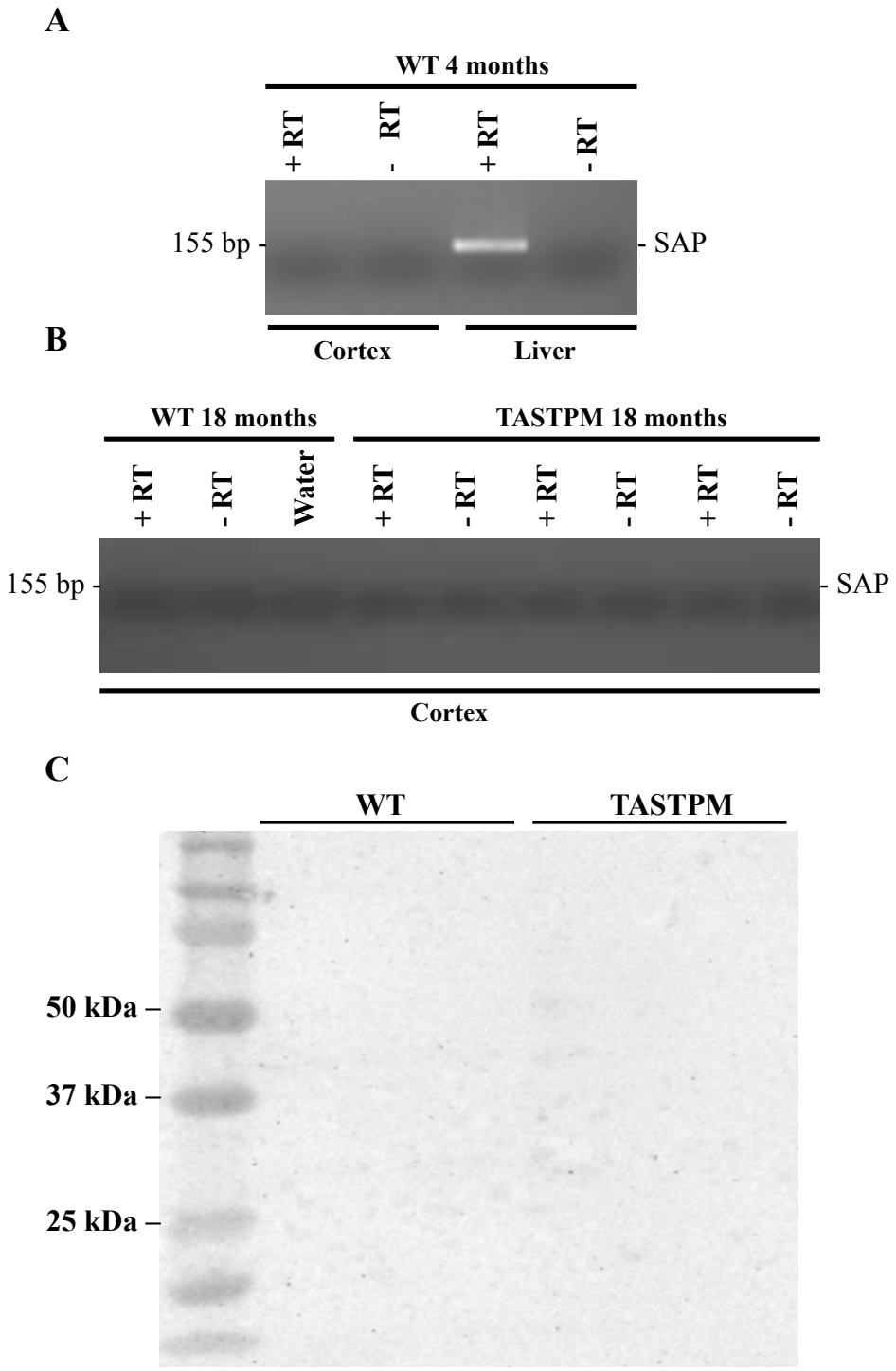

Figure 3.2. SAP RNA is not detected in the cortex of WT or TASTPM mice. A) *Apcs* (SAP) transcription was detected by RT-PCR in liver but not the cortex of 4-month old WT mice or in B) 18-month old WT or TASTPM mice. During the cDNA synthesis, RNA samples lacking the reverse transcriptase (-RT) enzyme served as a negative control to test for contamination. C) No SAP detected in whole-brain lysates from 20 month-old TASTPM or WT mice.

We next sought to determine if the higher concentrations of NPTX1 protein reportedly found in the brains of AD patients (Abad et al., 2006) corresponds to mRNA levels in the TASTPM mice. Using the same transgenic mouse database at www.mouseac.org, along with independently verified data from RT-qPCR experiments performed in our lab (Dr. Dervis Salih) we found that NPTX1 mRNA expression levels are dysregulated and actually decreased in the TASTPM mouse model of AD pathology, with expression significantly lower in the homozygous TASTPM mice at 4 and a trend toward a significant decrease (p=0.07) at 18 months of age (Fig. 3.3). This finding was unexpected, given the increase in NPTX1 immunoreactivity that is associated with dystrophic neurites in the brain tissue of the APP/PS1 mouse model of AD pathology previously reported (Abad et al., 2006).

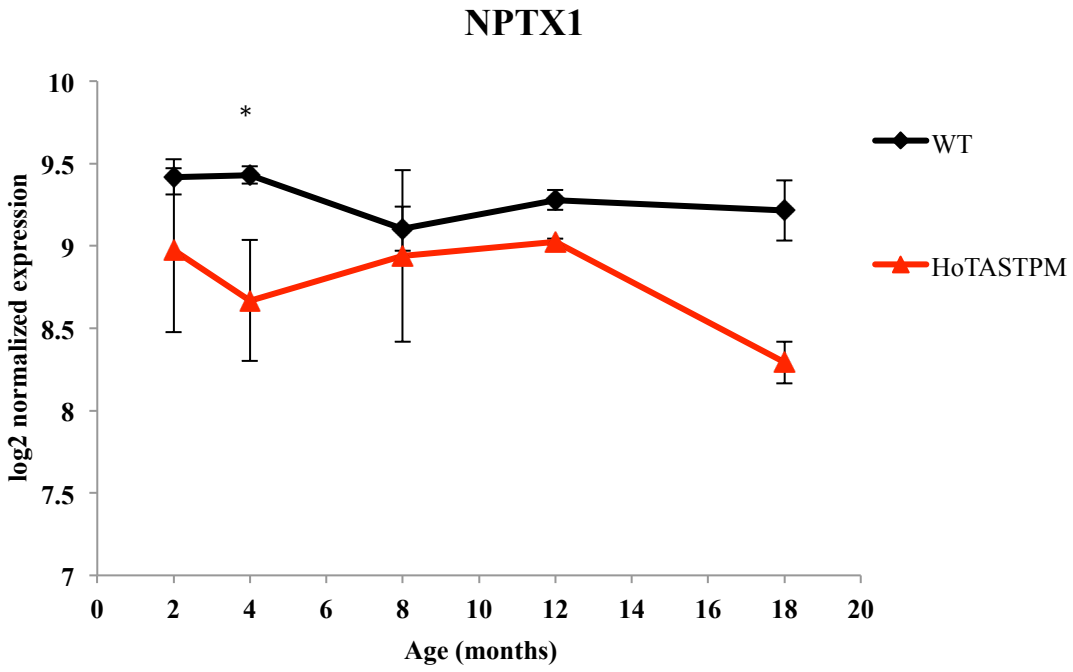

Figure 3.3. NPTX1 expression is dysregulated in the hippocampus of TASTPM mice. Gene expression changes (compared to WT) of NPTX1 in the hippocampus of WT and TASTPM homozygous mouse models from (www.Mouseac.org; Matarin et al., 2015). Two-way ANOVA revealed a main effect of genotype. Sidak post hoc multiple comparison of control to normalized NPTX1 levels are indicated *p<0.05. Data presented as mean ± SEM.

Different mouse strains have been found to have endogenous serum SAP levels that range from 20 µg/ml to 150 µg/ml, and to be classified as high and low SAP-responder strains after stimulation (Le et al., 1982). Given these variations, it was important to establish whether any SAP detection was possible with the consideration that compromises in the BBB of these mice may have occurred over the course of their lifespan. To investigate SAP and NPTX1 at the protein level in this mouse

model, western blots were run for 18-month old WT and homozygous TASTPM mice. No SAP could be detected in these mice at this advanced age, corresponding to the lack of any mRNA expression found and suggesting very low levels not detectable by our specific antibody, thus indicating that SAP is unlikely to cross the BBB in mice.

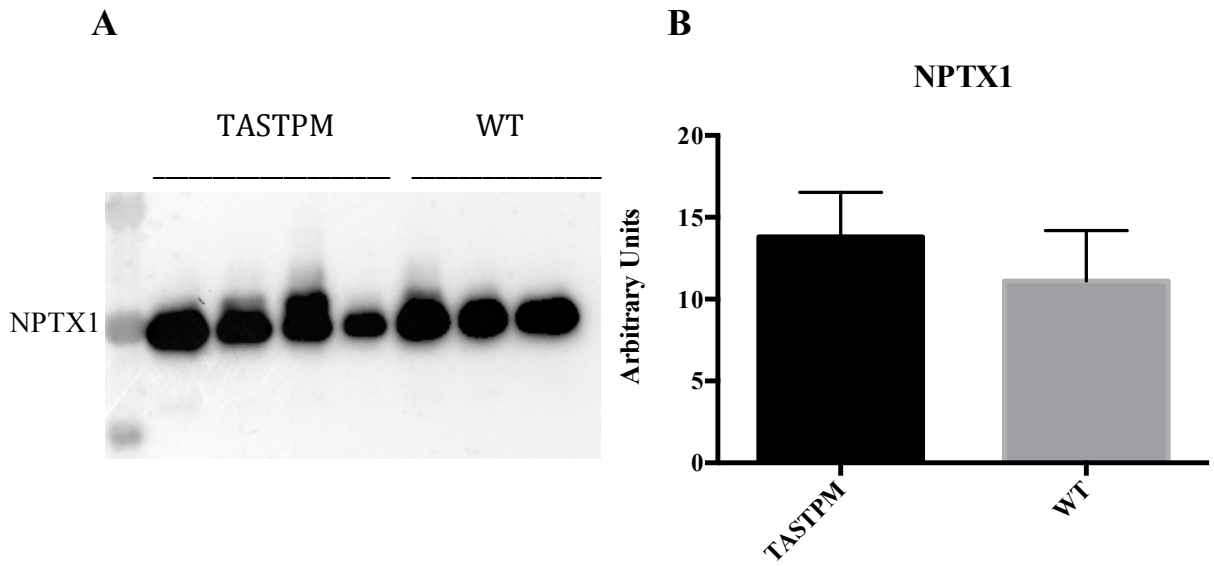

Figure. 3.4. NPTX1 protein concentration is not significantly different between the brains of old WT or TASTPM mice. (A) Western blot showing NPTX1 levels in 18-month old WT and homozygous TASTPM mice. (B) NPTX1 levels were normalized to prominent band protein levels using Ponceau-S. Data presented as mean ± SEM from WT (n=3) and TASTPM (n=4). Unpaired t-test revealed no significant difference.

Interestingly, NPTX1 protein levels in the 18-month old homozygous TASTPM mice were not found to be significantly different from those in the WT mice, despite the expression levels showing a trend for decreased NPTX1 expression at this age, (Fig. 3.4 A, B). Two-way ANOVA on the expression data revealed a significant effect of genotype [$F(1,54) = 10.78$, $p=0.0018$], and post hoc tests found a significant decrease in NPTX1 at 4 months ($p=0.0369$) and a trend toward a significant decrease at 18 months ($p=0.0708$). Although we find a difference between NPTX1 expression and protein levels in this mouse model, it is important to note that cellular homeostasis is likely taking place in this instance, as elevated protein concentrations (possibly due to accumulation around amyloid plaques) may be causing downregulation in mRNA synthesis. Also, it is generally accepted within the field that it is the concentration and interactions of proteins that dictate the causative forces in the cell (Greenbaum et al., 2003).

SAP and NPTX1 accumulate around plaques in hippocampus and cortex of AD patients

Table 3.1. Post-mortem sporadic Alzheimer's disease cases

Case number	Age at onset	Age at death	Duration (years)	Gender
1	80	85	5	M
2	46	52	6	F
3	58	68	10	M
4	54	64	9	M

As both NPTX1 and SAP have been reported to be associated with neuritic plaques in post-mortem brain tissue of AD patients (Crawford et al., 2012; Yasojima et al., 2000), we next compared the localization of these two pentraxins in post-mortem brains from AD patients (Table 3.1; Fig. 3.5 A, B). As the antibodies tested above detect both mouse and human NPTX1 and SAP, the same antibodies were used for the staining of the AD patient tissue.

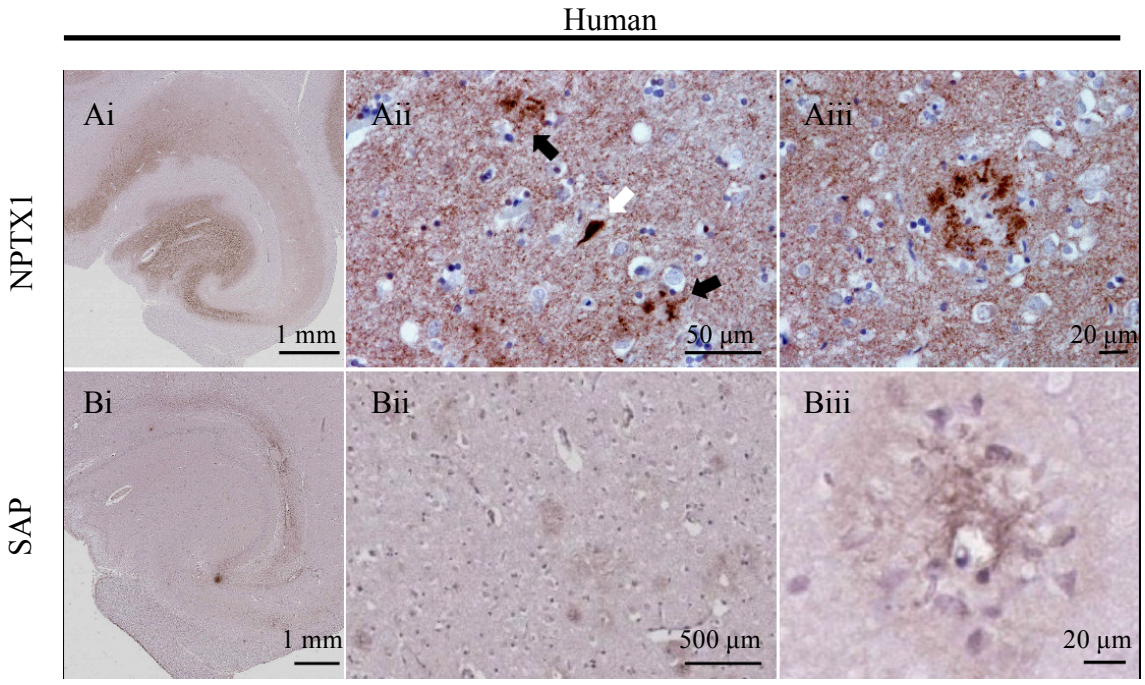

Figure 3.5. Comparison of the distribution of NPTX1 and SAP in hippocampus and on amyloid plaques in AD patients. A) Post-mortem AD hippocampus stained for NPTX1 (brown diaminobenzidine staining). Ai) NPTX1 is evident in the hippocampus, particularly within the polymorphic layer of the dentate gyrus, stratum lucidum of CA3 and stratum radiatum of CA1. 4x objective. Aii) A neurofibrillary tangle (white arrowhead) distal to neuritic plaques (black arrowheads) in the hippocampus. Both are heavily stained for NPTX1. 20x objective. Aiii) A higher magnification (40x objective) image showing NPTX1 associated with a neuritic plaque in the temporal cortex. B) Post-mortem AD hippocampus stained for SAP. Bi) Note the lower level of staining compared to NPTX1. 4x objective. Bii) Cortical plaques stained for SAP. Biii) Higher magnification image (40x objective) of plaques stained for SAP. Panels A-B: Brown staining is SAP or NPTX1, as labeled.

NPTX1 showed a high level of staining in dystrophic neurites around the periphery of plaques and general diffuse staining between the neurons with only faint staining in the core of the plaque. In addition, there was a general staining of NPTX1 in the polymorphic layer of the dentate gyrus in the tissue in human (Fig. 3.5 Ai). NPTX1 staining was also seen filling dystrophic neurons remote from plaques in the human AD brain samples, possibly representing neurons with tau pathology (Figure 3.5 Aii).

SAP staining was also seen in association with plaques in post-mortem brains from AD patients (Figure 3.5 Bi, Bii, Biii). Although very faint, this staining was present diffusely around the plaques but was not evident elsewhere in the tissue. As the SAP antibody showed higher affinity than the NPTX1 antibody for their respective targets (Figure 3.1 D), the relative strength of antibody staining suggests that only a small amount of SAP is present on the plaque compared to NPTX1. This is perhaps not surprising as the NPTX1 is reportedly produced in glutamatergic nerve terminals and so this staining likely represents locally released NPTX1, possibly from the dystrophic neurites themselves. Therefore, with the possible exception of structural changes of the proteins occurring when bound around amyloid plaques resulting in a differential change in the binding of the antibodies, the pentraxin binding to plaques appears to be strongly dominated by NPTX1 when compared to SAP.

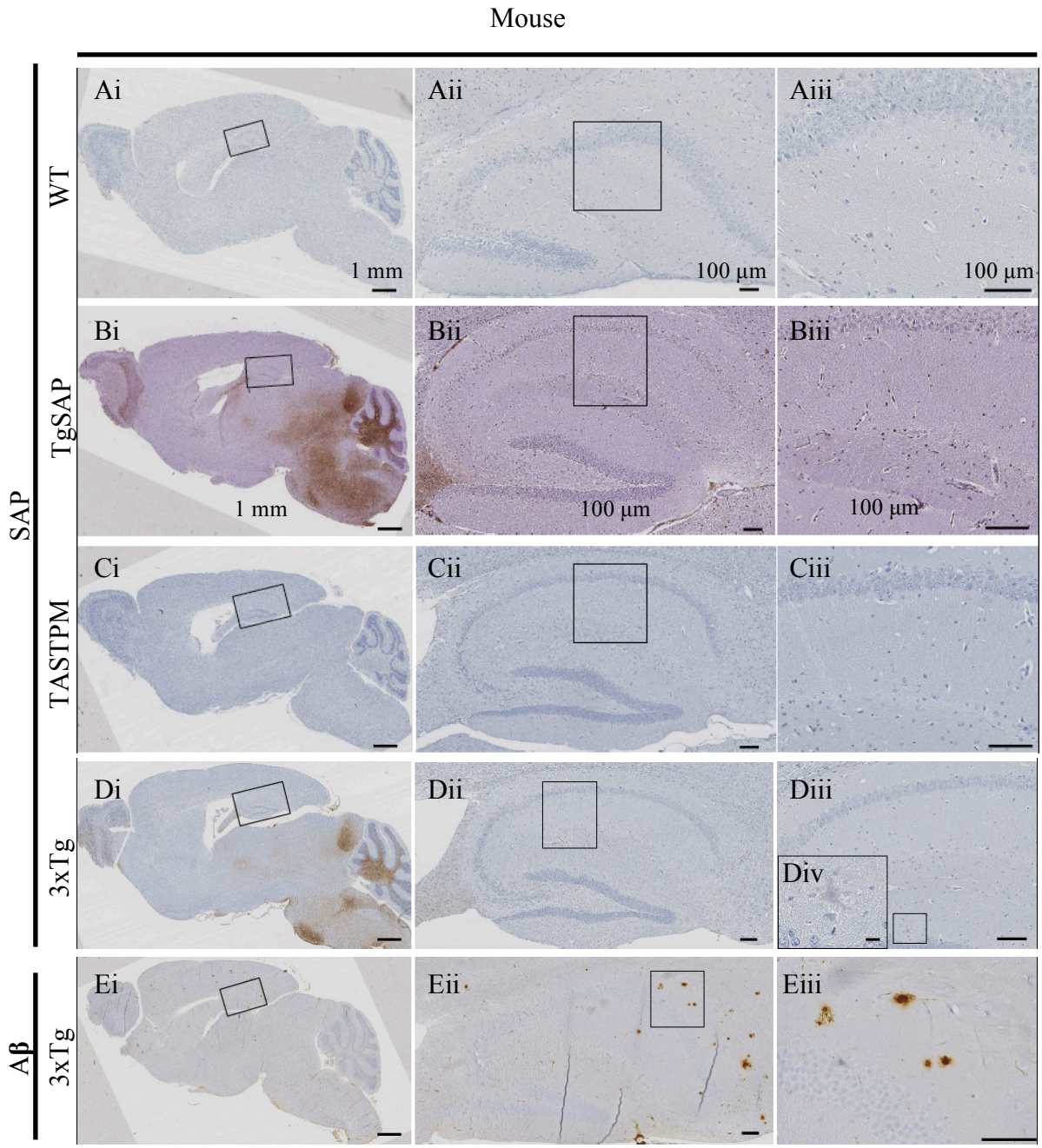

Figure 3.6. Distribution of SAP in WT, TgSAP and in TASTPM mice at 12 months of age. A) No SAP can be detected in the brain of WT mice. B) SAP staining can be seen in TgSAP mice. Bi) SAP is evident in the fiber tracts of the cerebellum, pons, medulla and inferior colliculus, and diffuse staining is present throughout the thalamus, hippocampus and cortex. Bii) Faint, diffuse staining of SAP in the hippocampus. Area of interest indicated by box on Bi. Biii) Higher magnification image of CA1, with very faint SAP staining. Area of interest indicated by box on Bii. C) No SAP can be detected in the brain of TASTPM mice. D) In 3xTg mice, a similar SAP staining pattern is seen to the TgSAP mice (B), with faint staining that can be seen in the hippocampus (Dii, Diii) as well as around plaques (Div, area of interest indicated in Diii). E) Confirmation of Aβ plaques in the 3xTg model with amyloid beta 6F3D Dake, showing a high number of dense-core plaques in the hippocampus (Eii, Eiii). Panels A-E: Brown staining is SAP or Aβ, as labeled.

SAP can enter the brain and is present on plaques in 3xTg (APP/PS1/SAP) mice

For the human SAP staining in the mice, an in-house monospecific polyclonal rabbit antiserum was used to detect SAP. This SAP antibody was independently validated for specificity by the lab's collaborators as described in Bodin et al. (2010). No SAP staining could be detected in the WT or TASTPM mice at 12 months of age (Fig. 3.6 A, C), demonstrating that mouse SAP is not likely being produced or leaking into the brain in this model of AD pathology, at least not at significant enough levels to be detected at this age. In the case of the TgSAP mice, diffuse staining was present in the hippocampus, with slightly stronger staining present in the regions of the fornix/fimbria (Fig. 3.6 Bi, Bii).

To determine the extent to which human SAP can enter the brain of a mouse model with both AD pathology and a high steady-state plasma SAP concentration we examined staining in our 3xTg model, which express approximately (at least) twice as much human SAP in the liver at the TgSAP mice (Al-Shawi et al., 2016). It can clearly be seen that SAP staining is present throughout several regions of the brain in the 3xTg mouse, with higher levels in the cerebellum, pons, medulla and some in the thalamus. There is also diffuse staining present throughout the hippocampus and cortex (Fig. 3.6 Di). In examining the hippocampus, the level of staining is very similar to the lower-expressing TgSAP model (Fig. 3.6 Bi), restricted to mostly diffuse staining associated with the amyloid plaques (Fig. 3.6 Dii, Diii, Div). Amyloid-β plaque staining was also performed in these models to confirm this attribute of the TASTPM phenotype (Fig. 3.6 E).

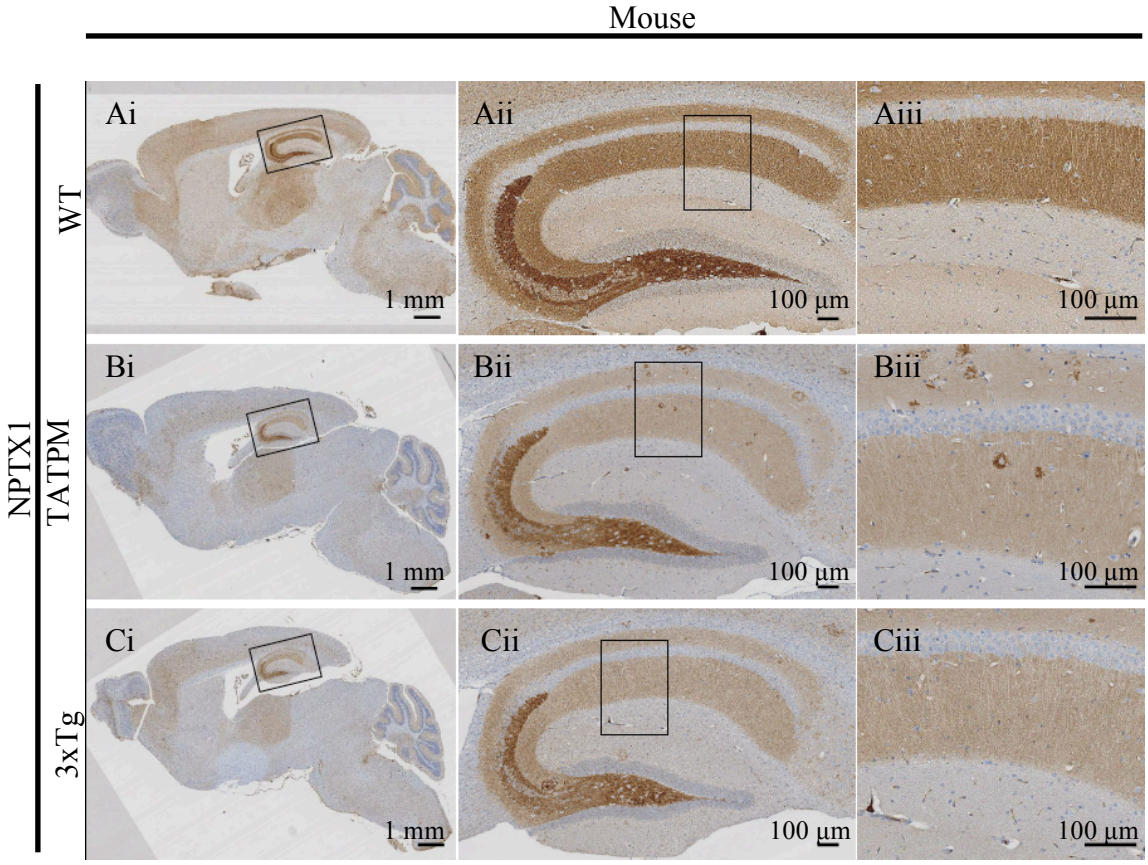

Figure 3.7. Distribution of NPTX1 in WT, TgSAP and in TASTPM mice at 12 months of age. A) NPTX1 staining in the hippocampus of an adult WT mouse. Note the similar pattern of staining to human (Fig. 3.5 A; i.e. polymorphic layer of dentate gyrus, particularly heavy staining in stratum lucidum of CA3 and lighter staining in stratum radiatum of CA1; but in the case of the mouse, also in all layers of CA3 and in stratum oriens in CA1). Aii) Higher magnification image of the CA1. The area of interest is indicated in Ai). Note the presence of NPTX1, particularly in stratum radiatum (SR) and stratum oriens but a near-absence in stratum pyramidale (SP) and stratum lacunosum moleculare (SLM). B) NPTX1 staining in the hippocampus of a TASTPM mouse. A similar pattern of staining to WT, with dense staining around the periphery of the plaque and only faint staining in the center (Biii, with area of interest in Bii). C) NPTX1 staining in the hippocampus of a 3xTg mouse. A similar pattern of staining to the WT and TASTPM mice, with staining around the outside of plaques that can be seen in Cii, but less intense than the staining around plaques in the TASTPM mice. Panels A-C: Brown staining is NPTX1, as labeled.

In examining NPTX1 staining in these mouse models (Fig. 3.7), a similar pattern of staining to humans is observed (from Fig. 3.5), particularly in the hippocampus. All three genotypes showed high levels present in the polymorphic layer of DG with heavy staining in stratum lucidum of CA3 and slightly less amount in stratum radiatum of CA1 and all layers of CA3 (Fig. 3.7 Aii, Bii, Cii). The level of staining of NPTX1 was again relatively higher around plaques found in the hippocampus, as compared to SAP, even in the higher-expressing TgSAP models (Fig. 3.7 Cii). A high

degree of staining can also be seen around plaques in the TASTPM mouse model, (Fig. 3.7 Biii) particularly with a greater extent of staining around the outside of plaques than in the TgSAP mouse (Fig. 3.7 Cii).

SAP can enter the brain under conditions of BBB breakdown

Under physiologically normal conditions, SAP is not expected to cross the BBB, but evidence from (Veszelka et al., 2013) has demonstrated that SAP can permeate an LPS-challenged BBB into the brain. Moreover, both Yasojima et al. (2000), and later Crawford et al. (2012), have shown significantly higher SAP levels in the brains of AD patients. We therefore hypothesize that it may cross the BBB under conditions of breakdown, as has been reported to occur in AD (Montagne et al., 2015), as well as in other conditions of inflammation or diseased states (Reinhold and Rittner, 2017).

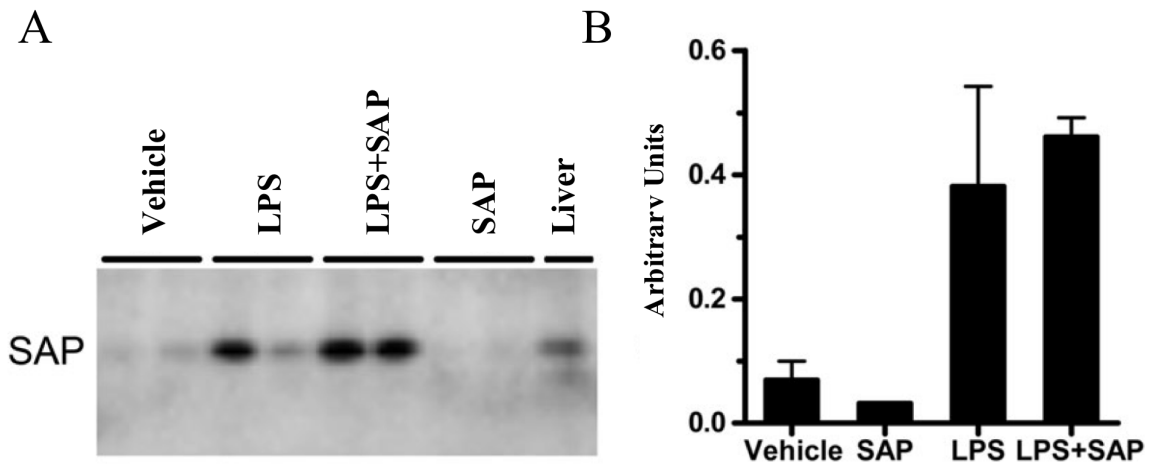

Figure 3.8. SAP crosses the compromised BBB. Mice were administered LPS to compromise the BBB and injected with native human SAP or PBS, then each hippocampus was probed for SAP. A) Western blot showing SAP levels in the four groups of mice. Liver from an animal injected with SAP is shown in the last lane as a positive control. B) SAP levels were normalized to total protein levels (Ponceau-S). Data presented as mean ± SEM from 2 animals per group. Two-way ANOVA confirmed a significant effect of LPS ($p= 0.01$) and no significant effect of SAP injection and no interaction. Figure adapted from Cummings, Benway et al. (2017).

We thus tested for levels of mouse and/or human SAP in the brain using Western blot in WT mice after injection of human SAP with or without compromising the BBB by treatment with LPS (Fig. 3.6 A). In the absence of LPS, we could detect only very low levels of SAP in the brain of untreated mice or mice injected with human SAP (250 μg). However, 22 hours after the first of two LPS administrations, injection of human SAP resulted in a strong SAP signal in both hippocampus and cerebellum. Furthermore, even without injection of human SAP, endogenous mouse SAP levels were increased in the brain, albeit at rather variable levels (Fig. 3.6 B). Two-way ANOVA confirmed a significant effect of LPS ($p=0.01$) and no significant effect of SAP injection and no interaction.

SAP binds to NPTX1 in HEK cells overexpressing pentraxins

Given the evidence that SAP can cross a compromised BBB and its presence in the brain of AD patients, we next sought to investigate whether SAP can interaction with the neuronal pentraxins. The coimmunoprecipitation procedure used was adapted from that of (O'Brien et al., 1999), using HEK293T cells transfected with the constructs that I made expressing each murine pentraxin fused to GFP and the appropriate antibodies that were verified. Here, we confirmed the results previously reported (Kirkpatrick et al., 2000; Xu et al., 2003) and showed that NPTX1, NPTX2 and NPTXR form heteropentamers when they are overexpressed together in 293T HEK cells (Fig. 3.7). Interestingly, we found that the peripheral pentraxin SAP can form a complex with NPTX1, NPTX2, and NPTXR (Fig. 3.7). This finding further supports the hypothesis that SAP can interact with the neuronal pentraxins, and potentially their downstream targets.

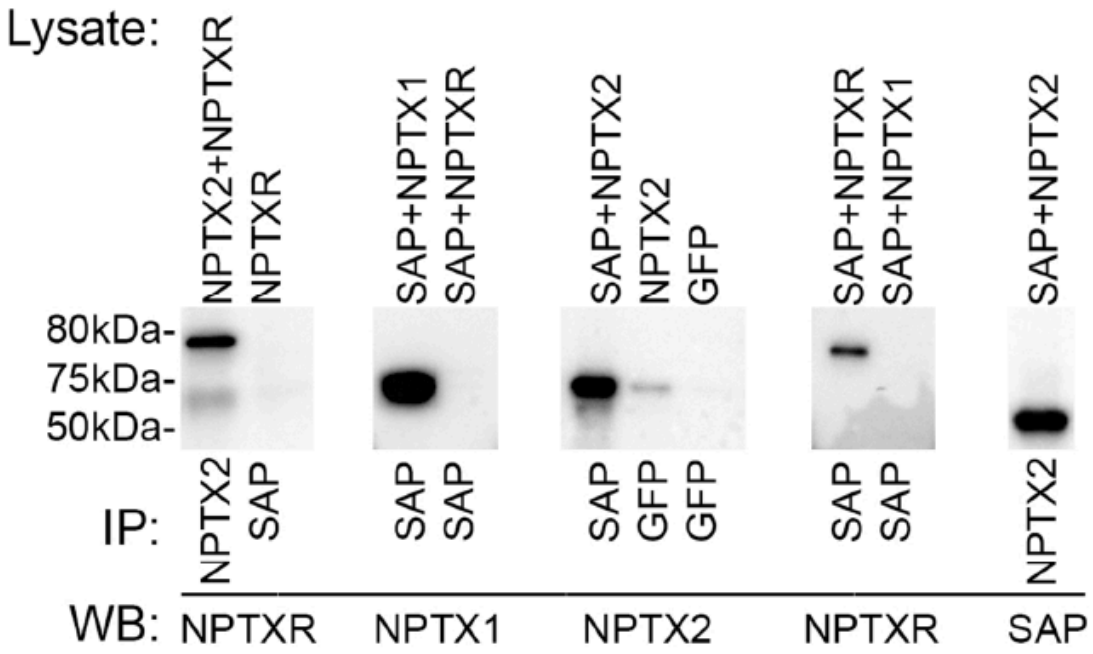

Figure 3.9. SAP forms complexes with each of the neuronal pentraxins. HEK293T cells were transfected with constructs expressing the combinations of pentraxins indicated, each fused to GFP. After 48 hours, lysates were collected and tested by immunoprecipitation (IP) followed by Western blotting with antibodies specific to each pentraxin. The bands correspond to the molecular weight predicted for each full-length pentraxin fused to GFP, with molecular weights for GFP ~27 kDa, SAP ~25 kDa, NPTX1/2 ~47 kDa and NPTXR ~53 kDa (Fig. 3.1 A). Note: the NPTX1 and NPTXR antibodies were not effective at immunoprecipitation, even for NPTX1 and NPXTR themselves, in part due to lower affinity (Fig. 3.1 D). Experiment undertaken by Benway, T.; Figure adapted from Cummings, Benway et al. (2017).

Summary

Previous studies have reported both SAP and NPTX1 to be associated with features of AD pathology (Abad et al., 2006; Yasojima et al., 2000), though none have examined either pentraxin in relation to the other in this context. After performing a multitude of experiments testing for the specificity and affinity of different antibodies, we were able to successfully identify ones for SAP and NPTX1 that could be used for examining the location of both pentraxins in the brains of AD patients and mouse models of AD pathology. In the post-mortem human AD tissue, these experiments revealed the presence of both pentraxins around plaques, confirming previous findings (ibid). Additionally, the results suggest that only a relatively small amount of SAP is present around plaques compared to NPTX1, considering the different levels that we found for the affinity of the antibodies used.

In mice, heavy staining for NPTX1 was found throughout the regions of the hippocampus, as previously reported (Cho et al., 2008). Interestingly, SAP staining was present, albeit diffuse and at low levels, in the hippocampus of transgenic mice expressing human SAP in the liver with plasma concentrations within the human range (Iwanaga et al. 1989). This suggests that SAP is capable of crossing the BBB in mice when at higher levels in the serum.

In the TASTPM mouse models of AD pathology, we found no evidence for SAP mRNA expression up to the age of 18 months, in line with previous results (Shi et al., 1999). Interestingly, a dysregulation of NPTX1 mRNA was found between the ages of 2 and 18 months, but the examination of protein levels revealed no differences between TASTPM and WT mice at 18 months of age, suggestive of a feedback mechanism that may be occurring due to high levels of NPTX1 deposition around plaques.

In TASTPM mice crossed with high-expressing SAP mice (3xTg), we show further evidence of SAP penetrance into the brain, with evidence of both SAP and NPTX1 staining around the plaques in these mice. The ability of SAP to cross the BBB was confirmed using an LPS-mediated experimental condition to cause a disruption of the BBB, in line with the findings from (Veszelka et al., 2013).

With the high degree of structural similarity between SAP and NPTX1, and the evidence for their co-localization in the brain, we hypothesized that the two pentraxins may be capable of interacting with one another. This was confirmed in our co-immunoprecipitation experiments. SAP was found to bind to not only NPTX1, but to NPTX2 and NPTXR as well. This finding raises the question of what other effects SAP may therefore be capable of eliciting in the brain via its interaction with the NPTXs, particularly with NPTX1, given that it ahs also been implicated in AD.

Overall, we can confirm previous reports that SAP is present in the brains of patients with AD and is particularly associated with plaques. Our novel finding that SAP can form a complex with NPTX1, NPTX2, or NPTXR (Fig. 3.7), together with the evidence that SAP can enter the brain if there is a breakdown of the BBB, suggest that this peripheral pentraxin may be capable of influencing other effects in the brain,

beyond its proposed role in possibly stabilizing plaques, as previously reported (Tennent et al., 1995). In fact we have recently reported that SAP causes direct regulation of synaptic function, interacting with the neuronal pentraxin family members in this context (Cummings, Benway et al., 2017). In considering the role of SAP in the brain, it is therefore crucial that the effects of SAP are examined in respect to other neuronal pentraxins as well.

Chapter 4

Chronic application of NPTX1 decreases spine density in primary cultured neurons

Introduction

As the main postsynaptic targets of excitatory synapses on pyramidal cells in the cortex and hippocampus of mammals, dendritic spines are key features of synaptic transmission (DeFelipe and Farinas, 1992). The strength of the synapse is directly related to different features of dendritic spines and is highly plastic, making spines important homeostatic modulators (Matsuzaki et al., 2001). Structural changes in the number and shape of dendritic spine are the key features mediating synaptic plasticity in the brain (Fu and Zuo, 2011), although following adolescence spines become more stable and last for the majority of a lifetime (Zuo et al., 2005). However, with advanced age, is it not uncommon for spine loss to occur. Synapse density in old monkeys was found to be 30-60% reduced from that of adults (Peters et al., 1998), while in mice the use of chronic, in vivo two-photon imaging has revealed that the density of the dendritic spines of apical dendrites in cortical pyramidal neurons is stable in mice from 8–15 months of age, but the long-term retention of spines is significantly lower in old mice, with spines that are smaller in size with age (Mostany et al., 2013).

There are several pathophysiological factors that can contribute to dendritic spine loss, including excitotoxicity induced by glutamate overspill, reduced presynaptic neurotransmitter release, interaction of protein oligomers with synaptic molecules, inflammation, altered Ca^{2+} release from stores, and disruptions in mitochondria function (Herms and Dorostkar, 2016). Neuropathological lines of evidence supporting synaptic pathology for AD have been well characterized in AD patients (Penzes et al., 2011) and in some mouse models of AD pathology (Herms and Dorostkar, 2016). Synaptic loss is consistently reported in studies analyzing post-mortem tissue samples from patients diagnosed with AD (DeKosky and Scheff, 1990; Selkoe, 2002). In these patients, loss of dendritic spines has been shown in both the hippocampus and cortex, which are the areas most significantly affected by AD pathology (DeKosky and Scheff, 1990; Walsh and Selkoe, 2004). While there is

substantial synapse loss in AD, there is also notable loss in patients with MCI, indicating that this loss progresses as the pathology advances (Arendt, 2009).

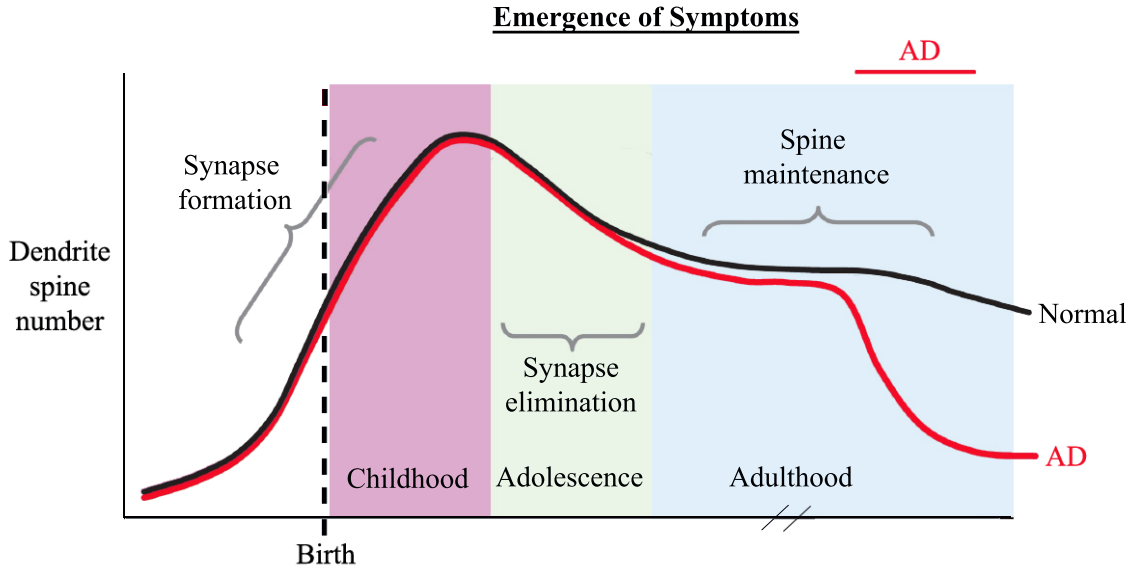

Figure 4.1. Putative lifetime trajectory of dendritic spine number in the in a normal subject and in AD. Bar across the top indicates the emergence period of symptoms and diagnosis. In normal subjects (black line), spine numbers increase before and after birth, then spines are selectively eliminated during childhood and adolescence to adult levels. In AD (red line), spines are rapidly lost in late adulthood, suggesting perturbed spine maintenance mechanisms that may underlie cognitive decline. Figure modified from Penzes et al. (2011).

Some mouse models of AD pathology also display dendritic and synaptic perturbations, similar to findings in human studies. In the Tg2576 mouse model that overexpresses a mutant form of APP (isoform 695) with the Swedish mutation (KM670/671NL), significant decreases in spine density are found in the outer molecular layer of the DG beginning as early as 4 months of age, far before the first detection of plaque deposition at 18 months of age (Jacobsen et al., 2006). Wu et al. (2004) found similar results in 90-day-old PDAPP mice that possess the APP V717F mutation, as they had significant decreases in spine densities of superficial granule cells in the posterior region of the DG. Additionally, examining both of the aforementioned models, (Lanz et al., 2003) found decreases in spine density in the CA1 region of the hippocampus for the Tg2576 and PDAPP mouse lines, at 4.5 and 2 months of age, respectively. Importantly, these reductions have been found to precede overt AD pathology in these models. Given that changes in spine density can occur before significant AD pathology in humans and some mouse models of AD

pathology, the question arises as to what other factors may be contributing to this effect.

NPTX1 and SAP are both present at higher concentrations in the brains of AD patients (Abad et al., 2006; Yasojima et al., 2000) and we have confirmed the distribution of both pentraxins in the hippocampus of such patients. We have also shown that SAP is capable of entering the brain under conditions of BBB breakdown and of interacting with the neuronal pentraxins. Given the results that both SAP and NPTX1 have presynaptic effects on glutamate release in the hippocampus (Benway, Cummings et al., 2017), with the application of either each separately or both together producing an increase in glutamate release probability, the question arises as to whether there are corresponding effects of these pentraxins at the postsynaptic terminal as well.

In parallel to our work, a recent study by Figueiro-Silva et al. (2015) looked at spine numbers in primary cultures of cortical neurons after NPTX1 knockdown and found a significant increase in dendritic protrusions, as well as an increase in the number of excitatory synapses. This finding led to our hypothesis that NPTX1 negatively regulates excitatory synapse formation. Therefore, it is the purpose of our study to determine whether increased levels of NPTX1 and/or SAP will correspondingly decrease synaptic density of hippocampal neurons, and investigate whether the effect, if any, is modulated by SAP, given the evidence provided for their interaction.

In the following results section, all immunohistochemistry and imaging experiments were performed by myself.

Aims

The aim of the following chapter is to investigate whether chronic exposure of NPTX1 and/or SAP elicits changes in the number of spines in primary neurons. This will help to provide a clearer understanding of synaptic alterations that may be occurring over the course of AD, when the concentrations of these proteins are at higher levels in the brain.

Results

Determining influence of SAP and NPTX1 on spine density in primary neurons

To determine the effects of exogenously applied SAP, NPTX1, or both pentraxins together, recombinant human NPTX1 protein and/or purified native SAP protein was added to the medium of hippocampal neurons at concentrations that first evoked significant changes in synaptic transmission (Cummings, Benway et al., 2017). In these experiments, exogenous application was our chosen paradigm in order to avoid any potentially confounding neomorphic effects of overexpression, and to best reflect a potential physiological condition. The following concentrations were added to the media of hipppcampal neurons from P0 GFP-mice at 7 DIV for 7 days: NPTX1 at 60 nM and SAP at 20 nM. Untreated neurons were used as the controls, and the data from 3 independent neuronal preparations for each type of treatment was pooled.

A section of approximately 100μm in length was sampled per dendrite, for two dendrites per neuron. An average of 5-6 neurons was sampled per coverslip, and the average spine density per coverslip (n) was then analyzed. Sample areas were taken from primary, secondary and tertiary dendrites of clearly immunolabeled GFP neurons (Fig. 4.3). Even sampling was performed as much as possible, where dendrite location and image quality allowed. Numbers generated for "all dendrites" are the mean spine densities of each dendrite in a coverslip sampled, regardless of the order.

In order to determine whether NPTX1, SAP or co-application of SAP and NPTX1 can exert postsynaptic effects, spine density of hippocampal neurons was measured after 7 days of treatment, at DIV 14. Importantly, we first established that there were no differences in spine density between dendrites of different orders. Our results confirmed those of previous studies (Duan et al., 2003) showing no difference between primary (emerging from the cell soma), secondary (first branches from a primary), or tertiary (first branches from a secondary) dendrites (Fig. 4.2), and so we initially examined the effects of the pentraxins on overall spine density for all types of dendrites examined.

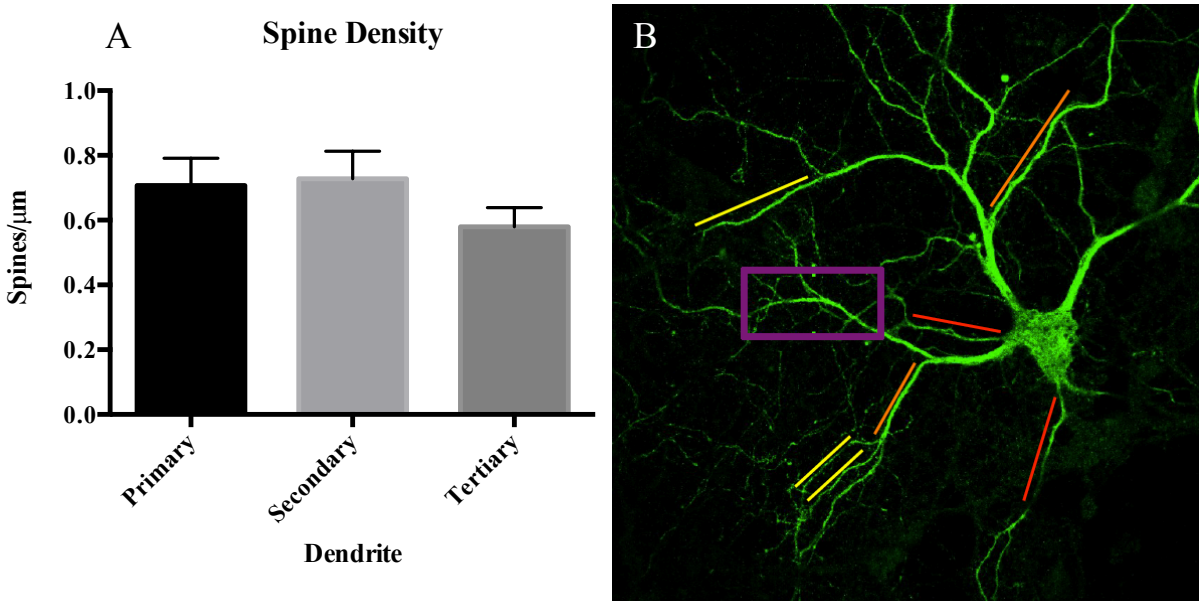

Figure 4.2. No differences in spine density were observed between different order dendrites of hippocampal neurons. One-way ANOVA revealed no difference in the average spine densities between primary (n=5), secondary (n=14) and tertiary (n=10) dendrites. Data presented as mean ± SEM.

In analyzing all hippocampal dendrites, two-way ANOVA revealed a main effect of NPTX1 [$F(1,40)=6.162$, $p=0.0174$], and post hoc tests showed that exogenously applied NPTX1 significantly decreased the overall spine density of GFP neurons after chronic exposure from a mean of 0.67 ± 0.05 spines/µm in the controls to 0.47 ± 0.04 spines/µm in the NPTX1-treated neurons (Figure 4.4 $p=0.0488$).

In examining the effects of SAP treatment alone and the effects of the co-application of SAP and NPTX1 on neurons, no significant changes were found in spine density (Fig. 4.4 The maintenance of dendritic spines with SAP treatment would therefore suggest that, while SAP has similar effects to NPTX1 at the presynaptic terminal on glutamate release probability, it differs from NPTX1 in its influence on spine density and interestingly counteracts the effect of NPTX1.

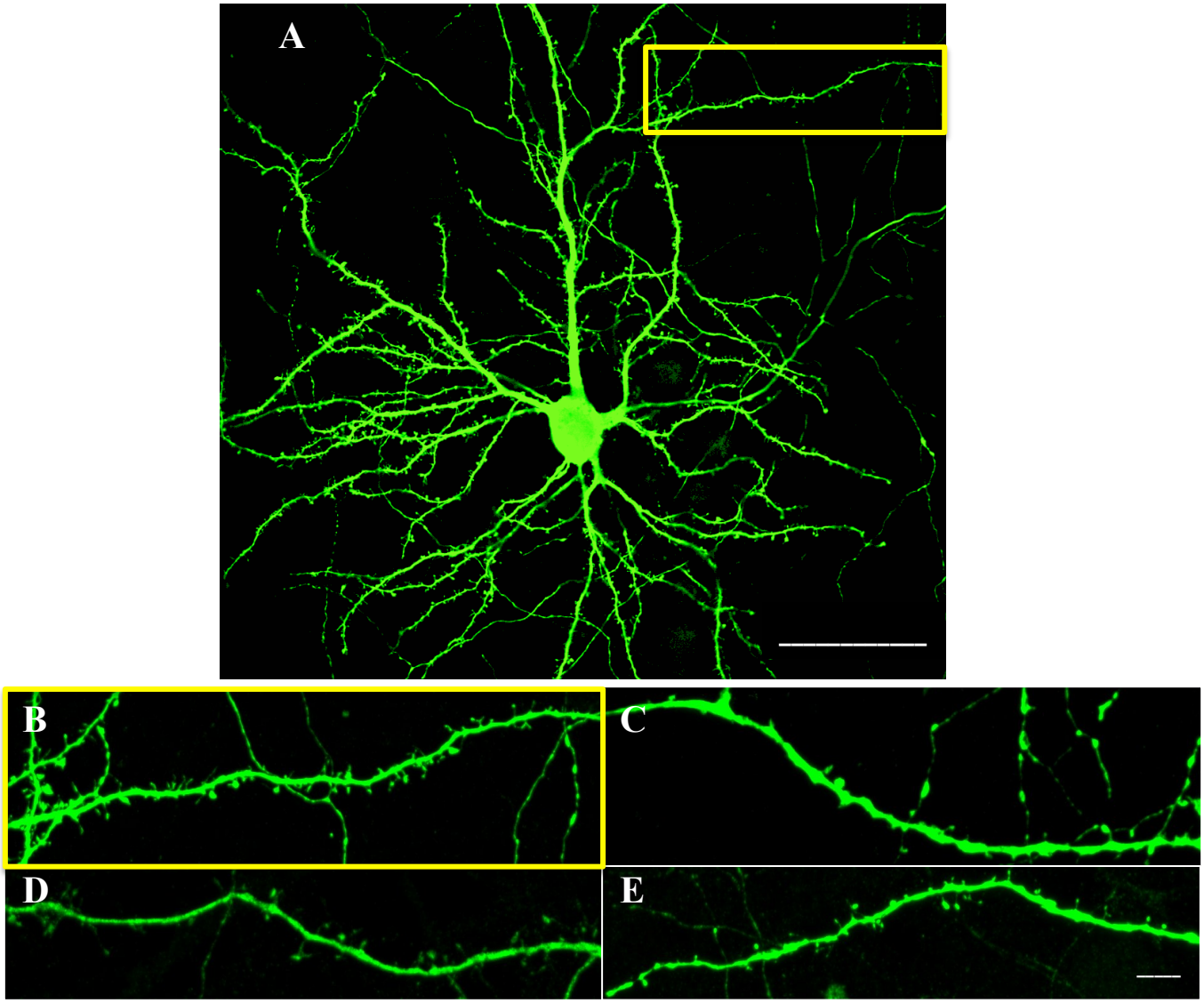

Figure 4.3. Dendrites of hippocampal neurons chronically treated with NPTX1 show a decrease in spine density, but co-application of SAP attenuates this effect. A) Immunolabeling with GFP in representative control GFP-immunolabeled hippocampal neuron from mice expressing GFP. Scale bar 50µm. B) Control tertiary dendrite from insert in A). C) 20 nM SAP-treated tertiary dendrite. D) 60 nM NPTX1-treated tertiary dendrite. E) 20 nM SAP+60 nM NPTX1-treated tertiary dendrite. Scale bar, 10µm.

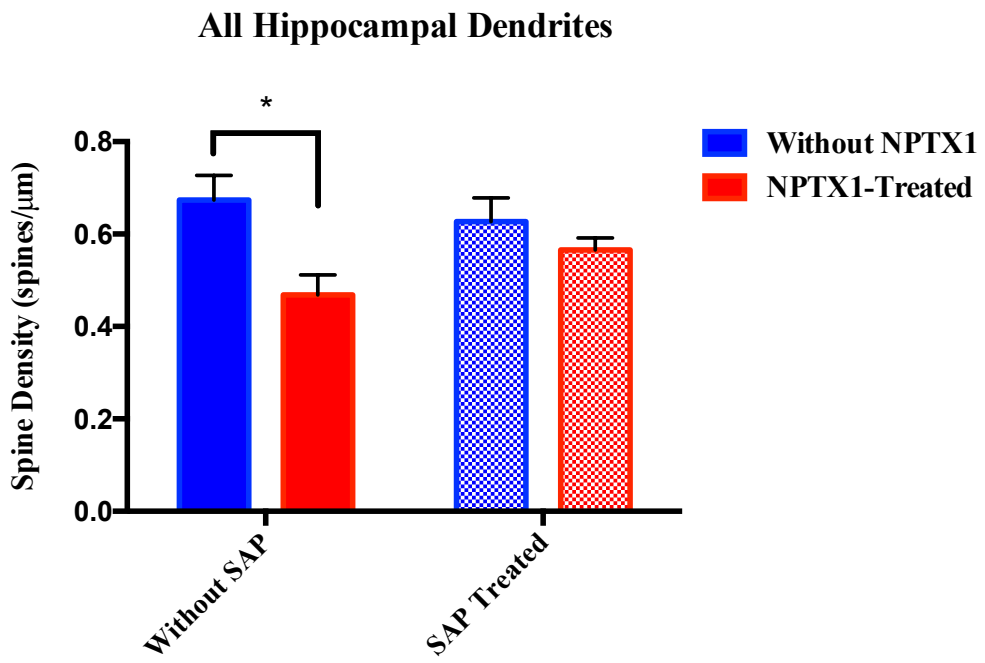

Figure 4.4. Application of NPTX1 at 60nM decreases spine density in hippocampal neurons, while application of SAP at 20nM blocks the effect of NPTX1. Two-way ANOVA with presence/absence of NPTX1 as one factor, and the presence/absence of SAP as the other factor, revealed a significant main effect of NPTX1, with a decrease in spine density for NPTX1-treated neurons (n=9) compared to controls (n=13). SAP treatment alone (n=15) produced no effect, but for neurons treated with SAP+NPTX1 (n=7), the effect of NPTX1 was blocked by SAP. Sidak post hoc multiple comparison of control to NPTX1-treated are indicated *$p<0.05$. Data presented as mean ± SEM.

Interestingly, these results show that SAP blocks the effect of NPTX1 on overall hippocampal spine density, rather than adding to its effect. This lack of an additive effect is reminiscent of the paired-pulse ratio data from Cummings, Benway et al. (2017), providing further evidence that SAP and NPTX1 interact at the synapse and likely act on similar targets. In this case a higher concentration of NPTX1 was used (60 nM) than the sub-maximal concentration (6 nM) used in the aforementioned study, and yet the effect of the addition of SAP not only failed to be additive, but was instead blocked by the same concentration of SAP (20 nM) used in both experiments.

In looking separately at the different types of dendritic projections, two-way ANOVA revealed a significant main effect of NPTX1 [Fig. 4.5 A; $F(1,17)=9.468$, $p=0.0068$] on primary hippocampal dendrites and a significant interaction between NPTX1 and SAP in secondary dendrites [Fig. 4.5 B; $F(1,38)=5.265$, $p=0.0274$]. While the blocking effect of SAP does not appear to be evident in primary dendrites, we still find that there is a lack of any additive effect of the SAP application. In considering why only the primary dendrites are significantly affected by NPTX1, it is important to consider that different order dendrites have different diameters, with primary dendrites being thicker than secondary or tertiary (Lu et al., 2015). It was predicted that tertiary dendrites may be more susceptible to changes in the milieu of the culture system given their tendency to form varicosities and show spine loss (relative to primary and secondary dendrites) under conditions of ischemia (Meller et al., 2008). However, we found the opposite; primary dendrites showed a higher susceptibility to spine loss, which is likely to be explained by the cytonuclear signaling being more efficient in primary dendrites due to their proximity to the cell soma (Li et al., 2015).

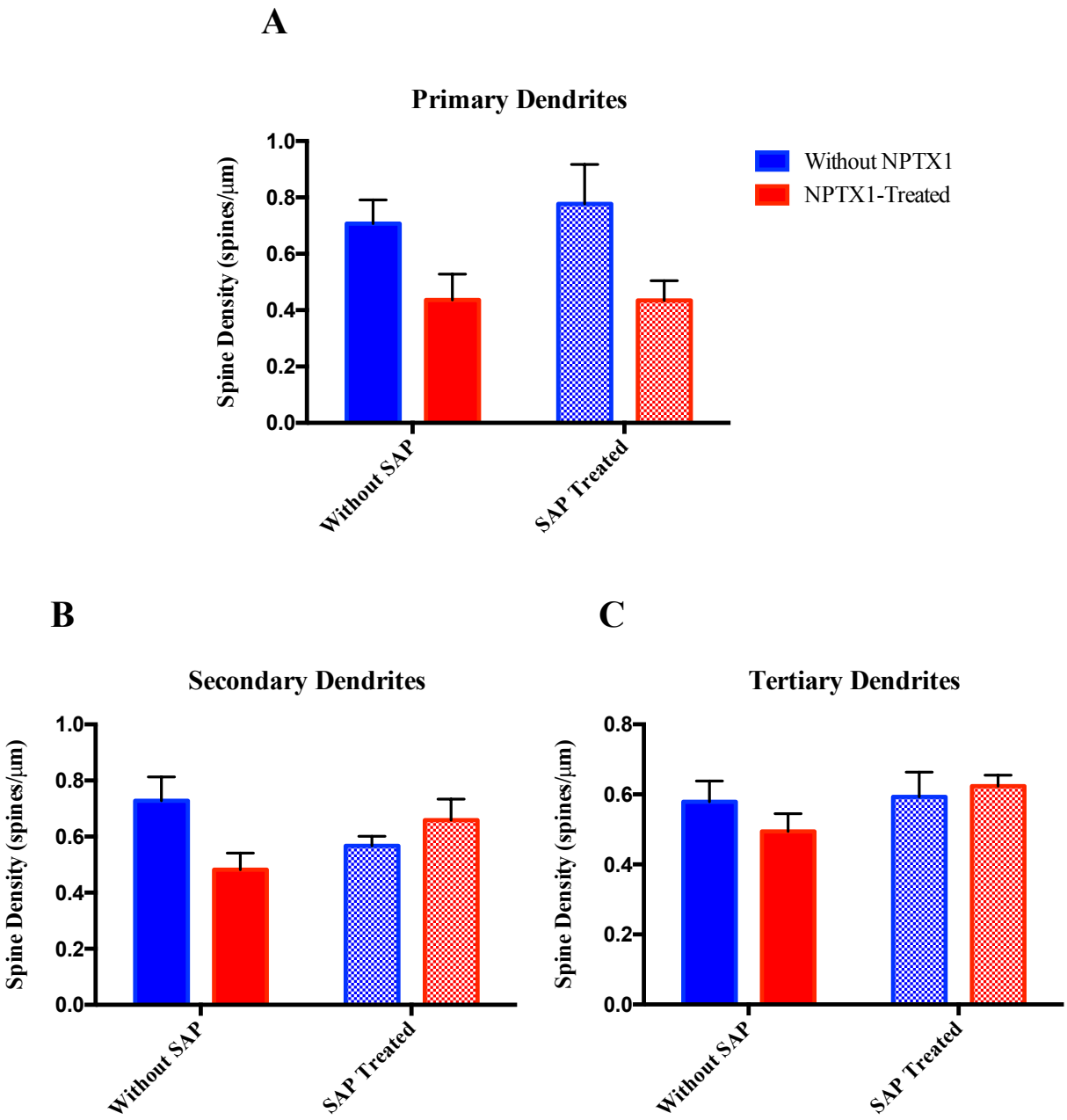

Figure 4.5. Application of NPTX1 at 60nM decreases spines of primary hippocampal dendrites. A) Two-way ANOVA revealed a significant main effect of NPTX1 on primary dendrites ($p=0.007$) with a decrease in spine density for neurons treated with NPTX1; with control (n=5), NPTX1-treated (n=6), SAP-treated (n=5), and NPTX1+SAP-treated (n=5). B) Two-way ANOVA revealed a significant interaction of SAP and NPTX1 on secondary dendrites ($p=0.027$), with control (n=14), NPTX1-treated (n=7), SAP-treated (n=13), and NPTX1+SAP-treated (n=8). C) No significant effects on spine density were found for tertiary dendrites, with control (n=10), NPTX1-treated (n=5), SAP-treated (n=5), and NPTX1+SAP-treated (n=6). Two-way ANOVA performed with presence/absence of NPTX1 as one factor, and the presence/absence of SAP as the other factor. Data presented as mean ± SEM.

Summary

Excitatory synaptic contacts are formed on dendritic spines, and the loss of spines is highly correlated to the loss of synaptic function. Changes in number and shape of dendritic spines are key modulators of synaptic plasticity (Fu and Zuo, 2011). There is substantial evidence that dendritic spine dysfunction is an important factor in the pathogenesis of AD (see review by (Herms and Dorostkar, 2016).

Determining the factors that play a role in the pathological lead-up to AD, and precede the rise in amyloid and tau pathology, are of the utmost importance in further deciphering the mechanisms that produce the devastating effects that occur. Here, we sought to determine whether two proteins found to be upregulated in AD, SAP and NPTX1 (Abad et al., 2006; Yasojima et al., 2000), are capable of exerting an effect on primary hippocampal neurons, independent of the influence of Aβ. This was important in establishing whether these pentraxins are capable of exerting effects that may occur before the onset of Aβ deposition, when it may be possible that the levels of these proteins are rising in the brain.

Previously it has been shown that treatment with both SAP and NPTX1 can elicit presynaptic changes in glutamate release (Cummings, Benway et al., 2017). Interestingly, no additive effect of SAP was found in these experiments when co-applied with NPTX1, suggesting that these two pentraxins do not act independently of each other. Here, our results further support this hypothesis; while there was a significant decrease in spine density in NPTX1-treated hippocampal neurons, the co-application of SAP and NPTX1 similarly did not produce an additive effect.

Taken together, the observations that SAP alone does not influence spine density, but can interfere with the effects of NPTX1 on spine density when co-applied, support the hypothesis that these two pentraxins have different effects at the synapse, but can interact or affect the same targets. It is important to note, however, that previous results in our lab have found that LTP is impaired in SAP transgenic mice (Cummings et al., 2017). Concordantly, Figueiro-Silva et al. (2015) also report enhanced LTP after NPTX1 knockdown. These results therefore suggest that both pentraxins could

be capable of influencing synaptic plasticity, but to different degrees of severity that may depend on length of exposure and concentration.

Chapter 5

The effect of NPTX1 and SAP on microglia in organotypic cultures

Introduction

A major risk factor for the development of neurodegenerative disease is age. Age-dependent changes in microglia morphology are likely to be a key factor in the pathological process (Conde and Streit, 2006). This hypothesis is based upon the evidence that microglia populations in the brain are maintained over a lifetime with the findings that the CNS microglial population is maintained without peripheral, bone marrow-derived influences (Ajami et al., 2007) and that microglial cells have a low proliferative rate (Saijo & Glass, 2011). It therefore follows that this long-lived microglial cell population would be susceptible to the aging effects that occur over the lifespan.

In healthy aged brains, microglia numbers show a significant increase with age, with higher numbers likely accounting for the decrease of the surveillance volume as shown by shorter process lengths, as assessed by comparing mice at different ages (Hefendehl et al., 2014). Aged microglia respond with more severe and longer-lasting pro-inflammatory activation that is associated with neuronal death and lack of functional recovery (Njie et al., 2012; Sierra et al., 2007).

It can therefore been hypothesized that ageing microglia can contribute to the brain's susceptibility of neurodegeneration, whereby they are neuroprotective in healthy brains, but subsequently undergo morphological changes that result in a buildup to the homeostatic tipping point upon which they lose their neuroprotective capacity and instead contribute to pathology. In the case of AD, the progressive buildup of Aβ poses added stress to the ageing microglia (Streit et al., 2009). Although microglia are able to respond to Aβ early in progression (Bamberger et al., 2003; Koenigsknecht and Landreth, 2004; Koenigsknecht-Talboo and Landreth, 2005; Mandrekar et al., 2009), it is likely that the battling of this toxic species over such a prolonged period of time promotes accelerated senescence and, in turn, inhibits Aβ phagocytosis.

The complement cascade is a line of defense that plays a major role in phagocytosis by microglia (Frank and Fries, 1991), as well as immune complex removal and synaptic maturation (Sunyer et al., 1998), and it is known to be activated by the versatile pattern recognition molecule C1q (Gaboriaud et al., 2004). C1q is localized to the synapse and signals phagocytic microglia to facilitate beneficial synapse elimination in early development (Bialas and Stevens, 2013; Schafer et al., 2012; Stevens et al., 2007). However, C1q levels have been found to rise and accumulate at the synapse early in AD, with the synaptic deposition being induced by prefibrillar oligomeric Aβ. C1q expression is upregulated in microglia in pre-plaque brains and is shown to be required for oligomeric Aβ synaptic loss *in vivo*, determined using C1qa KO mice and looking at downstream effects of activation (Hong et al., 2016).

SAP can directly interact with C1q by forming a complex with its collagen-like domain to cause activation (Roumenina et al., 2006). NPTX1 has been found to bind to C1q through a region in the C-terminal (Stevens et al., 2007), but the effects of this binding, if any, have yet to be studied. Given the results that SAP and NPTX1 are associated with amyloid plaques and NFTs in AD brains (Duong et al., 1989; Tennent et al., 1995)Cummings, Benway et al., 2017), and that levels of both pentraxins are at higher concentrations in the AD brain (Duong et al., 1997) (Abad et al., 2006), the question is raised whether this may correspondingly lead to higher levels of microglial activation, as both can interact with C1q. It is therefore important to consider whether such activation may be part of the process leading up to the tipping point for microglia in AD.

While the role of the peripheral pentraxins in the immune response has been well established, it is unclear whether the neuronal pentraxins play such a significant role in this response as well. Neuronal pentraxins are known to be involved in synaptic plasticity, synapse formation and synaptic clearance, which are all influenced by microglia (Osera et al., 2012). (Miskimon et al., 2014) recently provided some evidence for NPTX2 in immune function using NPTX2 KO mice by examining the microglial response to sciatic nerve transection, an injury known to result in increased glial activation (He et al., 1997). In this case, NPTX2 deletion resulted in a significant increase in microglial activation. From this result it would suggest that NPTX2 somehow regulates the immune response, though how it is able to do so requires

further investigation. Therefore, it may be the case that the other neuronal pentraxins are capable of influencing the immune response as well. In particular, given its high degree of structural similarity to NPTX2, NPTX1 may also be capable of somehow influencing the immune response. This becomes an important point to consider provided the evidence that NPTX1 co-localizes with the pathological amyloid and tau proteins in AD (Abad et al., 2006), and the role of the immune system in the disease progression.

To test whether chronic exposure of SAP and NPTX1 can influence the regulation of microglia numbers or activation at levels observed to cause pre- and postsynaptic effects, organotypic cultures were used to provide a model that preserves the neuronal circuits and cellular architecture seen *in vivo* including astrocytes and microglia - an important consideration in the examination of proteins initially studied with respect to synapses, such as the pentraxins.

In the following results section, all immunohistochemistry and imaging experiments were performed by myself.

Aims

This chapter investigates the effects of SAP and NPTX1 in the brain in relation to conditions present in AD using a 3D *ex vivo* model that preserves both cytoarchitecture and cell interactions that form the mouse hippocampus. Specifically, microglia numbers and rates of activation were measured to determine whether exposure to levels of pentraxins that are known to affect synaptic transmission will also elicit a response from the immune system.

Results

Hippocampal organotypic slices show a high proportion of activated microglia

The age at which to observe microglial activity in organotypic slices was chosen to be at DIV 20-22, as this allowed for an appropriate amount of time for slices to recover (based on previous observations from our lab) and allowed for an appropriate amount of time for chronic treatment with the pentraxins. Electrophysiological recordings previously discussed (Benway, Cummings et al., 2017) were also performed at this age, which us to compare and characterize these slices at the same timepoint.

The proportion of activated microglia in the untreated control slices was 57.5 ± 0.02% (mean ± SEM). This result is consistent with findings from (Gerlach et al., 2016), who also examined microglia activation using double-immunolabeling of Iba1 and CD68 in hippocampal organotypic slices. Their findings revealed rapid and long-lasting activation microglial activation through to DIV 7 using CD68 immunoreactivity, but also confirmed this extended activation state by examining gene expression profiles of two markers of microglial activation MHCIIAB and IL-1B (Graeber et al., 2011; Kettenmann et al., 2011) up through DIV 15. Gerlach et al. (2016) also provide profiles of microgliosis in organotypic slices over the course of 15 DIV, where spikes in activation are reported in the first 3 days, followed by a plateau and then steady but gradual increase in activation levels over time. Additionally, previous results from our lab show no significant changes in number of microglia or in activation levels between DIV 7 and DIV 21, confirming the minimal, if any, increase in activation levels or numbers of microglia that occur following the first week of adjustment in culture (Nair MSci Dissertation, 2015).

Effects of SAP, NPTX1 and SAP+NPTX1 application on microglia in organotypic slice cultures

In order to determine whether SAP and NPTX1 have effects either separately or together on microglia in the hippocampus, organotypic hippocampal slices were exposed to human pentraxin protein levels that first evoked changes in release probability as found in Cummings, Benway et al. (2017). Given these concentrations

produced both presynaptic and postsynaptic changes, the question is then raised about other effects the pentraxins may be having on other cell types that influence neural function.

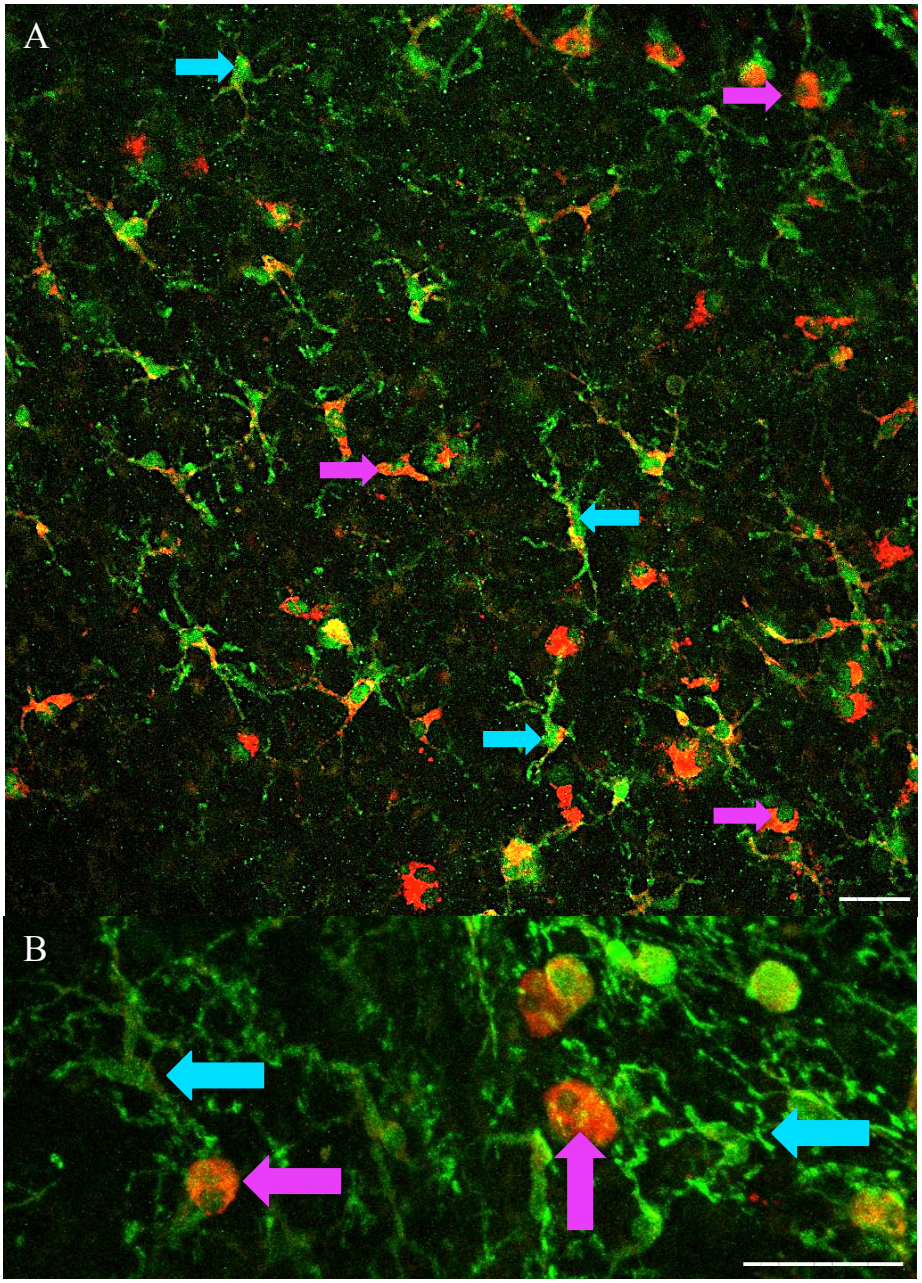

Figure 5.1. **Representative image of microglia in the hippocampus of an organotypic slice.** A) Microglia stained with Iba1 (green) and CD68 (red) in the CA1 of WT mouse organotypic slices (DIV 21) showing representative images of resting microglia (blue arrows) and activated microglia (purple arrows). B) Higher power image of representative resting microglia (blue arrows) and active microglia (purple arrows), where characteristics are clearly shown. Scale bars, 20µm.

Microglia were characterized based upon both their morphology and immunolabeling with Iba1 and CD68 (Fig. 5.1). Inactivated microglia were defined as Iba1-positive cells with a resting phenotype of highly ramified processes and a small somata, and each microglia occupying a small distinct area (Boche et al., 2013). Microglia were defined as "resting" even with exhibiting some CD68-positive staining, based upon the criteria that CD68 staining was restricted to the periphery of the cell body, the cell body was not increased in size, and the microglia still possessing normal projections from its cell body. Activated microglia were defined as Iba1- and CD68-positive cells with an amoeboid phenotype of a larger, swollen cell body of approximately 2-3 times larger than resting microglia, with clearly rescinded projections from the soma. Morphological features based upon a physiological review of microglia morphology, as described in Kettenmann et al. (2011).

As performed previously to investigate the chronic effects of pentraxins at the synapse, native purified human SAP 20 nM and/or recombinant human NPTX1 60 nM was applied to the media of organotypic slices for a period of 7 days, beginning at DIV 13-15. Untreated organotypic slices of the same age were used as the controls, and the data from 3 independent experiments for each type of treatment were pooled. The CA1 and the DG were the two regions of the hippocampus examined, as they show high levels of vulnerability to pathology in human AD patients as well as in mouse models of AD.

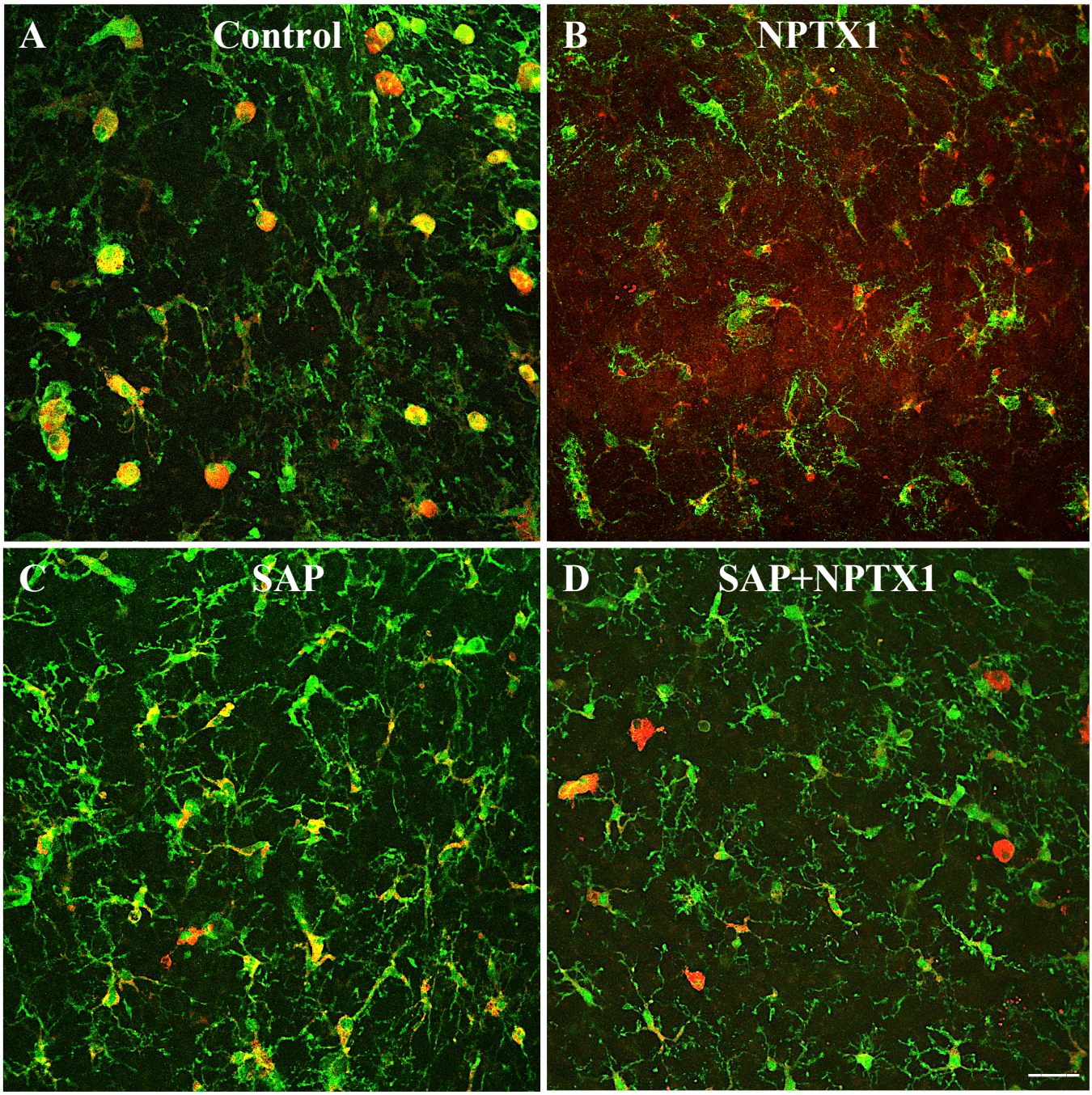

Figure 5.2. Application of NPTX1 decreases number of microglia and co-application of SAP and NPTX1 suppresses activation of microglia in DIV 20-22 organotypic slices. Immunolabeling with Iba1 (green) and CD68 (red) in: A) Control CA1; B) 60 nM NPTX1-treated CA1; C) 20 nM SAP-treated CA1; and D) 60 nM NPTX1+ 20 nM SAP-treated DG. Scale bar, 20μm.

Effect of SAP and NPTX1 on microglia numbers

In organotypic cultures treated with NPTX1 (60nM; Fig. 5.2 B), SAP (20nM; Fig. 5.2 C) or both pentraxins (Fig. 5.2 D), two-way ANOVA revealed a significant interaction between SAP and NPTX1 treatment [Fig. 5.3 A; $F(1,70)=16.24$, $p=0.0001$], and significant main effects of both SAP [$F(1,70)=16.92$, $p=0.0001$] and NPTX1 [$F(1,70)=18.10$, $p=0.0001$]. Post hoc tests found that microglia numbers in the hippocampus significantly decreased after the chronic 7-day treatment of NPTX1 ($p<0.0001$). However, this effect of NPTX1 was blocked by SAP, as hippocampal slices treated with both pentraxins showed no change compared to those of the control, and the co-treated slices showed a significantly higher number of microglia than the NPTX1-treated slices ($p<0.0001$).

In the CA1 (Fig. 5.3 B), two-way ANOVA showed a strong trend toward significance of the interaction between SAP and NPTX1 ($p=0.0585$), and main effects of SAP treatment [$F(1,59)=10.89$, $p=0.0016$] and NPTX1 treatment [$F(1,59)=13.39$, $p=0.0005$]. Post hoc tests again revealed NPTX1 treatment significantly decreased the number of microglia ($p=0.0002$), which SAP again blocked ($p=0.0041$).

In the DG (Fig. 5.3 C), two-way ANOVA revealed a significant interaction between SAP and NPTX1 [$F(1,62)=22.53$, $p<0.0001$], and main effects of SAP treatment [$F(1,62)=20.58$, $p<0.0001$] and NPTX1 treatment [$F(1,62)=13.22$, $p=0.0006$]. Post hoc tests again revealed NPTX1 treatment significantly decreased the number of microglia ($p<0.0001$), which SAP again blocked ($p<0.0001$).

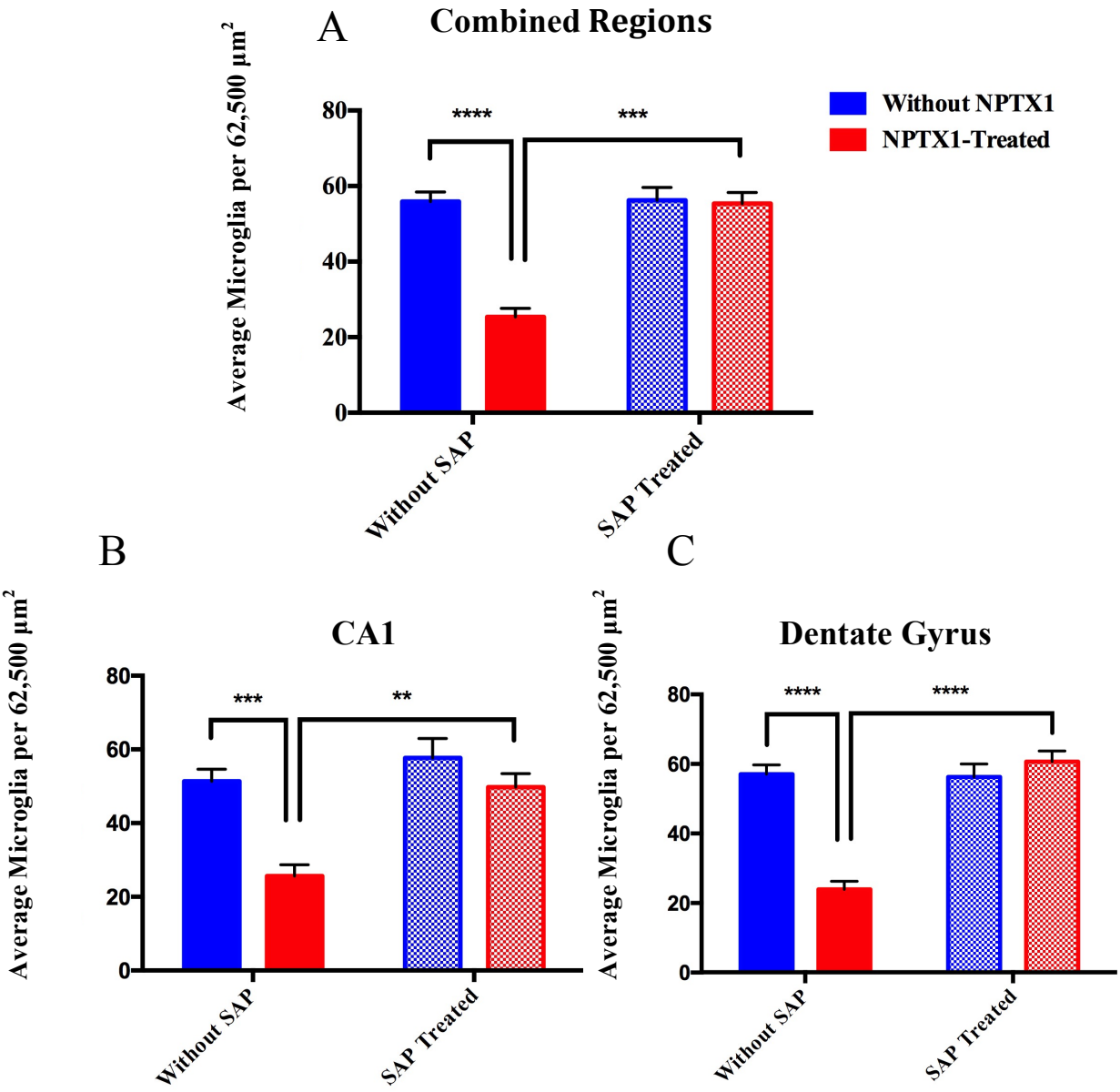

Figure 5.3. Application of NPTX1 at 60nM decreases number of microglia in hippocampal organotypic slices, while application of SAP at 20nM has no effect alone but blocks the effect of NPTX1. A) Two-way ANOVA revealed an interaction between SAP and NPTX1 treatment (p=0.0001), with total (CA1 + DG) microglia numbers in the hippocampus decreased for NPTX1-treated slices (n=10) compared to controls (n=39), but increased in SAP+NPTX1 (n=16) compared to only NPTX1-treated. SAP treatment alone (n=9) produced no effect. B) In the CA1, two-way ANOVA revealed a strong trend for interaction between SAP and NPTX1 treatment (p=0.0585), with microglia numbers decreased for NPTX1-treated slices (n=10) compared to controls (n=32), but increased in SAP+NPTX1 (n=13) compared to only NPTX1-treated. SAP treatment alone (n=8) produced no effect. C) In the DG, Two-way ANOVA revealed an interaction between SAP and NPTX1 treatment (p<0.0001), with microglia numbers decreased for NPTX1-treated slices (n=10) compared to controls (n=35), but increased in SAP+NPTX1 (n=14) compared to only NPTX1-treated. SAP treatment alone (n=7) produced no effect. Sidak post hoc comparison to control and to NPTX1-treated are indicated **p<0.01; ***p<0.001; **** p<0.0001. Data presented as mean ± SEM.

Effect of SAP and NPTX1 on microglia activation

In looking at microglial activation levels in organotypic cultures treated with NPTX1 and SAP (Fig. 5.4 A), two-way ANOVA revealed a significant interaction between SAP and NPTX1 treatment [$F(1,70)=4.799$, $p=0.0318$], and a significant main effect of NPTX1 [$F(1,70)=24.79$, $p<0.0001$]. Post hoc tests found that the proportion of activated microglia numbers in the hippocampus significantly decreased after the chronic 7-day treatment of both SAP and NPTX1 ($p<0.0001$), though no effects found with the application of either pentraxin on its own.

In the CA1 (Fig. 5.4 B), two-way ANOVA revealed a significant interaction between SAP and NPTX1 [$F(1,59)=7.832$, $p=0.0069$], and a main effect of NPTX1 treatment [$F(1,59)=8.979$, $p=0.0040$]. Post hoc tests again revealed a decrease in the proportion of activated microglia numbers after the treatment of both SAP and NPTX1 ($p=0.0020$), and no effect of either pentraxin on its own.

In the DG (Fig. 5.4 C), two-way ANOVA revealed a significant interaction between SAP and NPTX1 [$F(1,63)=4.557$, $p=0.0367$], and a main effect of NPTX1 treatment [$F(1,63)=6.950$, $p=0.0105$]. Post hoc tests showed a significant decrease in the proportion of activated microglia with co-application of both pentraxins compared to only SAP-treated slices ($p=0.0221$).

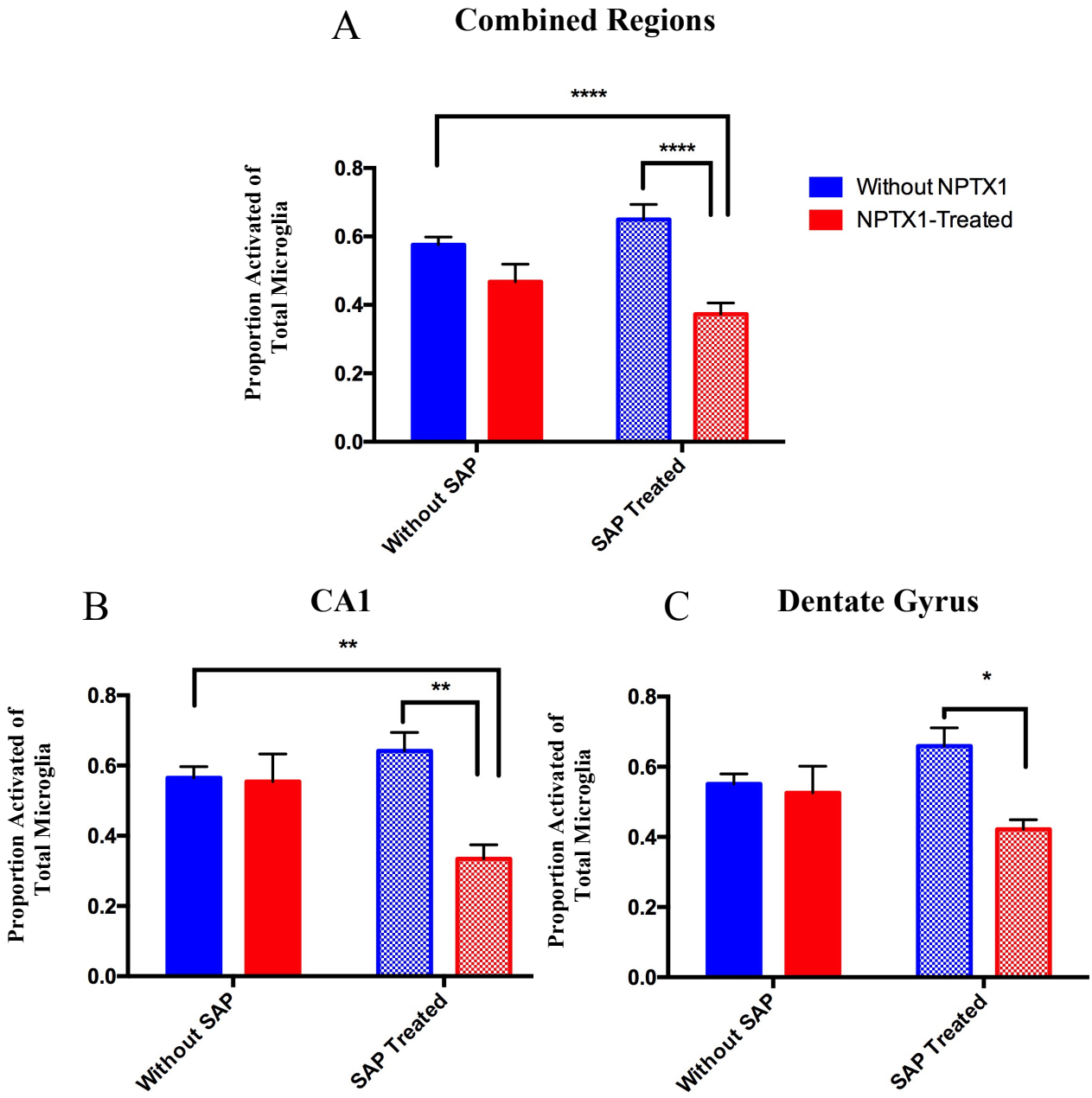

Figure 5.4. Co-application of NPTX1 at 60nM and SAP at 20nM decreases the proportion of activated microglia. A) Two-way ANOVA revealed an interaction between SAP and NPTX1 treatment ($p=0.0318$), with co-application of SAP+NPTX1 (n=17) decreasing the proportion of total (CA1+DG) activated microglia in the hippocampus compared to controls (n=38) and SAP-treated (n=9). NPTX1-treatment alone (n=10) produced no effect. B) In the CA1, two-way ANOVA revealed an interaction between SAP and NPTX1 treatment ($p=0.0069$), with co-application of SAP+NPTX1 (n=13) decreasing the proportion of activated microglia compared to controls (n=32) and SAP-treated (n=8). NPTX1-treatment alone (n=10) produced no effect. C) In the DG, two-way ANOVA revealed an interaction between SAP and NPTX1 treatment ($p=0.0367$), with co-application of SAP+NPTX1 (n=14) decreasing the proportion of activated microglia compared to SAP-treatment alone (n=7), but not controls (n=36). NPTX1-treatment alone (n=10) produced no effect. Sidak post hoc comparison to control and to NPTX1-treated are indicated *$p<0.05$; **$p<0.01$; ***$p<0.001$; **** $p<0.0001$. Data presented as mean ± SEM.

Summary

The overall aim of the current study is to investigate the effects of the peripheral pentraxin SAP and the neuronal pentraxin NPTX1 in the brain at higher levels, considering the evidence for increased concentrations of both proteins found in AD brains (Abad et al., 2006; Yasojima et al., 2000). We have used organotypic cultures in our study to examine the effect of SAP and NPTX1 on microglia in a region of the brain where both pentraxins have been shown to localize around amyloid plaques in brains of AD patients. The results of this chapter show that these pentraxins are capable of affecting microglia number and activation, and demonstrate that there is an interaction between both that influences the immune response.

In the CA1 and DG regions of the hippocampus where, earlier in this thesis, we confirmed both pentraxins are distributed (Fig. 3.5), NPTX1 has a significant effect in decreasing the number of microglia (Fig. 5.3). Interestingly, this effect is completely blocked by SAP, with co-application of both pentraxins bringing microglia numbers back to those in the controls. However, SAP treatment alone has no effect on total numbers of microglia. Increases in NPTX1 protein levels and expression have been shown to lead to apoptotic neuronal death (Abad et al., 2006; DeGregorio-Rocasolano et al., 2001), and these results now indicate that NPTX1 may also be involved in the process of cell death in microglia. This blocking effect of SAP on NPTX1 toxicity can be supported by previous findings from Cummings, Benway et al. (2017), where co-application of the two pentraxins in organotypic slices produced no additive effect in paired-pulse ratios, suggesting that they are competing for the same target with SAP blocking the effect.

While activation levels of microglia were unaffected by treatment of either pentraxin alone, the co-application of SAP and NPTX1 produced a significant decrease in the proportion of activated microglia in both regions of the hippocampus (Fig. 5.4). This further confirms the conclusion from Cummings, Benway et al. (2017) that the two pentraxins are not acting independently, but instead interacting either together or on the same targets when applied together.

Overall, these results suggest that SAP, upon entry into the brain, can interact with endogenous NPTX1 to alter the role that NPTX1 plays in affecting microglia number and activation. While we hypothesized that chronic SAP and NPTX1 treatment would cause increased microglial activation levels, this was not the case. Treatment with SAP or NPTX1 alone did not cause an increase in activation of microglia, but, interestingly, their co-application caused a decrease in activation levels.

Chapter 6

Mice expressing human SAP demonstrate no spatial working memory impairment

Introduction

In AD, it is widely accepted that the degree of synaptic loss provides a much stronger indication of cognitive decline than does the extent of Aβ plaque burden (Scheff et al., 2006; Terry et al., 1991). When considering the data from Cummings, Benway et al. (2017), it is clear that chronic exposure to SAP modulates synaptic transmission, as electrophysiological recordings from both organotypic brain slices with exogenous application of SAP and acute brain slices of TgSAP mice demonstrated increases in glutamate release probability. Further, the latter result also revealed that sufficient SAP can enter the brain of the mouse to cause this effect, even when only expressed at normal human levels in the liver (Cummings et al., 2017; Iwanaga et al., 1989). With these results clearly demonstrating that SAP can influence central transmission and synaptic plasticity, the question arises whether the effects that SAP produces at the synapses will translate to cognitive effects.

To examine this question in relation to AD, we used the TASTPM mouse model. Alterations in hippocampal synaptic paired pulse facilitations have been found in this model at very young ages (2 months), before detectable deposition of amyloid plaques (Cummings et al., 2015). However, in previous behavioral tests, cognitive performance of TASTPM mice up to the age of 9 months showed no impairment in hippocampus-specific memory tasks, using the same measures employed in the current study (Benway MSc Dissertation, 2011). However, an age of 9 months may have been too young for any cognitive changes to occur, given the brain's resilience and capability of sustaining normal cognitive functioning even in the presence of pathology up to, in many cases, well advanced ages (Negash et al., 2013). Therefore, an older age of 13-14 months with increased pathology was chosen as the time point at which to compare any difference in cognitive performance between genotypes.

It has been shown that human SAP promotes the aggregation of amyloid *in vitro* at physiological concentrations of SAP at 0.01 μM and $A\beta_{1\text{-}40}$ at a concentration of 1 nM

(Hamazaki, 1995). Given $A\beta_{1-40}$ is found in human plasma and cerebrospinal fluid at concentrations around 0.6 nM (Seubert et al., 1992), the observation of the effects with using 1 nM $A\beta_{1-40}$ with SAP are of physiological relevance. Further, it has been shown that this binding of SAP to Aβ fibrils prevents their digestion, with *in vitro* experiments showing two aggressive proteinases (human neutrophil cathepsin G and extent elastase) and phagocytic cells to be inhibited in their degradation of fibrils by bound SAP blocking their actions (Tennent et al., 1995).

In humans, SAP in the periphery binds to and stabilizes amyloid fibrils (Kolstoe et al., 2009). The dissociation of SAP from these peripheral fibrils has been show to result in their partial clearance from the plasma, and may aid in the symptoms of amyloidosis (Pepys et al., 2002). Given the role SAP in stabilizing amyloid deposits in the periphery, it led to the suggestion that it may do the same with amyloid plaques in the brains of AD patients, particularly with the significantly higher levels of SAP reported in the hippocampus and cortex of AD patients compared to controls (Crawford et al., 2012). Additionally, SAP knockout mice with casein-induced amyloidosis showed a significantly decreased and delayed amyloid deposit load in the body as compared to WT mice with induced amyloidosis, but it is important to note that this study reflects amyloid deposits in the body, and not in the brain (Botto et al., 1997).

The aim of the present study is to focus on the peripheral pentraxin SAP after having established in Chapter 3 that it can enter the brain, deposit on plaques, and likely interact with the neuronal pentraxins at the synapse. To accomplish this, we will examine the effect of human SAP in the $TgSAP_{L38}$ and 3xTg ($TgSAP_{L38}$/TASTPM) mouse models in an attempt to determine whether there are any behavioral effects of SAP or the amyloid mutations and, if so, whether these changes are additive or interact. With the finding that human SAP expressed in the liver can enter the brains of mice (Fig. 3.6), it was hypothesized that human SAP could bind to the plaques in the brains of the TASTPM mouse and thus result in enhanced plaque pathology that may then contribute to cognitive impairment. This was also proposed in light of the finding by Cacucci et al., (2008) of a correlation between plaque load and cognitive impairment; while many studies find no such correlation, it is important to note that

this study examined the hippocampal plaque load and neocortex plaque load separately, and only found this correlation only with plaques in the hippocampus.

T-maze forced alternation task

Our present investigation has thus far concentrated on examining the effects of SAP and NPTX1 in the hippocampus, in light of findings that these proteins are localized in this area and at elevated levels in patients with AD (Abad et al., 2006; Crawford et al., 2012). Therefore, the behavioral task chosen for testing was one that shows high sensitivity to hippocampal dysfunction (Deacon and Rawlins, 2006; Dudchenko, 2001).

The T-maze forced alternation task tests the spatial working memory of the mouse, as it must remember what arm of the maze it has previously visited and alter its choice on the second run in order to receive a food reward. Mice employ the use of distal cues to determine which arm to next visit, and this type of short-term memory is utilized within the one trial, and once used, is typically forgotten (Dudchenko, 2004). Rodents tend to naturally alter their choice of goal arm, which is an instinctive behavior that is necessary for location of food, water, shelter and mates within their natural habitat. As this tendency is encouraged during the habituation period using the food reward, it is often found that even prior to training, WT mice will show a ~75% correct response rate in the task, with this increasing to >90% correct following the training period (Cacucci et al., 2008; Deacon and Rawlins, 2006).

The cognitive demand of the T-maze can be increased by adding delays between the sample and choice runs. To test for subtle memory deficits, we used delays of 2.5, 5 and 10 minutes for the test phase of the task. Also, to prevent demotivation, trials using longer delays were always interspersed pseudorandomly with trials of the shortest delay period.

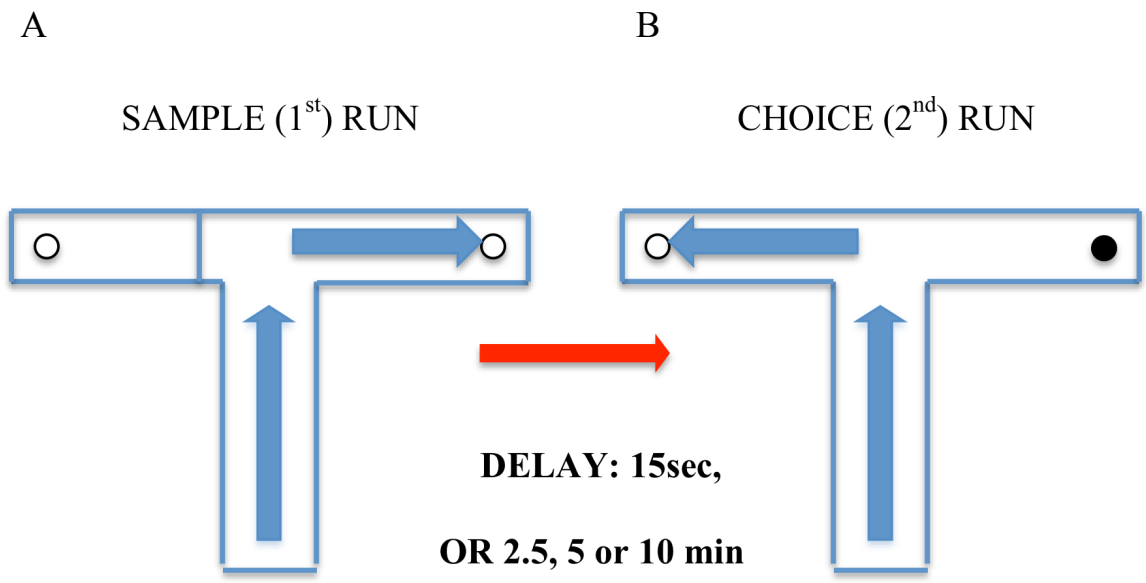

Figure 6.1. Schematic of forced-choice alternation T-maze task. Mice first ran the A) sample run with one blocked arm followed by the B) choice run with both arms open and reward in arm not previously visited. One drop of reward was placed on top of a barrier covering a small cup full of reward, designed to prevent the use of olfactory cues. Maze was cleaned with 70% EtOH between trials.

Locomotor and Anxiety testing

To further investigate cognitive function in our novel TgSAP$_{L38}$ mouse models, mice were also evaluated in terms of locomotor activity and anxiety levels. To accomplish this, mice were tested in the open field and the elevated plus maze (EPM). Both tests are based on the approach-avoidance conflict, which is established by the contradiction of the innate exploratory behavior of a mouse, with the aversive properties of a large open space or brightly lit environment (Ohl, 2005).

Open field

The open field test consists simply of an inescapable open arena, and has been shown to be successful for use on mice (Prut and Belzung, 2003). With its ability to quickly measure many clearly defined behaviors, it is one of most common tests for locomotor activity, exploration and anxiety-related behaviors (ibid). For the purposes of our study, the open field was used to test two main parameters: 1) the proportion of time spent in center as an indicator of anxiety, and 2) total distance travelled as a measure of overall exploratory/locomotor activity.

Elevated plus maze (1 trial only test)

The EPM is another simple method for assessing anxiety responses of rodents (Pellow et al., 1985). The task consists of a platform that includes an elevated open alley that produces a strong approach–avoidance conflict, and a dark enclosed alley, which does not. Assessment of anxiety behavior of rodents is evaluated by using the ratio of time spent on the open arms to the time spent on the closed arms. The benefit to using this assay over ones that present noxious stimuli (i.e. foot shock), is that it relies on the preference of the rodents for dark, enclosed spaces (approach) and their fear of open spaces and heights (avoidance), without eliciting a conditioned response (ibid).

In the following results section, all behavioral experiments were performed by myself.

Aims

Here we aim to evaluate the cognitive performance of mice with the transgene for human SAP and determine whether SAP can influence the phenotype of mice with AD pathology to produce effects on memory.

Results

Hippocampal-dependent memory

No deficit in either TASTPM or TgSAP$_{L38}$ mice at 13-14 months of age

In the current study, mice between the ages of 13-14 months were tested in the forced-choice T-maze. The following four genotypes of mice were tested over three mixed cohorts: WT, TgSAP$_{L38}$, TASTPM and 3xTg (TgSAP$_{L38}$+TASTPM). Additionally, tests of motor function and anxiety were conducted in order to assess for confounding factors. Given the higher levels of anxiety reported in AD patients (Horning et al., 2014), these control measures were particularly relevant here.

The protocol used within the present study for testing within the T-maze was adapted from that previously published for use on mice (Cacucci et al., 2008). However, because previous results showed no memory impairment with advanced plaque deposition in the TASTPM mice (Benway MSc Dissertation 2011), the current study modified the protocol from Cacucci et al. (2008) by increasing the delay time between sample and choice runs in order to increase cognitive demand in an attempt to best discern any memory impairment.

For the T-maze task, correct responses were pooled into 2-day blocks for analysis. Two-way ANOVA of choice response over the 5 training blocks revealed no significant effect of interaction but main effects of block [$F(4,156)=5.68$, $p=0.0003$], genotype [$F(3,39)=3.383$, $p=0.028$], and subjects (matching) [$F(39,156)=5.749$, $p<0.0001$]. Post hoc analysis revealed that the TgSAP$_{L38}$ and TASTPM mice fail to show a significant improvement across the blocks as compared to the WT and 3xTg (Fig. 6.2), as they unexpectedly began training with a high percentage (>80%) of correct choices, which therefore left little room for improvement.

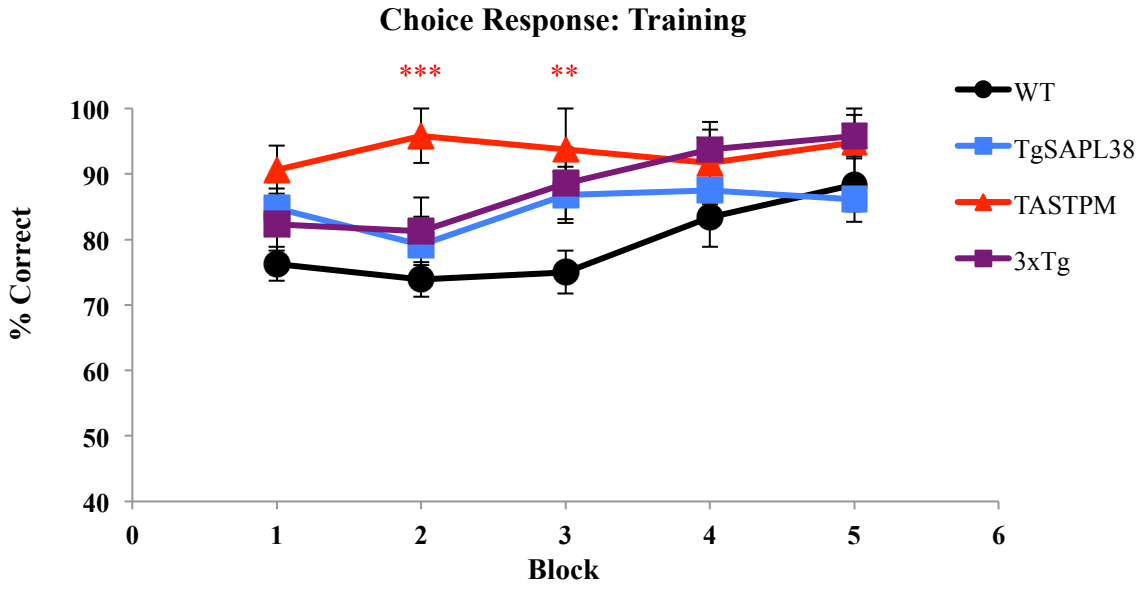

Figure 6.2. TASTPM and TgSAP$_{L38}$ mice fail to show improvement in T-maze task. Percent correct for choice runs of each genotype during the blocked training period for WT (n=15), TgSAP$_{L38}$ (n=12), TASTPM (n=8) and 3xTg (n=8). Each block is 2 pooled days of training, with 6 trials per mouse per day. Two-way ANOVA revealed main effects of block and genotype. Sidak's post hoc multiple comparison of control to TASTPM genotype are indicated **p<0.01, ***p<0.001. Data presented as mean ± SEM.

In the analysis of response times (Fig. 6.3), two-way ANOVA did not reveal a significant interaction, but there were main effects of block [$F(4,156)=22.17$, $p<0.0001$], genotype [$F(3,39)=3.344$, $p=0.029$] and subjects (matching) [$F(39,156)=7.149$, $p<0.0001$]. Post hoc tests found that all genotypes were able to improve their performance time over the course of the five blocks (WT: $p<0.0001$; TgSAP$_{L38}$: $p<0.001$; TASTPM: $p<0.001$; 3xTg: $p<0.0001$). These tests also showed that the 3xTg mice took a significantly longer time to respond at the beginning of training, during block 2 ($p=0.0045$). The increased amount of time required for the 3xTg mice to make a choice may possibly indicate a higher level of anxiety in this mouse model. To determine whether higher levels of anxiety might account for this difference, subsequent anxiety tests were performed.

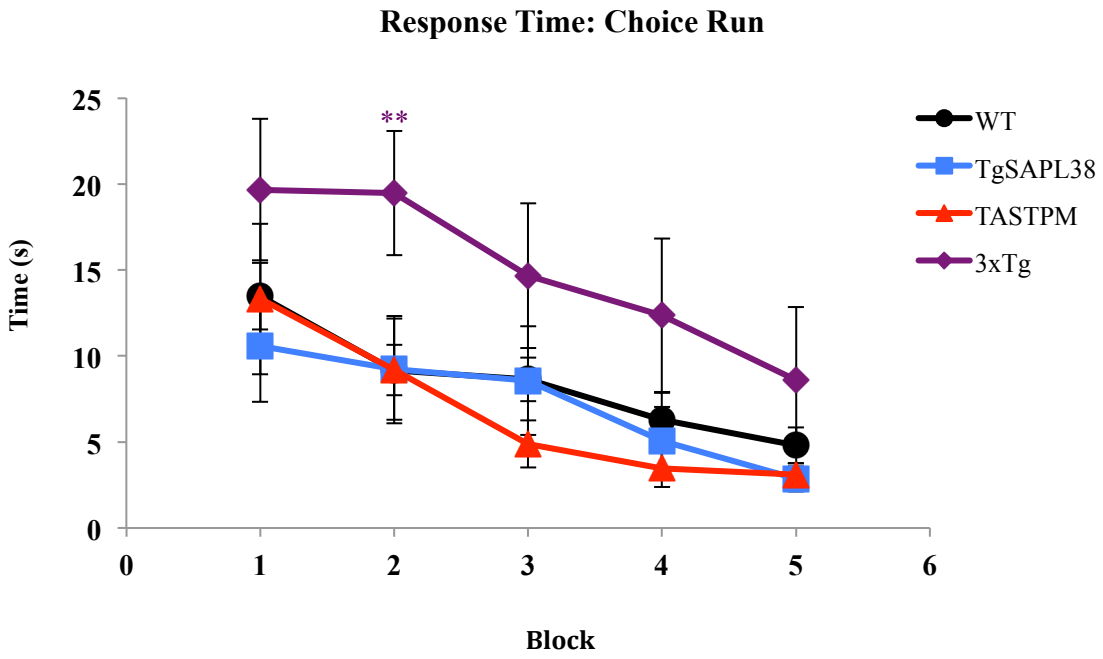

Figure 6.3. **3xTg mice require more time to make choice response in T-maze**. Response times for choice runs during blocked training period for WT (n=15), $TgSAP_{L38}$ (n=12), TASTPM (n=8) and 3xTg (n=8). Two-way ANOVA revealed main effects of block, genotype, and subjects (matching). Sidak's post hoc multiple comparison of control to 3xTg genotype are indicated **p<0.01. Data presented as mean ± SEM.

To further increase cognitive demand, "long" delay tests of 2.5, 5 and 10 minutes were introduced between sample and choice runs in the T-maze task. In looking at the performance in this long delay version, two-way ANOVA revealed significant main effects of genotype [$F(3,117)=4.256$, $p=0.0068$] and delay [$F(2,117)=5.094$, $p=0.0076$], though no significant effect of interaction was found.

Post hoc tests revealed that the 3xTg mice performed significantly better than the WT mice with the 2.5 min delay test ($p=0.0191$). Interestingly, no differences were found between genotypes at either the 5 or 10-minute delays (Fig. 6.4). Overall, these delay results demonstrate that mice with the TASTPM AD transgenes, a human SAP transgene, or both, do not exhibit spatial working deficits at 13-14 months of age.

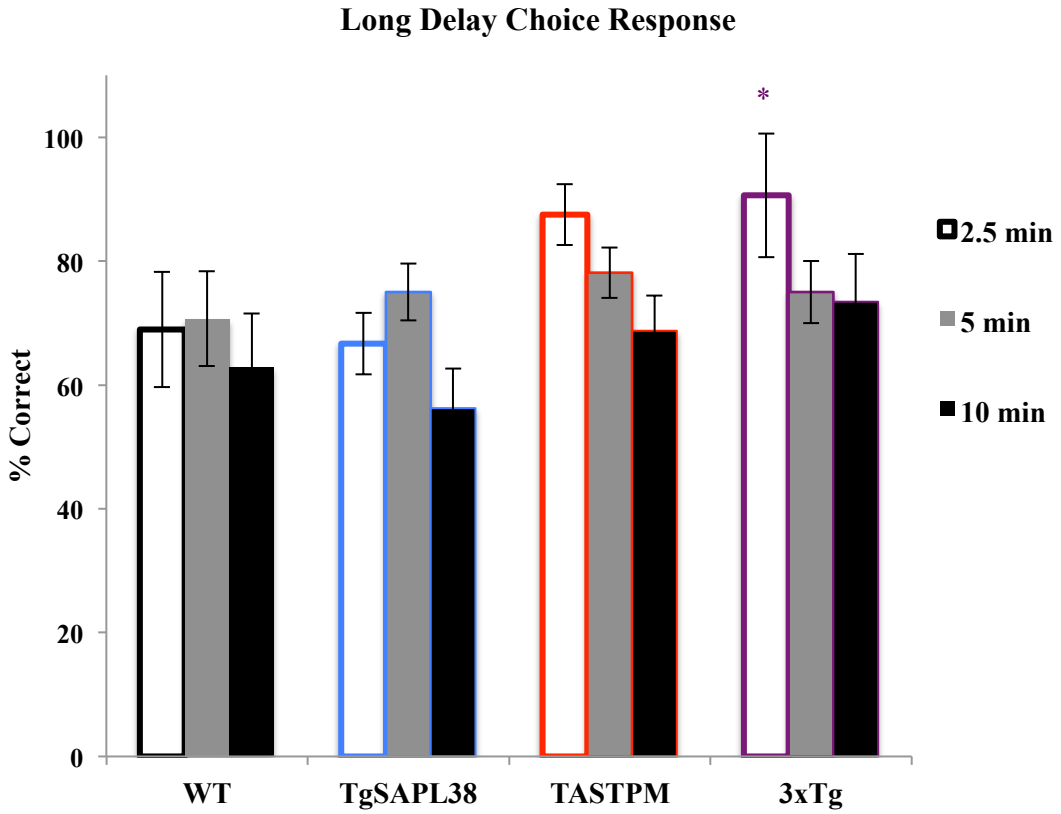

Figure 6.4. Mice with TASTPM transgenes make more correct choices with a 2.5-minute delay. Percentage of correct arm choices for WT (n=15), $TgSAP_{L38}$ (n=12), TASTPM (n=8) and 3xTg (n=8). Two-way ANOVA revealed significant effects of genotype and delay. Sidak's post hoc multiple comparison of control to 3xTg genotype are indicated *$p<0.05$. Data presented as mean ± SEM.

To further elucidate cognitive performance, an additional probe trial was included in the training on days 5 and 10, in which the orientation of the maze was reversed to provide a greater spatial memory challenge. This test allows for the assessment of the animals' use of external visuospatial cues (place response) versus an egocentric strategy utilizing only intramaze cues in order to make a correct choice (O'Keefe and Nadel, 1978). Results from these probe trials (Fig. 6.5 A,B) showed that genotype did not influence place or response choice at either time point during the training period.

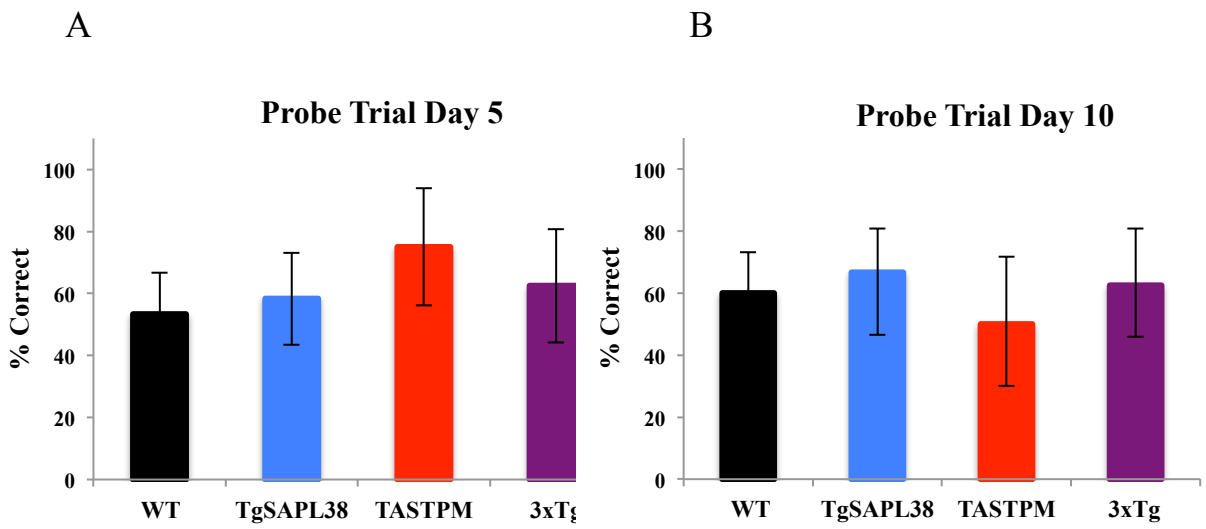

Figure 6.5. No difference between genotypes for probe trials. Probe trial place response scores for A) day 5 and B) day 10, with WT (n=15), $TgSAP_{L38}$ (n=12), TASTPM (n=8), and 3xTg (n=8). Data represented as mean +/- S.E.M.

Locomotor and anxiety testing

In order to further characterize the phenotype of the novel $TgSAP_{L38}$ transgenic mice, two additional tests of anxiety were performed. The open field and EPM tests represent standard measures of mouse anxiety commonly employed in behavioral studies (Pugh et al., 2007b; Scullion et al., 2011).

Open field test

The open field test allows for free exploration in a circular enclosure, and exploits a rodents' natural tendency to display thigmotaxis - their preference to explore the periphery of a novel environment and remain closer to the walls. The open field is used to measure anxiety by quantifying the time spent in the inner, more anxiogenic area, versus the periphery.

First, in order to assess overall locomotor activity in the different genotypes compared to WT mice, total distance travelled within the open field arena was measured. Two-way ANOVA revealed a significant effect of the TASTPM genotype on the total

distance accumulated [F(1,37)=34.65, p<0.001] over the course of 15 minutes in the open field test (Fig. 6.6 A). Post hoc tests performed again revealed the anxiogenic effect of the TASTPM genotype, with both the TASTPM and 3xTg mice exploring the arena significantly less than the WT (p<0.0001 and p<0.01, respectively).

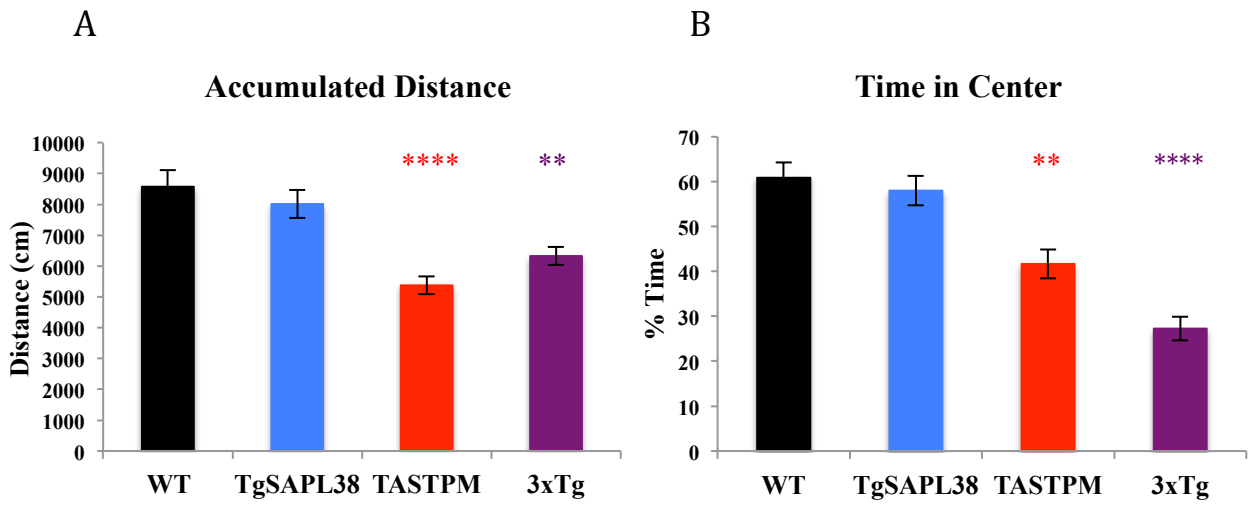

Figure 6.6. Mice with TASTPM transgenes have lower exploratory drive and spend less time in center of open field. A) Total accumulated distance in the open field, and B) percentage of time spent in the center of the open field arena for the 15-min test, for WT (n=14), $TgSAP_{L38}$ (n=11), TASTPM (n=8), and 3xTg (n=8). Two-way ANOVA revealed significant effects of TASTPM in A), and of TASTPM and SAP in B). Sidak's post hoc multiple comparison to control are indicated **p<0.01, ****p<0.0001. Data presented as mean ± SEM.

In examining the percentage of time mice spent in the center of the open field task (Fig. 6.6 B), two-way ANOVA again revealed a significant main effect of the TASTPM genotype [F(1,36)=48.59, p<0.0001], and of SAP [F(1,36)=5.48, p=0.0249]. Post hoc Sidak tests revealed that mice with the TASTPM AD transgenes, both with and without high SAP levels, demonstrated significantly greater levels of anxiety than the WT mice (p<0.0001 and p<0.01, respectively). These results are in line from those of Benway MSc Dissertation (2011), which found that TASTPM mice at the ages of 7-9 months of age displayed significantly higher levels of anxiety than WT mice. It can be seen from these results however that mice only expressing higher levels of human SAP do not demonstrate higher levels of anxiety.

Elevated Plus Maze

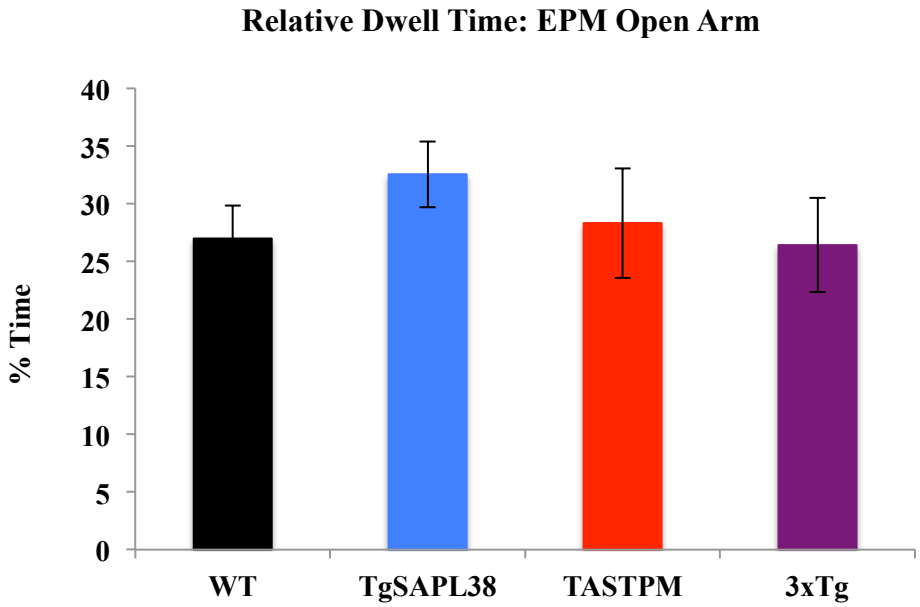

Figure 6.7. No difference between genotypes for time spent in the open arm of the EPM. Relative dwell times in open arm for WT (n=15), $TgSAP_{L38}$ (n=12), TASTPM (n=8), and 3xTg (n=8). Data represented as mean +/- S.E.M.

In the EPM, anxiety is measured by the preference of rodents for the closed arms over the open, more 'anxiogenic' ones (McDermott and Kelly, 2008). The interpretation is that the more time spent in the open arms of the maze, the less anxious the animal. However, with this measure, two-way ANOVA revealed no differences between genotypes (Fig. 6.7).

Summary

In order to assess possible deficits in hippocampal-dependent spatial working memory in our $TgSAP_{L38}$ and 3xTg models, the T-maze forced alternation task was chosen, due to its high sensitivity to dysfunction within the hippocampus (O'Keefe and Nadel, 1978). The T-maze task used was adapted from the protocol in Cacucci et al. (2008) in order to provide a greater cognitive challenge to elucidate any impairment in spatial working memory.

In our examination of T-maze training performance, we found that the WT and the 3xTg mice were able to learn the task and show an improvement in performance over

the 10-day training period. Unexpectedly, the TASTPM and the $TgSAP_{L38}$ mice began training at levels that left little room for improvement (Fig. 6.2). This failure to 'improve' could therefore be interpreted as an inability to forget the training that they experienced during habituation. However, the high percentages in correct choices made suggest that these mice do not necessarily display spatial memory impairments at this age tested. As TASTPM mice already possess a significant plaque load at this age of 13-14 months (Howlett et al., 2004; Matarin et al., 2015), our results further support the view that the plaques are not the cause of memory impairment. These results are also in line with previous work from our lab examining the spatial memory performance in younger TASTPM compared to WT mice in the same task at 4 and 8 months of age, where TASTPM mice start at the same levels as the WT and end training at levels comparable to WT, with no significant differences found between the genotypes (Benway, MSc Dissertation, 2011; Fig. 6.8).

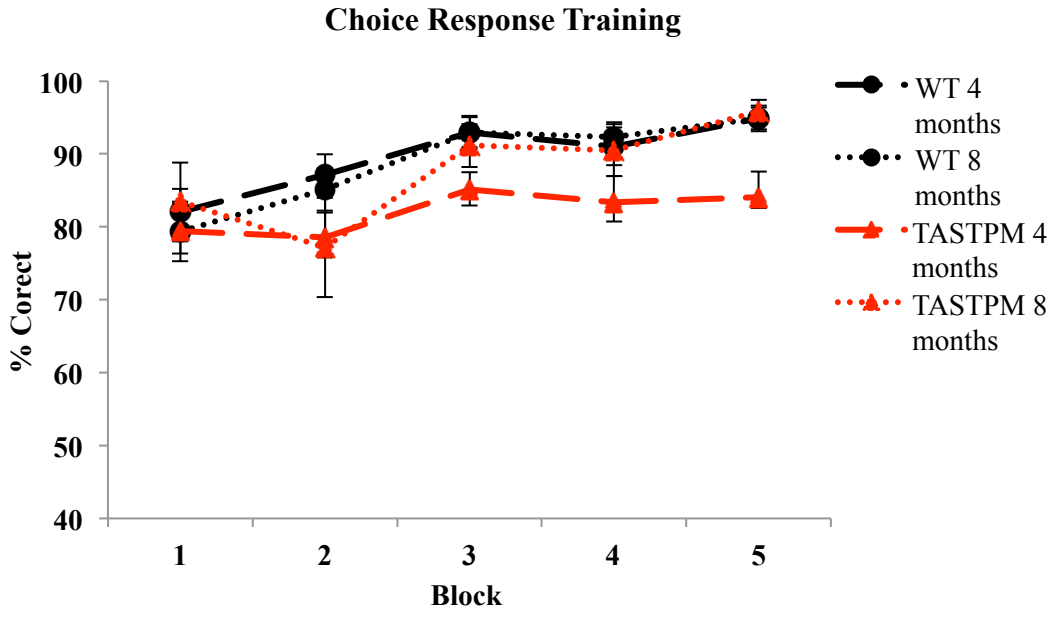

Figure 6.8. TASTPM mice at 4 and 8 months of age show no difference in performance to WT in T-maze training. Percent correct for choice runs of each genotype during the blocked training period for WT 4 months (n=13), WT 8 months (n=13), TASTPM 4 months (n=11) and TASTPM 8 months (n=10). Two-way ANOVA revealed main effects of block [$F(2.94, 172) = 9.30$, $p<.001$], indicating again that all groups were able to learn and improve their performance in the 15-sec delay version of the task, and a main effect of genotype [$F(1, 43) = 7.14$, $p=.011$]. Data presented as mean ± SEM, adapted from Benway, MSc Dissertation, 2011.

Unimpaired spatial memory function in these transgenic mice, with or without SAP, is further demonstrated in the analysis of the trials with long delays, in which all transgenic mice show comparable (if not better, in the case of the 3xTg) performance to WT mice. These results therefore suggest that cognitive function remains intact in mice expressing higher levels of human SAP, with and without the AD transgenes, at least in measures of this test. These results are again in line with previous work shown in Fig. 6.9 with younger TASTPM mice compared to WT that found no significant differences between genotypes in performance of the task with longer delays (Benway, MSc Dissertation, 2011).

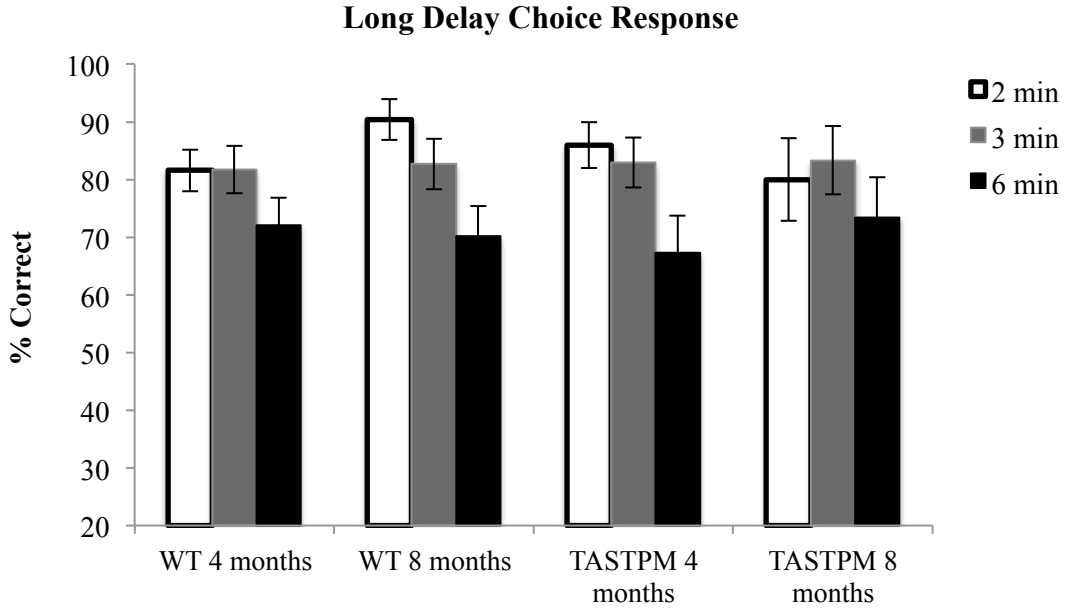

Figure 6.9. TASTPM mice at 4 and 8 months of age show no difference in performance to WT in longer delay. Percentage of correct arm choices for WT 4 months (n=13), WT 8 months (n=13), TASTPM 4 months (n=11) and TASTPM 8 months (n=10). Two-way ANOVA revealed a significant effect of delay [F(1.86, 78.10) = 7.09, p=.002]. Data presented as mean ± SEM.

The additional test of the probe trial similarly revealed no differences in performance when mice were required to utilize only external visuospatial cues instead of a mix of external and egocentric cues in the choice response phase of the task. When examining other factors of the task, we find that with response time, 3xTg mice took a significantly longer amount of time to make a choice in the earlier trials of training, which likely indicates higher levels of anxiety in this mouse model. This was also demonstrated in the open field test in which mice with the AD transgenes spent

significantly less time exploring than the WT or the $TgSAP_{L38}$ mice, as measured by less distance travelled in the field. This anxiogenic effect of the TASTPM transgenes was further confirmed with these mice spending less time in the center of the open field than the WT and $TgSAP_{L38}$ mice. However, no differences were found between genotypes in the EPM anxiety test, indicating that the anxiogenic effects of the AD transgenes may only be mild at the age of 13-14 months.

Overall, these results suggest that mice expressing human SAP alone or with the human genes $APP_{SWE}/PSEN1_{M146V}$ for AD have normal spatial working memory. While there was an effect of the AD transgenes on the open field measures of anxiety, the high levels of human SAP in these mice did not augment this effect. However, in looking at the data from the T-maze and anxiety tests together, it appears that there may be changes in cognitive flexibility in mice with the TASTPM transgenes, but that overexpression of human SAP alone does not result in this effect at the ages tested.

Chapter 7

Discussion

In this thesis I have investigated the influences of the two pentraxins SAP and NPTX1 in the brain in relation to AD, and to one another, using a range of different techniques. In order to best determine prevention or treatment strategies for AD, it is imperative that we gain a better understanding of the factors potentially contributing to the progression of the disease. As both SAP and NPTX1 had previously been associated with pathological features of AD, the novel findings reported herein contribute to the field of neurodegenerative disease by building upon and clarifying the effects of both pentraxins at elevated concentrations in the brain.

Molecular and histological investigation: SAP and NPTX1 in the hippocampus

Due to the particular vulnerability to pathology and high levels of neuronal loss displayed by the hippocampus in AD (Braak and Braak, 1991; Scahill et al., 2002), the features and functions of this region were chosen as the focus for the experiments of this thesis. Using the tools that we generated or independently verified we were able to confirm previous reports that a sufficient level of SAP crossed the BBB into the brain, or was possibly also expressed at low levels, to allow for it to be detected in the brains of patients with AD (Kalaria et al., 1991a; Perlmutter et al., 1995). This peripheral pentraxin was found to localize around plaques in these patients, where NPTX1 presence was also confirmed. Additionally, we have been able to approximate the relative amounts of both pentraxins on plaques and find that there is substantially more NPTX1 than SAP in these regions. However, the presence of SAP around the plaques, at least qualitatively, in the same location as NPTX1 suggests it still may be able to influence Aβ deposition, possibly via an interaction with the neuronal pentraxin.

An observation of interest in the experiments in AD patient brains was that strong NPTX1 staining was also found in the dystrophic neurites around plaques. It is likely that these neurites in the plaques are axonal boutons, rather than dendrites, as we found no evidence of NPTX1 being taken up by dendrites. Previous studies from our lab have found an increase in glutamate release probability to be both the first effect

of rising Aβ to occur in the TASTPM mouse model of AD pathology (Cummings et al., 2015), and also to occur after chronic exposure to NPTX1 (Cummings, Benway et al., 2017). Together these findings are in line with the effects produced from Aβ release in response to specific stimulus paradigms in normal rats (Abramov et al., 2009), which is consistent with the evidence that increasing NPTX1 levels can mediate the effects of Aβ (Abad et al., 2006).

In considering what factors may be influencing the dysregulation of the role of NPTX1 at the synapse in mediating the synaptic clustering of AMPA glutamate receptors to mediating the effects of Aβ, recent research has revealed possible routes by which this change may take place. Lee et al. (2017) investigated the role of NPTXR at the synapse using overexpression and knockdown of the 'receptor' in cultured neurons, and interestingly found that NPTXR knockdown resulted in a decrease in NPTX2, but had no effect on levels of secreted NPTX1. Overall, they found that NPTXR was a rate-limiting factor in synapse organization, where it recruits and stabilizes the other two neuronal pentraxins in a complex on the presynaptic membrane. Interestingly, this condition parallels what may be occurring in AD; microarray data from Matarin et al. (2015) shows the expression levels of NPTXR in TASTPM homozygous mice decreasing with age (Fig. 7.1). While this evidence might suggest that a decrease in the amount of NPTXR at the synapse could lead to an excess amount of unbound NPTX1, the decrease shown in the TASTPM data is only modest, and would require further investigation to determine whether NPTXR levels decrease in AD patient brains. However, as unbound NPTX1 has previously been shown to result in apoptosis (DeGregorio-Rocasolano et al., 2001), it may be the case that an excess of this pentraxin builds up at the synapse when there is a decrease in the level of NPTXR to bind it in complex, which may therefore contribute to the pathological progression in AD, particularly in the presence of increasing levels of Aβ.

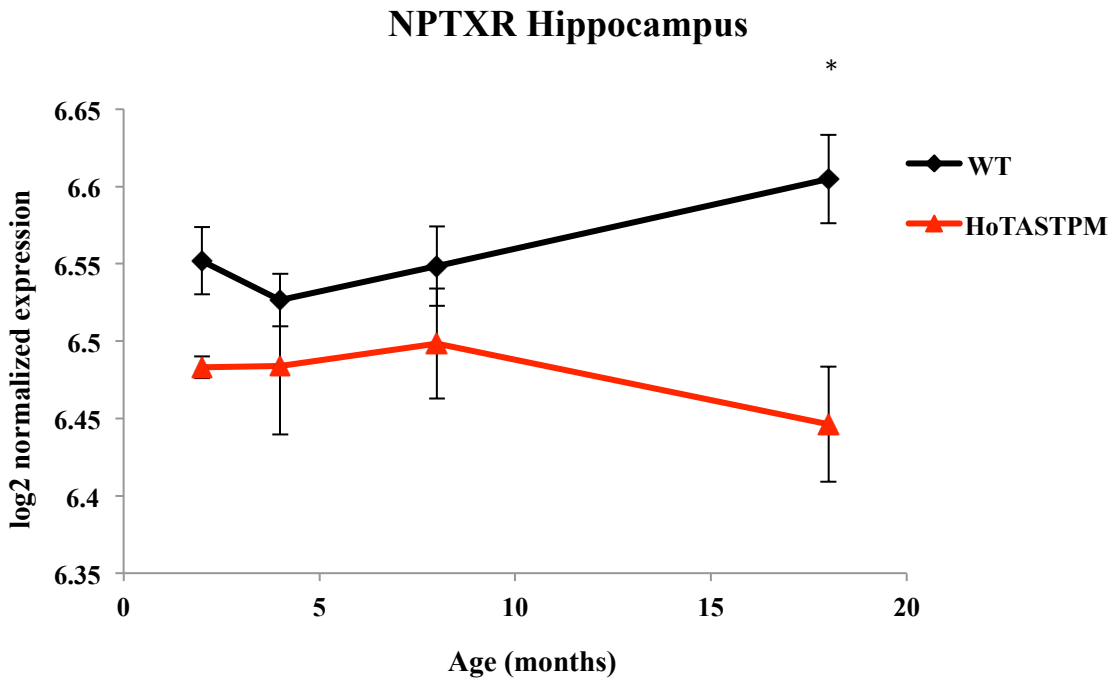

Figure 7.1. NPTXR expression is dysregulated in the hippocampus of TASTPM mice. Gene expression changes (compared to WT) of NPTXR in the hippocampus from (www.Mouseac.org; Matarin et al., 2015) in the hippocampus of WT and TASTPM homozygous mouse models. Two-way ANOVA revealed a main effect of genotype. Sidak post hoc multiple comparison of control to normalized NPTX1 levels are indicated *p<0.05. Data presented as mean ± SEM.

In the examination of a mouse model of AD pathology, the inability to detect SAP mRNA or protein in WT or TASTPM mice corroborates our understanding that in mice, SAP is most likely only expressed in the liver (Pepys et al., 1997), and that mouse SAP does not readily cross the blood brain barrier in mice under normal physiological conditions (Winkler et al., 2001). This is in line with recent evidence by (Bien-Ly et al., 2015) who reported no breakdown of the BBB in multiple mouse models of AD pathology using protein markers of multiple different sizes. Our results therefore suggest that BBB breakdown does not occur in mice to the extent that evidence suggests in humans (Blennow et al., 1990; Hartz et al., 2012; Kalaria and Grahovac, 1990). However, it is also important to consider that the pathology of sporadic AD in humans progressively builds over the course of several decades, whereas the pathological process in transgenic mouse models is accelerated via the insertion of human genes for familial AD. Transgenic mice therefore lack many key neurological features comprising the brain milieu that accumulate during the long course of the disease, including periphery molecules that may have entered the brain

during times of infection, which are common in the old age (Manepalli et al., 1990), or a buildup of damage caused by cerebrovascular lesions, another common observation in aged samples (Bridges et al., 2014; Farrall and Wardlaw, 2009), with one study reporting the presence of infarcts in 43% of elderly brains in their donation program (Beach et al., 2015).

In the same TASTPM mouse model, although previous work has found NPTX1 mRNA expression to be dysregulated and actually decreased at the ages of 4 and 18-months (Matarin et al., 2015), we find no decrease in protein levels in the mice with advanced AD pathology at 18-months of age. As we also find a high degree of NPTX1 concentrated around Aβ plaques in these models, it is likely that the mRNA expression is being downregulated via a feedback mechanism detecting higher levels of this protein accumulating around plaques. Moreover, a study using the measurements of the absolute concentrations of mRNAs and proteins from various organisms, including mammalian cells, worms, flies, yeast and a few species of bacteria found that in both bacteria and eukaryotes, the cellular concentrations of proteins showed a squared Pearson correlation coefficient of ~0.40 with the abundances of their corresponding mRNAs (Vogel and Marcotte, 2012). This implies that only ~40% of the variation in protein concentration can be explained by knowing mRNA abundances, but that there is a remaining ~60% variation due to a combination of post-transcriptional regulation and measurement noise (ibid). An additional point to consider is that protein multimerization can influence a feedback circuit that regulates transcription/translation rates that can increase negative feedback strength (Singh, 2011; Singh and Hespanha, 2009; Thattai and van Oudenaarden, 2001), and given NPTX1 is prone to multimerization, the downregulation of mRNA may be explained by NPTX1 forming a higher number of complexes at the synapse in AD.

Our interesting finding came with the examination of the TgSAP, $TgSAP_{L38}$ and 3xTg mice expressing human SAP, where diffuse SAP staining could be seen throughout several regions of the brain, including the hippocampus, and around plaques in the mice with the TASTPM transgenes. Given that the affinity for the SAP antibody for its target is significantly higher than the affinity of the NPTX1 antibody that we used, it would lead us to conclude that the SAP concentration in the brains of these mice is

low, but at levels that are high enough to elicit impaired synaptic transmission with chronic exposure (Cummings, Benway et al., 2017). However, this still raises the question of how the SAP gets into the brain of the transgenic mice. The three lines of mice listed above are exposed to human SAP throughout life and so it is possible that the BBB is compromised from time to time during the life of the mouse and that this results in slightly higher levels in the brain, or that there is a leaky expression of the promoter in the brain. Corroborating evidence for these findings was shown in a recent study by Al-Shawi et al. (2016), in which the same 3xTg human SAP-expressing mice were examined at 20 months of age. This study confirmed high levels of hSAP staining in the cerebrovasculature, at a level at least 1000-fold higher (in the case of the TgSAP, and even higher in the TgSAPL38 and 3xTg mice) than the plasma and extracerebral interstitial fluid concentration. This further supports the hypothesis that SAP is capable of penetrating the BBB across such a high concentration gradient and entering the brain. Finally, although we and others (Hawrylycz et al., 2012; Mulder et al., 2012) [www.brainmap. org]; (Matarin et al., 2015)[www.mouseac.org]) find little or no evidence for expression of SAP within the brain, there still remains the possibility of local synthesis (Yasojima et al., 2000), which may be below detection thresholds in most studies.

SAP crossing the BBB

Our results using peripherally evoked LPS inflammation confirm the finding by Veszelka et al. (2013) that SAP can enter the brain under conditions of BBB breakdown. This result is compatible with the reported 1000-fold concentration gradient for SAP between the plasma and brain (Kolstoe et al., 2009; Nelson et al., 1991b). While soluble SAP would be expected to be broken down or be otherwise removed from the brain (Veszelka et al. 2013), its ability to infiltrate the brain through a compromised BBB in AD suggests that it may possibly be binding to plaques and preventing their removal, thus reflecting the higher concentrations of SAP found in the brains of AD patients (Crawford et al., 2012). However, it is also possible that SAP is binding to dystrophic neurites or damaged synapses, where NPTX1 has previously been reported in the brains of AD patients (Abad et al., 2006), or even to NPTX1 on the plaque. The *in vitro* and *in vivo* evidence from Veszelka et al. (2013) shows that rapid efflux of SAP is greatly preferred at the BBB, with rapid

clearance following intrahippocampal administration and significantly higher release of SAP from endothelial cells to the luminal than that to the abluminal side. These findings support the hypothesis that the binding of SAP to amyloid may be what is preventing its removal from the brain and allowing levels, albeit low, to be maintained.

The question arises as to what causes BBB disruption and preferential localization to the hippocampus in conditions of advanced age or disease (Montagne et al., 2015). As the hippocampus is a site of early pathology in aging and AD (Braak and Braak, 1991), it would be logical to hypothesize that Aβ or tau might play a role. The accumulation of Aβ occurs earlier than tau (though tau cannot be completely excluded), is toxic to pericytes (Verbeek et al., 1997), and can induce cerebral endothelial dysfunction. Specifically, Aβ is able to increase BBB permeability via the activation of transient receptor potential melastatin-2 channels (TRPM-2) and through causing dysregulation of endothelial intracellular Ca^{2+} (Park et al., 2014). Importantly, SAP has also been shown to potentiate the BBB-weakening effect of Aβ, as their combination *in vitro* was found to increase BBB permeability (Veszelka et al., 2013), suggesting that the crossing of SAP through the BBB could be capable of propagating the acceleration of BBB breakdown that has been shown to occur in AD (Montagne et al., 2015).

SAP can interact with the neuronal pentraxins

Interestingly, our coimmunoprecipitation results have shown a novel finding that SAP can bind to each of the neuronal pentraxins (NPTX1, NPTX2 and NPTXR), which suggests that SAP may be able to contribute to heteromultimeric complexes of NPTXs and, in doing so, possibly alter their activity. It is important to note however that they could also be pulled down together because they can simultaneously bind to other common partners, and so it is possible that SAP may therefore be able to compete for the same cell surface targets that the neuronal pentraxins bind to. Importantly, this result drastically expands the scope of SAP's possible influence in the brain, beyond its interaction with plaques; if SAP can interact with each of the neuronal pentraxins, it is possible that this interaction could also cause disruption to the normal synaptic functions of the NPTXs in the brain (Fig. 7.2). However, it is

important to note that this would only be likely to occur under conditions of significant BBB breakdown, in order for the concentration of SAP to be high enough to exert any possible effects in the brain.

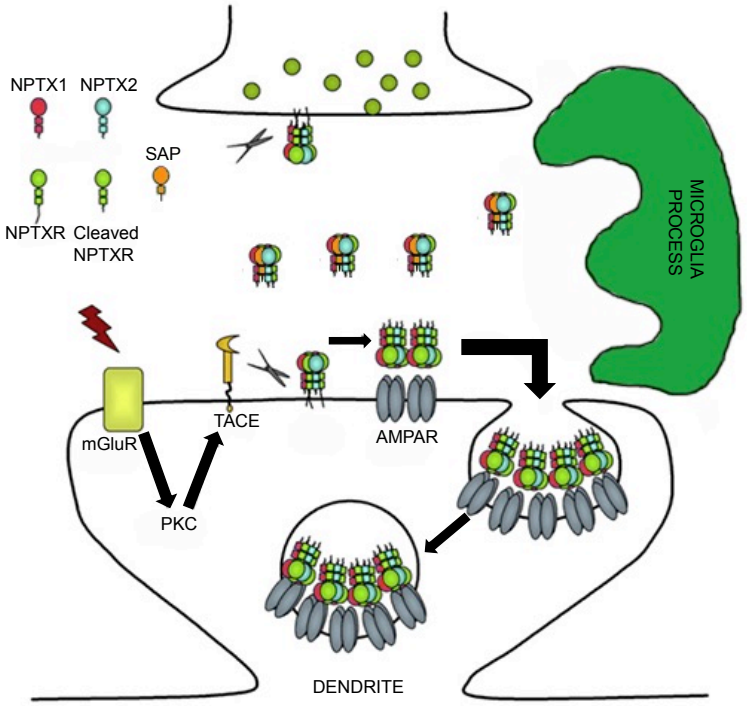

Figure 7.2. SAP is capable of interacting with the neuronal pentraxins and may be able to influence their function if high enough levels cross the BBB. Schematic depicting possible interactions that SAP could be having with the neuronal pentraxins at the synapse. Molecular biology data presented in this thesis has indicated that SAP can form part of the pentamer with the other neuronal pentraxins, and cell culture work has shown that SAP can also influence the function of NPTX1 on neurons and microglia.

In summary, both SAP and NPTX1 are present around Aβ plaques in post-mortem brains of people with AD and, although mouse SAP is not present in the brains of TASTPM mice with advanced AD pathology, human SAP can be seen in the brains of mice when it is expressed at levels that are within a physiologically range in humans. The evidence presented here therefore strongly suggests that SAP is capable of entering the brain under some conditions of BBB breakdown, where it would have the opportunity to interact with the NPTXs and, as has been previously shown, influence central synaptic transmission (Cummings, Benway et al., 2017) in AD.

Spine density changes with treatment of SAP and/or NPTX1

As changes in synapse function have been shown to occur before the onset of plaques in AD (Busche et al., 2012; Cao et al., 2012; Cummings et al., 2015), the examination of related factors that may play roles in the development of the disease is vital. Here, I have investigated the effects that increased levels of SAP and NPTX1 may be having on healthy neurons, representing what may be occurring in the brain prior to the development of plaques or the presence of increased levels of soluble Aβ. Developing a better understanding of how normal functions can go awry and contribute to disease pathology is key to the identification of targets for treatment and prevention of such disorders.

Our finding that NPTX1 treatment at a concentration first found to elicit changes in synaptic transmission significantly decreased spine density in hippocampal neurons is in accordance with previous research by (Figueiro-Silva et al., 2015), where it was hypothesized that NPTX1 negatively regulates excitatory synapses. This role for NPTX1 was proposed based upon the results seen after its knockdown, which they found to cause: 1) an increase in the number of excitatory synapses, 2) a localization of extrasynaptic amino acid receptors to the new synapses, 3) higher frequency mEPSCs demonstrating functionality, and 4) an increase in the amplitude of spontaneous calcium oscillations. With this increase in excitatory synapse number from knockdown, they correspondingly found a significantly higher number of spine protrusions. As we found the opposite effect with chronic exposure of NPTX1, our results support this hypothesis. This role of NPTX1 as a limiting factor in excitatory synapses is further supported by the finding that overexpression of NPTX1 decreased the number of excitatory synapses (ibid). In the context of AD, given the increase in NPTX1 protein levels (Abad et al., 2006), it can be hypothesized that NPTX1 acts as a key mediator in driving the synaptic loss that is one of the hallmarks of the disease (Selkoe, 2002). Supporting this hypothesis, evidence from Abad et al. (2006) found that NPTX1 significantly contributes to synapse loss, neurite damage, and the subsequent apoptotic toxicity that is induced by Aβ in cortical neuronal cultures.

It was initially hypothesized that NPTX1 and SAP may be capable of inducing changes in synaptic density due to excitotoxicity produced as a result of their application at the same experimental concentrations that cause increases in glutamate release (Cummings, Benway et al., 2017). However, given only NPTX1 application caused a decrease in spine density and the finding that SAP co-application blocked, rather than augmented, the effect of NPTX1, an excitotoxic mechanism is therefore unlikely. Importantly, these results suggest that SAP may be capable of interacting with NPTX1 at the synapse and mediating the negative regulatory function that NPTX1 has been proposed to have on spines (Figueiro-Silva et al., 2015).

While the application of SAP to hippocampal neurons did not cause a decrease in spine density, previous findings from our lab have shown that the long-term exposure of SAP that occurs in the brains of transgenic mice with human SAP can impair LTP (Cummings, Benway et al., 2017). While the latter results would seem to contradict the finding in the present study, given the correlation of spine formation with LTP (Segal, 2005), it may be the case that the concentration used and the extent of treatment time was not sufficient enough to produce changes in spine number. It should also be considered that LTP is associated with changes in the size of spine heads, as their enlargement is consistently reported to occur in response to the expansion of the postsynaptic density after LTP induction (Desmond and Levy, 1986; Fifkova and Anderson, 1981). It may therefore be the case that SAP could be causing changes in spine structure, rather than in density – at least at the concentration used. However, for NPTX1, the finding of spine density reduction with increased levels of NPTX1 correlates to the enhancement in LTP after NPTX1 knockdown that was reported by Figuero-Silva et al. (2015). Together, these results suggest that NPTX1 is likely to mediate more potent effects at the postsynaptic density than SAP. Additionally, the blocking effect of SAP when applied with NPTX1, rather than an additive effect, suggests SAP is interacting with NPTX1 or blocking the targets used by NPTX1 to regulate synapse formation.

Effect of SAP and NPTX1 on microglia numbers and activation

The functions of microglia in the CNS are inherently linked to the development, clearance and plasticity of synapses, which the pentraxins have also been shown to

influence (Osera et al., 2012; Cummings, Benway et al., 2017). The treatment of organotypic hippocampal slices with NPTX1 was found to cause a decrease in the number of microglia, and the co-treatment with SAP was again found to block the effect of NPTX1, which was the same effect that was observed with the hippocampal neurons. The blocking effect of SAP on NPTX1 in both cultured neurons and hippocampal slices further supports the hypothesis that SAP is interacting with NPTX1, and curiously poses the question of whether it may be capable of providing protection to cells by counteracting the negative effects elicited by NPTX1 or competing for binding to the same targets. If SAP is forming a complex with NPTX1, as I have shown is feasible, then it is possible that the binding of SAP to NPTX1 is preventing or decreasing the potency of the interaction that NPTX1 would otherwise be involved in at the synapse.

As NPTX1 has been found to contribute to the neuronal damage evoked by Aβ, it raises the possibility that this may also be the case in regard to microglia. It has been shown that transgene overexpression of NPTX1 reproduces the neurotoxic effects of Aβ, and that Aβ exposure to cultured microglia promotes their degeneration (Korotzer et al., 1993). If NPTX1 can mimic the effects of Aβ on neurons, the possibility that it may also be capable of mediating the same effects of Aβ on microglia is an important point for consideration. NPTX1 may therefore be a target worth further investigation for the treatment of AD.

The activation of microglia requires a high level of metabolic energy from the cell, and prolonged periods of activation of aging microglia often result in senescence due to the strains placed on the cell (Streit, 2006). It was therefore hypothesized that NPTX1 may cause a decrease in microglia numbers as a result of the pentraxin inducing high levels of activation, given the report that NPTX1 binds to C1q (Stevens et al., 2007), the initiator of the complement cascade. Interestingly however, it was found that neither pentraxin had an effect on activation levels when applied on its own, but their co-application resulted in a decreased activation. This surprising finding indicates that the spine density changes that were observed from NPTX1 application were unlikely to have been mediated via a microglia ‘pruning’ effect mediated by C1q, as previously suggested. It is possible however that the decreased

activation levels may in part be due to both pentraxins binding to C1q in a manner that instead prevents or reduces the potency of the activation of complement.

In relation to AD, increases in SAP and NPTX1 levels inhibiting microglial activation in key areas where phagocytosis of Aβ should be occurring may be a pathological feature of these two proteins that is important to consider. Moreover, these results suggest that an increase in NPTX1 level in the brain, as shown to occur in Abad et al., (2006), may be a factor that promotes dystrophy of aging microglial and subsequent death, further impeding the clearance of Aβ that microglia should be mediating. The latter point is particularly important considering that NPTX1 levels are clearly much higher around plaques and in dystrophic neurites than those of SAP in the brain (see Chapter 3), as the relatively small amount of SAP would be unlikely to block most of the effects of NPTX1.

Spatial memory in mice expressing human SAP

In our investigation into whether the synaptic effects of human SAP in the brains of transgenic mice would translate into memory problems, no spatial memory impairment could be detected up to an age of 14-months old, in any of the genotypes. This surprising finding raises the question of how mice with the AD transgenes were able to perform as well as WT in the task, particularly given the changes in LTP commonly observed in mouse models of AD pathology at earlier ages (Tozzi et al., 2015)Jacobsen et al., 2006). Additionally, we have found that the magnitude of LTP is significantly smaller in hippocampal slices from TgSAP mice compared with WT mice (Cummings et al., 2017), and this model expresses only approximately (at least) half the amount of SAP as the $TgSAP_{L38}$ mice (as described previously). However, sensitivity of the T-maze task has been confirmed in a previous experiment that used the Tg2576 mouse model of AD pathology in the task and found correlations between hippocampal plaque burden and behavioral performance (Cacucci et al., 2008). It is important to note that the aforementioned study examined older mice at 16 months of age, after significant impairments in LTP have been found in both the CA1 and DG (Chapman et al., 1999), and additional measures of response time and anxiety were not taken into account in the results. Despite the reports from Cacucci et al. (2008), a direct link between the amount of Aβ plaque deposits and behavioral deficits has not

been clearly identified in transgenic mouse models of AD or in patients, and that it is only synaptic loss that has been shown to correlate to cognitive impairment (Terry et al., 1991).

The training results of the TASTPM and $TgSAP_{L38}$ mice beginning at such high levels may indicate the inability for these models to extinguish the memory of the task. The lack of extinction of fear memory has been shown in the TASTPM mice as early as 4 months of age (Pardon et al., 2009; Rattray et al., 2009), suggesting it may be a more sensitive measure for memory assessment that the explicit forced-choice T-maze memory task. The extinction of fear memory is the learned inhibition of fear, and is a less explored but complex cognitive process. It is possible that the T-maze environment induces some level of fear in the animals, which would be expected to occur during habituation, but this should be followed by an inhibition of the acquired association by learning that the task is not aversive by the start of training (given their gained familiarity of the task and the reward provided). This would then suggest that the exposure to the maze can induce a reconsolidation of the learned behavior, rather than its extinction, thus demonstrating a reduction in cognitive flexibility (Pardon et al., 2009). It can therefore be suggested that the $TgSAP_{L38}$ mice show similar memory extinction impairment as the TASTPM mice at 13-14 months of age, given both genotypes began training (following habituation) at such a high correct rate. However, the 3xTg display a learning curve similar to WT - an unexpected result, but one that has been supported by electrophysiological findings from our lab that have shown a decrease in paired pulse ratio and decreased LTP in TASTPM and $TgSAP_{L38}$ mice, but no change in the 3xTg (Liu et al., unpublished data). Importantly, this could suggest that SAP may be capable of reducing the progression of, rather than negatively augmenting, the TASTPM phenotype. A possible explanation for this may be that SAP is promoting plaque formation and thus contributing to the removal of Aβ from the synapses, based upon the evidence from SAP knockdown mice that showed delayed and decreased amyloid plaque formation from experimentally induced amyloidosis (Botto et al., 1997). However, it is important to note that the findings from the aforementioned study were based upon plaques in the periphery, not in the brain, and therefore reflect very different physiological conditions.

Evidence supporting a protective function of amyloid aggregation has been shown by (Cohen et al., 2009) in a study that examined the effect of a reduction in insulin-like growth factor 1 (IGF-1) signaling in a mouse model of AD pathology with the human transgenes APP_{swe} and presenilin-1 ΔE9. This study found that a reduction of IGF-1 signaling resulted in an increased quantity of densely packed, larger fibrillar plaques later in life, which were found to protect from proteotoxicity associated with Aβ. The hyper-aggregation of Aβ was correlated with reductions in neuronal and synaptic loss, neuroinflammation, and behavioral impairment. These findings suggest that the accumulation of tightly packed and ordered plaques results in possible sequestering of the soluble Aβ oligomers that are consistently found to be more toxic than aggregated Aβ (Haass and Selkoe, 2007). This hypothesis has been supported in findings that enhanced Aβ fibrillization in mice by a different means (insertion of AβE22G mutation in hAPP mice) reduced Aβ toxicity (Cheng et al., 2007), and that small, oligomeric Aβ impairs LTP to a greater extent than fibrillar Aβ (Shankar et al., 2008).

Another surprising result was found during the test phase of the task, with the introduction of long delays. With greater memory challenge, mice with the TASTPM transgene performed better with the 2.5-minute delay, but then performed at the same levels as WT when challenged with the two longer delays. This further suggests that the TASTPM mice may lack the ability to forget. These results may therefore indicate that the T-maze test may not be sensitive enough to detect explicit alteration in memory function, or that significant compensatory mechanisms exist in the brains of the mice that allow perceived normal functioning up to significantly advanced ages. This result is in line with recent findings from (Beglopoulos et al., 2016) that showed normal learning in the PDAPP mouse model of AD pathology (with the APP_{V717F} mutation, exhibiting 10-fold higher human APP expression than endogenous murine APP) in the spatial memory-dependent water maze task. However, while the PDAPP mice showed no impairment in learning of the task at 3-4 months of age, the study reports that the transgenic mice had increased levels of forgetting the task, when long intervals of 7 days were introduced between trials (ibid). As this was a novel design feature of the maze, it is an important point to consider in animal behavior work that it may be necessary to incorportate such modifications for more sensitive detection of cognitive changes.

While no impairments in spatial memory were found, it was important to also determine whether any potentially confounding factors were apparent, particularly given that higher levels of anxiety are commonly reported in AD patients (Assal and Cummings, 2002; Brodaty and Low, 2003). An anxiogenic effect of the TASTPM transgenes was confirmed with these mice spending less time in the center of the open field than the WT and $TgSAP_{L38}$ mice. This result correlates to previous findings in TASTPM mice tested at 7-8 months of age, where significantly higher levels of anxiety were observed using the same measurement in the open field task (Benway, MSc Dissertation). This effect was also demonstrated in the open field test in which mice with the AD transgenes spent significantly less time exploring than the WT or the $TgSAP_{L38}$ mice, as measured by less distance travelled in the field. This finding is in agreement with increased levels of immobility observed in 5.5 month old TASTPM mice in retention and extinction trials in contextual fear conditioning experiments (Pardon et al., 2009). Additionally, hypoactivity has been displayed in 10-month old TASTPM mice previously, as measured using beam boxes and open field tests (Pugh et al., 2007a). It is important to note however that not all mouse models of AD pathology display increased levels of anxiety. While the Tg2576 and TgCRND8 (Swe/Indiana APP mutations) mice both exhibit increased anxiety (Lee et al., 2004; Ognibene et al., 2005), and even a correlated increase in the expression of genes implicated in anxiety (for the latter model), other studies report no changes, such as in the APP23 models (Lalonde et al., 2002). While the observation that other measures, such as alterations in circadian rhythms, which are known to affect activity levels in mice, and may partially account for some of the variation observed, it is still unclear as to what accounts for the differences among transgenic animals. This therefore demonstrates that there is a variation between mouse models in the manifestation of different behaviors, making it important to assess what could be confounding factors when examining the phenotypes of the different transgenic models. A possible way of resolving this may be through the use of knock-in mice rather than transgenic models, which would avoid some of the issues related to overexpression and possible influences of transgene insertions.

Conclusion

In the field of AD research, there is still a great deal yet to be understood about the underlying mechanisms that go awry and culminate in the tipping of the homeostatic balance in the brain towards disease. In this thesis I have investigated the influence of two members of the pentraxin family of proteins that have previously been implicated in AD, but focused my examination in a novel way that has considered not only the effects of each individually, but also their possible interaction, where possible, in relation to AD progression. Here I present evidence that the peripheral pentraxin SAP and the neuronal pentraxin NPTX1 can interact, and possibly affect the same targets within the brain.

By thoroughly performing a series of tests to determine the specificity and affinities of multiple antibodies, I have been able to confirm the localization of SAP and NPTX1 in the brains of patients with AD and in mice with AD transgenes, with and without human SAP. From these histological examinations, it is clear that SAP is capable of infiltrating the brain, and can be found in key locations that are vulnerable in AD along with NPTX1, particularly co-localized around amyloid plaques. To investigate the possible implications of these findings, we considered the evidence that the neuronal pentraxins form complexes with one another and extended the possibility of this property to SAP, give the high degree of structural similarity. In our novel finding that SAP can bind to each of the neuronal pentraxins, we have broadened the lens through which SAP has been previously been viewed to mediate effects in the brain.

With the evidence for the penetration of SAP into the brain and its potential for interaction with NPTX1 that was presented in Chapter 3, it was critical for our follow up work to further investigate this interaction and the effects that it may be exerting on different cell types. The finding in Chapter 4 that SAP not only fails to produce an additive effect, but can actually block the effect of NPTX1 on spine density demonstrates the possibility of a protective role for SAP in the brain. Moreover, this same effect was found with microglia in organotypic slices as described in Chapter 5, corresponding to the findings in spine density changes, but using a more physiologically relevant culture system and examining different cell types.

Apart from the interaction of SAP with NPTX1 or the downstream targets of the neuronal pentraxin, we have uncovered another possible protective function for SAP in the brain, in the examination of behavior in Chapter 6. While it may be the case that SAP is stabilizing Aβ plaques in the brain as it does in the periphery, the result of it doing so may be contributing to the removal of the toxic soluble Aβ species from the extracellular space, which is a mechanism that has previously been shown to be protective (Cohen et al., 2009). The finding that the mice with AD transgenes and human SAP performed similar to the WT mice suggests that SAP may be capable of moderating the effects of soluble Aβ, which is the toxic species most highly associated with cognitive impairment.

However, in relating these results to humans, it is important to note that the likelihood of SAP being able to effectively block the effects of NPTX1 or stabilize Aβ plaques in the brain is quite low, given we have determined that qualitatively there is a much higher concentration of NPTX1 in the brain relative to SAP. Moreover, it is evident that SAP is also capable of exerting toxic effects on neurons as well, given the findings of it causing neuronal death in cell cultures (Duong et al., 1998; Urbanyi et al., 1994) and increasing glutamate release probability (Cummings, Benway et al., 2017). In considering the data that has been presented throughout this thesis, the scope of the possible influence of SAP in the brain and in AD has been significantly broadened. The interplay of SAP with the neuronal pentraxins has been shown here to be an important point for consideration in the future investigations of the functions of the NPTXs in the AD brain.

References

Abad, M.A., Enguita, M., DeGregorio-Rocasolano, N., Ferrer, I., and Trullas, R. (2006). Neuronal pentraxin 1 contributes to the neuronal damage evoked by amyloid-beta and is overexpressed in dystrophic neurites in Alzheimer's brain. J Neurosci *26*, 12735-12747.

Abramov, E., Dolev, I., Fogel, H., Ciccotosto, G.D., Ruff, E., and Slutsky, I. (2009). Amyloid-beta as a positive endogenous regulator of release probability at hippocampal synapses. Nat Neurosci *12*, 1567-1576.

Aisen, P.S., Schafer, K.A., Grundman, M., Pfeiffer, E., Sano, M., Davis, K.L., Farlow, M.R., Jin, S., Thomas, R.G., Thal, L.J.*, et al.* (2003). Effects of rofecoxib or naproxen vs placebo on Alzheimer disease progression: a randomized controlled trial. JAMA *289*, 2819-2826.

Ajami, B., Bennett, J.L., Krieger, C., Tetzlaff, W., and Rossi, F.M. (2007). Local self-renewal can sustain CNS microglia maintenance and function throughout adult life. Nat Neurosci *10*, 1538-1543.

Akiyama, H., Barger, S., Barnum, S., Bradt, B., Bauer, J., Cole, G.M., Cooper, N.R., Eikelenboom, P., Emmerling, M., Fiebich, B.L.*, et al.* (2000). Inflammation and Alzheimer's disease. Neurobiol Aging *21*, 383-421.

Akiyama, H., Yamada, T., Kawamata, T., and McGeer, P.L. (1991). Association of amyloid P component with complement proteins in neurologically diseased brain tissue. Brain Res *548*, 349-352.

Al-Shawi, R., Tennent, G.A., Millar, D.J., Richard-Londt, A., Brandner, S., Werring, D.J., Simons, J.P., and Pepys, M.B. (2016). Pharmacological removal of serum amyloid P component from intracerebral plaques and cerebrovascular Abeta amyloid deposits in vivo. Open Biol *6*, 150202.

Andersen, O., Vilsgaard Ravn, K., Juul Sorensen, I., Jonson, G., Holm Nielsen, E., and Svehag, S.E. (1997). Serum amyloid P component binds to influenza A virus haemagglutinin and inhibits the virus infection in vitro. Scand J Immunol *46*, 331-337.

Andra, K., Abramowski, D., Duke, M., Probst, A., Wiederhold, K.H., Burki, K., Goedert, M., Sommer, B., and Staufenbiel, M. (1996). Expression of APP in transgenic mice: a comparison of neuron-specific promoters. Neurobiol Aging *17*, 183-190.

Arendt, T. (2009). Synaptic degeneration in Alzheimer's disease. Acta Neuropathol *118*, 167-179.

Assal, F., and Cummings, J.L. (2002). Neuropsychiatric symptoms in the dementias. Curr Opin Neurol *15*, 445-450.

Association, A.s. (2017). 2017 Alzheimer’s Disease Facts and Figures. Alzheimer’s Dement *13*, 325-373.

Ballard, C., Gauthier, S., Corbett, A., Brayne, C., Aarsland, D., and Jones, E. (2011). Alzheimer's disease. Lancet *377*, 1019-1031.

Bamberger, M.E., Harris, M.E., McDonald, D.R., Husemann, J., and Landreth, G.E. (2003). A cell surface receptor complex for fibrillar beta-amyloid mediates microglial activation. J Neurosci *23*, 2665-2674.

Banks, W.A., Akerstrom, V., and Kastin, A.J. (1998). Adsorptive endocytosis mediates the passage of HIV-1 across the blood-brain barrier: evidence for a post-internalization coreceptor. J Cell Sci *111 (Pt 4)*, 533-540.

Bao, F., Wicklund, L., Lacor, P.N., Klein, W.L., Nordberg, A., and Marutle, A. (2012). Different beta-amyloid oligomer assemblies in Alzheimer brains correlate

with age of disease onset and impaired cholinergic activity. Neurobiol Aging *33*, 825 e821-813.
Beach, T.G., Adler, C.H., Sue, L.I., Serrano, G., Shill, H.A., Walker, D.G., Lue, L., Roher, A.E., Dugger, B.N., Maarouf, C.*, et al.* (2015). Arizona Study of Aging and Neurodegenerative Disorders and Brain and Body Donation Program. Neuropathology *35*, 354-389.
Beaudoin, G.M., 3rd, Lee, S.H., Singh, D., Yuan, Y., Ng, Y.G., Reichardt, L.F., and Arikkath, J. (2012). Culturing pyramidal neurons from the early postnatal mouse hippocampus and cortex. Nat Protoc *7*, 1741-1754.
Beglopoulos, V., Tulloch, J., Roe, A.D., Daumas, S., Ferrington, L., Watson, R., Fan, Z., Hyman, B.T., Kelly, P.A., Bard, F.*, et al.* (2016). Early detection of cryptic memory and glucose uptake deficits in pre-pathological APP mice. Nat Commun *7*, 11761.
Bell, R.D., Winkler, E.A., Singh, I., Sagare, A.P., Deane, R., Wu, Z., Holtzman, D.M., Betsholtz, C., Armulik, A., Sallstrom, J.*, et al.* (2012). Apolipoprotein E controls cerebrovascular integrity via cyclophilin A. Nature *485*, 512-516.
Bharadwaj, D., Mold, C., Markham, E., and Du Clos, T.W. (2001). Serum amyloid P component binds to Fc gamma receptors and opsonizes particles for phagocytosis. J Immunol *166*, 6735-6741.
Bialas, A.R., and Stevens, B. (2013). TGF-beta signaling regulates neuronal C1q expression and developmental synaptic refinement. Nat Neurosci *16*, 1773-1782.
Bien-Ly, N., Boswell, C.A., Jeet, S., Beach, T.G., Hoyte, K., Luk, W., Shihadeh, V., Ulufatu, S., Foreman, O., Lu, Y.*, et al.* (2015). Lack of Widespread BBB Disruption in Alzheimer's Disease Models: Focus on Therapeutic Antibodies. Neuron *88*, 289-297.
Binette, P., Binette, M., and Calkins, E. (1974). The isolation and identification of the P-component of normal human plasma proteins. Biochem J *143*, 253-254.
Bladen, H.A., Nylen, M.U., and Glenner, G.G. (1966). The ultrastructure of human amyloid as revealed by the negative staining technique. J Ultrastruct Res *14*, 449-459.
Blander, J.M., and Medzhitov, R. (2004). Regulation of phagosome maturation by signals from toll-like receptors. Science *304*, 1014-1018.
Blennow, K., de Leon, M.J., and Zetterberg, H. (2006). Alzheimer's disease. Lancet *368*, 387-403.
Blennow, K., Wallin, A., Fredman, P., Karlsson, I., Gottfries, C.G., and Svennerholm, L. (1990). Blood-brain barrier disturbance in patients with Alzheimer's disease is related to vascular factors. Acta Neurol Scand *81*, 323-326.
Bliss, T.V., and Gardner-Medwin, A.R. (1973). Long-lasting potentiation of synaptic transmission in the dentate area of the unanaestetized rabbit following stimulation of the perforant path. J Physiol *232*, 357-374.
Bliss, T.V., and Lomo, T. (1973). Long-lasting potentiation of synaptic transmission in the dentate area of the anaesthetized rabbit following stimulation of the perforant path. J Physiol *232*, 331-356.
Boche, D., Perry, V.H., and Nicoll, J.A. (2013). Review: activation patterns of microglia and their identification in the human brain. Neuropathol Appl Neurobiol *39*, 3-18.
Bodin, K., Ellmerich, S., Kahan, M.C., Tennent, G.A., Loesch, A., Gilbertson, J.A., Hutchinson, W.L., Mangione, P.P., Gallimore, J.R., Millar, D.J.*, et al.* (2010). Antibodies to human serum amyloid P component eliminate visceral amyloid deposits. Nature *468*, 93-97.

Bottazzi, B., Doni, A., Garlanda, C., and Mantovani, A. (2010). An integrated view of humoral innate immunity: pentraxins as a paradigm. Annu Rev Immunol *28*, 157-183.
Botto, M., Hawkins, P.N., Bickerstaff, M.C., Herbert, J., Bygrave, A.E., McBride, A., Hutchinson, W.L., Tennent, G.A., Walport, M.J., and Pepys, M.B. (1997). Amyloid deposition is delayed in mice with targeted deletion of the serum amyloid P component gene. Nat Med *3*, 855-859.
Braak, H., and Braak, E. (1991). Neuropathological stageing of Alzheimer-related changes. Acta Neuropathol *82*, 239-259.
Braak, H., Braak, E., and Bohl, J. (1993). Staging of Alzheimer-related cortical destruction. Eur Neurol *33*, 403-408.
Breitner, J.C., Gau, B.A., Welsh, K.A., Plassman, B.L., McDonald, W.M., Helms, M.J., and Anthony, J.C. (1994). Inverse association of anti-inflammatory treatments and Alzheimer's disease: initial results of a co-twin control study. Neurology *44*, 227-232.
Brickell, K.L., Steinbart, E.J., Rumbaugh, M., Payami, H., Schellenberg, G.D., Van Deerlin, V., Yuan, W., and Bird, T.D. (2006). Early-onset Alzheimer disease in families with late-onset Alzheimer disease: a potential important subtype of familial Alzheimer disease. Arch Neurol *63*, 1307-1311.
Bridges, L.R., Andoh, J., Lawrence, A.J., Khoong, C.H., Poon, W.W., Esiri, M.M., Markus, H.S., and Hainsworth, A.H. (2014). Blood-brain barrier dysfunction and cerebral small vessel disease (arteriolosclerosis) in brains of older people. J Neuropathol Exp Neurol *73*, 1026-1033.
Brightman, M.W., and Reese, T.S. (1969). Junctions between intimately apposed cell membranes in the vertebrate brain. J Cell Biol *40*, 648-677.
Brodaty, H., and Low, L.F. (2003). Aggression in the elderly. J Clin Psychiatry *64 Suppl 4*, 36-43.
Busche, M.A., Chen, X., Henning, H.A., Reichwald, J., Staufenbiel, M., Sakmann, B., and Konnerth, A. (2012). Critical role of soluble amyloid-beta for early hippocampal hyperactivity in a mouse model of Alzheimer's disease. Proc Natl Acad Sci U S A *109*, 8740-8745.
Busche, M.A., Eichhoff, G., Adelsberger, H., Abramowski, D., Wiederhold, K.H., Haass, C., Staufenbiel, M., Konnerth, A., and Garaschuk, O. (2008). Clusters of hyperactive neurons near amyloid plaques in a mouse model of Alzheimer's disease. Science *321*, 1686-1689.
Cacucci, F., Yi, M., Wills, T.J., Chapman, P., and O'Keefe, J. (2008). Place cell firing correlates with memory deficits and amyloid plaque burden in Tg2576 Alzheimer mouse model. Proc Natl Acad Sci U S A *105*, 7863-7868.
Cai, Y., An, S.S., and Kim, S. (2015). Mutations in presenilin 2 and its implications in Alzheimer's disease and other dementia-associated disorders. Clin Interv Aging *10*, 1163-1172.
Calhoun, M.E., Burgermeister, P., Phinney, A.L., Stalder, M., Tolnay, M., Wiederhold, K.H., Abramowski, D., Sturchler-Pierrat, C., Sommer, B., Staufenbiel, M.*, et al.* (1999). Neuronal overexpression of mutant amyloid precursor protein results in prominent deposition of cerebrovascular amyloid. Proc Natl Acad Sci U S A *96*, 14088-14093.
Candelario-Jalil, E., Yang, Y., and Rosenberg, G.A. (2009). Diverse roles of matrix metalloproteinases and tissue inhibitors of metalloproteinases in neuroinflammation and cerebral ischemia. Neuroscience *158*, 983-994.
Cao, L., Schrank, B.R., Rodriguez, S., Benz, E.G., Moulia, T.W., Rickenbacher, G.T., Gomez, A.C., Levites, Y., Edwards, S.R., Golde, T.E.*, et al.* (2012). Abeta alters the

connectivity of olfactory neurons in the absence of amyloid plaques in vivo. Nat Commun *3*, 1009.
Caroni, P., Donato, F., and Muller, D. (2012). Structural plasticity upon learning: regulation and functions. Nat Rev Neurosci *13*, 478-490.
Caserta, M.T., Caccioppo, D., Lapin, G.D., Ragin, A., and Groothuis, D.R. (1998). Blood-brain barrier integrity in Alzheimer's disease patients and elderly control subjects. J Neuropsychiatry Clin Neurosci *10*, 78-84.
Castano, A.P., Lin, S.L., Surowy, T., Nowlin, B.T., Turlapati, S.A., Patel, T., Singh, A., Li, S., Lupher, M.L., Jr., and Duffield, J.S. (2009). Serum amyloid P inhibits fibrosis through Fc gamma R-dependent monocyte-macrophage regulation in vivo. Sci Transl Med *1*, 5ra13.
Cathcart, E.S., Comerford, F.R., and Cohen, A.S. (1965). Immunologic Studies on a Protein Extracted from Human Secondary Amyloid. N Engl J Med *273*, 143-146.
Cathcart, E.S., Shirahama, T., and Cohen, A.S. (1967a). Isolation and identification of a plasma component of amyloid. Biochim Biophys Acta *147*, 392-393.
Cathcart, E.S., Wollheim, F.A., and Cohen, A.S. (1967b). Plasma protein constituents of amyloid fibrils. J Immunol *99*, 376-385.
Chapman, P.F., White, G.L., Jones, M.W., Cooper-Blacketer, D., Marshall, V.J., Irizarry, M., Younkin, L., Good, M.A., Bliss, T.V., Hyman, B.T.*, et al.* (1999). Impaired synaptic plasticity and learning in aged amyloid precursor protein transgenic mice. Nat Neurosci *2*, 271-276.
Charidimou, A., Gang, Q., and Werring, D.J. (2012). Sporadic cerebral amyloid angiopathy revisited: recent insights into pathophysiology and clinical spectrum. J Neurol Neurosurg Psychiatry *83*, 124-137.
Cheng, I.H., Scearce-Levie, K., Legleiter, J., Palop, J.J., Gerstein, H., Bien-Ly, N., Puolivali, J., Lesne, S., Ashe, K.H., Muchowski, P.J.*, et al.* (2007). Accelerating amyloid-beta fibrillization reduces oligomer levels and functional deficits in Alzheimer disease mouse models. J Biol Chem *282*, 23818-23828.
Cho, R.W., Park, J.M., Wolff, S.B., Xu, D., Hopf, C., Kim, J.A., Reddy, R.C., Petralia, R.S., Perin, M.S., Linden, D.J.*, et al.* (2008). mGluR1/5-dependent long-term depression requires the regulated ectodomain cleavage of neuronal pentraxin NPR by TACE. Neuron *57*, 858-871.
Cohen, E., Paulsson, J.F., Blinder, P., Burstyn-Cohen, T., Du, D., Estepa, G., Adame, A., Pham, H.M., Holzenberger, M., Kelly, J.W.*, et al.* (2009). Reduced IGF-1 signaling delays age-associated proteotoxicity in mice. Cell *139*, 1157-1169.
Conde, J.R., and Streit, W.J. (2006). Microglia in the aging brain. J Neuropathol Exp Neurol *65*, 199-203.
Coria, F., Castano, E., Prelli, F., Larrondo-Lillo, M., van Duinen, S., Shelanski, M.L., and Frangione, B. (1988). Isolation and characterization of amyloid P component from Alzheimer's disease and other types of cerebral amyloidosis. Lab Invest *58*, 454-458.
Crawford, J.R., Bjorklund, N.L., Taglialatela, G., and Gomer, R.H. (2012). Brain serum amyloid P levels are reduced in individuals that lack dementia while having Alzheimer's disease neuropathology. Neurochem Res *37*, 795-801.
Cummings, C.W. (2017). Ethics in the twenty first century otolaryngology. Braz J Otorhinolaryngol.
Cummings, D.M., Benway, T.A., Ho, H., Tedoldi, A., Fernandes Freitas, M.M., Shahab, L., Murray, C.E., Richard-Loendt, A., Brandner, S., Lashley, T.*, et al.* (2017). Neuronal and Peripheral Pentraxins Modify Glutamate Release and may Interact in Blood-Brain Barrier Failure. Cereb Cortex, 1-12.

Cummings, D.M., Liu, W., Portelius, E., Bayram, S., Yasvoina, M., Ho, S.H., Smits, H., Ali, S.S., Steinberg, R., Pegasiou, C.M*., et al.* (2015). First effects of rising amyloid-beta in transgenic mouse brain: synaptic transmission and gene expression. Brain *138*, 1992-2004.
Davalos, D., Grutzendler, J., Yang, G., Kim, J.V., Zuo, Y., Jung, S., Littman, D.R., Dustin, M.L., and Gan, W.B. (2005). ATP mediates rapid microglial response to local brain injury in vivo. Nat Neurosci *8*, 752-758.
Deacon, R.M., and Rawlins, J.N. (2006). T-maze alternation in the rodent. Nat Protoc *1*, 7-12.
Deane, R., Sagare, A., Hamm, K., Parisi, M., Lane, S., Finn, M.B., Holtzman, D.M., and Zlokovic, B.V. (2008). apoE isoform-specific disruption of amyloid beta peptide clearance from mouse brain. JClinInvest *118*, 4002-4013.
Deb, S., and Gottschall, P.E. (1996). Increased production of matrix metalloproteinases in enriched astrocyte and mixed hippocampal cultures treated with beta-amyloid peptides. J Neurochem *66*, 1641-1647.
Deban, L., Jaillon, S., Garlanda, C., Bottazzi, B., and Mantovani, A. (2011). Pentraxins in innate immunity: lessons from PTX3. Cell Tissue Res *343*, 237-249.
DeFelipe, J., and Farinas, I. (1992). The pyramidal neuron of the cerebral cortex: morphological and chemical characteristics of the synaptic inputs. Prog Neurobiol *39*, 563-607.
DeGregorio-Rocasolano, N., Gasull, T., and Trullas, R. (2001). Overexpression of neuronal pentraxin 1 is involved in neuronal death evoked by low K(+) in cerebellar granule cells. J Biol Chem *276*, 796-803.
DeKosky, S.T., and Scheff, S.W. (1990). Synapse loss in frontal cortex biopsies in Alzheimer's disease: correlation with cognitive severity. Ann Neurol *27*, 457-464.
del Rio, J.A., Heimrich, B., Soriano, E., Schwegler, H., and Frotscher, M. (1991). Proliferation and differentiation of glial fibrillary acidic protein-immunoreactive glial cells in organotypic slice cultures of rat hippocampus. Neuroscience *43*, 335-347.
Desmond, N.L., and Levy, W.B. (1986). Changes in the postsynaptic density with long-term potentiation in the dentate gyrus. J Comp Neurol *253*, 476-482.
Dodds, D.C., Omeis, I.A., Cushman, S.J., Helms, J.A., and Perin, M.S. (1997). Neuronal pentraxin receptor, a novel putative integral membrane pentraxin that interacts with neuronal pentraxin 1 and 2 and taipoxin-associated calcium-binding protein. Journal of Biological Chemistry *272*, 21488-21494.
Dowton, S.B., and McGrew, S.D. (1990). Rat serum amyloid P component. Analysis of cDNA sequence and gene expression. Biochem J *270*, 553-556.
Du Clos, T.W. (1989). C-reactive protein reacts with the U1 small nuclear ribonucleoprotein. J Immunol *143*, 2553-2559.
Du Clos, T.W. (1996). The interaction of C-reactive protein and serum amyloid P component with nuclear antigens. Mol Biol Rep *23*, 253-260.
Du Clos, T.W., Mold, C., and Stump, R.F. (1990). Identification of a polypeptide sequence that mediates nuclear localization of the acute phase protein C-reactive protein. J Immunol *145*, 3869-3875.
Duan, H., Wearne, S.L., Rocher, A.B., Macedo, A., Morrison, J.H., and Hof, P.R. (2003). Age-related dendritic and spine changes in corticocortically projecting neurons in macaque monkeys. Cereb Cortex *13*, 950-961.
Dudchenko, P.A. (2001). How do animals actually solve the T maze? Behavioral neuroscience *115*, 850-860.
Dudchenko, P.A. (2004). An overview of the tasks used to test working memory in rodents. Neurosci Biobehav Rev *28*, 699-709.

Duong, T., Acton, P.J., and Johnson, R.A. (1998). The in vitro neuronal toxicity of pentraxins associated with Alzheimer's disease brain lesions. Brain Res *813*, 303-312.
Duong, T., Doucette, T., Zidenberg, N.A., Jacobs, R.W., and Scheibel, A.B. (1993). Microtubule-associated proteins tau and amyloid P component in Alzheimer's disease. Brain Res *603*, 74-86.
Duong, T., and Gallagher, K.A. (1994). Immunoreactivity patterns in neurofibrillary tangles of the inferior temporal cortex in Alzheimer disease. Mol Chem Neuropathol *22*, 105-122.
Duong, T., Nikolaeva, M., and Acton, P.J. (1997). C-reactive protein-like immunoreactivity in the neurofibrillary tangles of Alzheimer's disease. Brain Res *749*, 152-156.
Duong, T., Pommier, E.C., and Scheibel, A.B. (1989). Immunodetection of the amyloid P component in Alzheimer's disease. Acta Neuropathol *78*, 429-437.
Dyck, R.F., Evans, D.J., Lockwood, C.M., Rees, A.J., Turner, D., and Pepys, M.B. (1980a). Amyloid P-component in human glomerular basement membrane. Abnormal patterns of immunofluorescent staining in glomerular disease. Lancet *2*, 606-609.
Dyck, R.F., Lockwood, C.M., Kershaw, M., McHugh, N., Duance, V.C., Baltz, M.L., and Pepys, M.B. (1980b). Amyloid P-component is a constituent of normal human glomerular basement membrane. J Exp Med *152*, 1162-1174.
Edison, P., Archer, H.A., Gerhard, A., Hinz, R., Pavese, N., Turkheimer, F.E., Hammers, A., Tai, Y.F., Fox, N., Kennedy, A.*, et al.* (2008). Microglia, amyloid, and cognition in Alzheimer's disease: An [11C](R)PK11195-PET and [11C]PIB-PET study. Neurobiol Dis *32*, 412-419.
Emsley, J., White, H.E., O'Hara, B.P., Oliva, G., Srinivasan, N., Tickle, I.J., Blundell, T.L., Pepys, M.B., and Wood, S.P. (1994). Structure of pentameric human serum amyloid P component. Nature *367*, 338-345.
Farrall, A.J., and Wardlaw, J.M. (2009). Blood-brain barrier: ageing and microvascular disease--systematic review and meta-analysis. Neurobiol Aging *30*, 337-352.
Feng, G., Mellor, R.H., Bernstein, M., Keller-Peck, C., Nguyen, Q.T., Wallace, M., Nerbonne, J.M., Lichtman, J.W., and Sanes, J.R. (2000). Imaging neuronal subsets in transgenic mice expressing multiple spectral variants of GFP. Neuron *28*, 41-51.
Fifkova, E., and Anderson, C.L. (1981). Stimulation-induced changes in dimensions of stalks of dendritic spines in the dentate molecular layer. Exp Neurol *74*, 621-627.
Figueiro-Silva, J., Gruart, A., Clayton, K.B., Podlesniy, P., Abad, M.A., Gasull, X., Delgado-Garcia, J.M., and Trullas, R. (2015). Neuronal pentraxin 1 negatively regulates excitatory synapse density and synaptic plasticity. J Neurosci *35*, 5504-5521.
Frank, M.M., and Fries, L.F. (1991). The role of complement in inflammation and phagocytosis. Immunol Today *12*, 322-326.
Frank-Cannon, T.C., Alto, L.T., McAlpine, F.E., and Tansey, M.G. (2009). Does neuroinflammation fan the flame in neurodegenerative diseases? Mol Neurodegener *4*, 47.
Frolich, L., Kornhuber, J., Ihl, R., Fritze, J., Maurer, K., and Riederer, P. (1991). Integrity of the blood-CSF barrier in dementia of Alzheimer type: CSF/serum ratios of albumin and IgG. Eur Arch Psychiatry Clin Neurosci *240*, 363-366.
Fu, M., and Zuo, Y. (2011). Experience-dependent structural plasticity in the cortex. Trends Neurosci *34*, 177-187.

Gaboriaud, C., Thielens, N.M., Gregory, L.A., Rossi, V., Fontecilla-Camps, J.C., and Arlaud, G.J. (2004). Structure and activation of the C1 complex of complement: unraveling the puzzle. Trends Immunol *25*, 368-373.
Garlanda, C., Bottazzi, B., Bastone, A., and Mantovani, A. (2005). Pentraxins at the crossroads between innate immunity, inflammation, matrix deposition, and female fertility. Annu Rev Immunol *23*, 337-366.
Gerlach, J., Donkels, C., Munzner, G., and Haas, C.A. (2016). Persistent Gliosis Interferes with Neurogenesis in Organotypic Hippocampal Slice Cultures. Front Cell Neurosci *10*, 131.
Gewurz, H., Zhang, X.H., and Lint, T.F. (1995). Structure and function of the pentraxins. Curr Opin Immunol *7*, 54-64.
Gillmore, J.D., Hutchinson, W.L., Herbert, J., Bybee, A., Mitchell, D.A., Hasserjian, R.P., Yamamura, K., Suzuki, M., Sabin, C.A., and Pepys, M.B. (2004). Autoimmunity and glomerulonephritis in mice with targeted deletion of the serum amyloid P component gene: SAP deficiency or strain combination? Immunology *112*, 255-264.
Giulian, D. (1987). Ameboid microglia as effectors of inflammation in the central nervous system. J Neurosci Res *18*, 155-171, 132-153.
Gogolla, N., Galimberti, I., DePaola, V., and Caroni, P. (2006). Staining protocol for organotypic hippocampal slice cultures. Nat Protoc *1*, 2452-2456.
Golde, T.E., Schneider, L.S., and Koo, E.H. (2011). Anti-abeta therapeutics in Alzheimer's disease: the need for a paradigm shift. Neuron *69*, 203-213.
Graeber, M.B., Li, W., and Rodriguez, M.L. (2011). Role of microglia in CNS inflammation. FEBS Lett *585*, 3798-3805.
Graeber, M.B., Tetzlaff, W., Streit, W.J., and Kreutzberg, G.W. (1988). Microglial cells but not astrocytes undergo mitosis following rat facial nerve axotomy. Neurosci Lett *85*, 317-321.
Greenbaum, D., Colangelo, C., Williams, K., and Gerstein, M. (2003). Comparing protein abundance and mRNA expression levels on a genomic scale. Genome Biol *4*, 117.
Grueninger, F., Bohrmann, B., Czech, C., Ballard, T.M., Frey, J.R., Weidensteiner, C., von Kienlin, M., and Ozmen, L. (2010). Phosphorylation of Tau at S422 is enhanced by Abeta in TauPS2APP triple transgenic mice. Neurobiol Dis *37*, 294-306.
Gunter, S.M., Jones, K.M., Zhan, B., Essigmann, H.T., Murray, K.O., Garcia, M.N., Gorchakov, R., Bottazzi, M.E., Hotez, P.J., and Brown, E.L. (2016). Identification and Characterization of the Trypanosoma cruzi B-cell Superantigen Tc24. Am J Trop Med Hyg *94*, 114-121.
Haass, C., and Selkoe, D.J. (2007). Soluble protein oligomers in neurodegeneration: lessons from the Alzheimer's amyloid beta-peptide. Nat Rev Mol Cell Biol *8*, 101-112.
Hamazaki, H. (1995). Amyloid P component promotes aggregation of Alzheimer's beta-amyloid peptide. Biochem Biophys Res Commun *211*, 349-353.
Harris, K.M., Fiala, J.C., and Ostroff, L. (2003). Structural changes at dendritic spine synapses during long-term potentiation. Philos Trans R Soc Lond B Biol Sci *358*, 745-748.
Hartz, A.M., Bauer, B., Soldner, E.L., Wolf, A., Boy, S., Backhaus, R., Mihaljevic, I., Bogdahn, U., Klunemann, H.H., Schuierer, G.*, et al.* (2012). Amyloid-beta contributes to blood-brain barrier leakage in transgenic human amyloid precursor protein mice and in humans with cerebral amyloid angiopathy. Stroke *43*, 514-523.

Hasbani, M.J., Schlief, M.L., Fisher, D.A., and Goldberg, M.P. (2001). Dendritic spines lost during glutamate receptor activation reemerge at original sites of synaptic contact. J Neurosci *21*, 2393-2403.
Hawkins, P.N., Myers, M.J., Epenetos, A.A., Caspi, D., and Pepys, M.B. (1988). Specific localization and imaging of amyloid deposits in vivo using 123I-labeled serum amyloid P component. J Exp Med *167*, 903-913.
Hawkins, P.N., Rossor, M.N., Gallimore, J.R., Miller, B., Moore, E.G., and Pepys, M.B. (1994). Concentration of serum amyloid P component in the CSF as a possible marker of cerebral amyloid deposits in Alzheimer's disease. Biochem Biophys Res Commun *201*, 722-726.
Hawrylycz, M.J., Lein, E.S., Guillozet-Bongaarts, A.L., Shen, E.H., Ng, L., Miller, J.A., van de Lagemaat, L.N., Smith, K.A., Ebbert, A., Riley, Z.L.*, et al.* (2012). An anatomically comprehensive atlas of the adult human brain transcriptome. Nature *489*, 391-399.
He, B.P., Tay, S.S., and Leong, S.K. (1997). Microglia responses in the CNS following sciatic nerve transection in C57BL/Wld(s) and BALB/c mice. Exp Neurol *146*, 587-595.
Hefendehl, J.K., Neher, J.J., Suhs, R.B., Kohsaka, S., Skodras, A., and Jucker, M. (2014). Homeostatic and injury-induced microglia behavior in the aging brain. Aging Cell *13*, 60-69.
Herms, J., and Dorostkar, M.M. (2016). Dendritic Spine Pathology in Neurodegenerative Diseases. Annu Rev Pathol *11*, 221-250.
Hicks, P.S., Saunero-Nava, L., Du Clos, T.W., and Mold, C. (1992). Serum amyloid P component binds to histones and activates the classical complement pathway. J Immunol *149*, 3689-3694.
Hind, C.R., Collins, P.M., Baltz, M.L., and Pepys, M.B. (1985). Human serum amyloid P component, a circulating lectin with specificity for the cyclic 4,6-pyruvate acetal of galactose. Interactions with various bacteria. Biochem J *225*, 107-111.
Holtmaat, A., and Svoboda, K. (2009). Experience-dependent structural synaptic plasticity in the mammalian brain. Nat Rev Neurosci *10*, 647-658.
Hong, S., Beja-Glasser, V.F., Nfonoyim, B.M., Frouin, A., Li, S., Ramakrishnan, S., Merry, K.M., Shi, Q., Rosenthal, A., Barres, B.A.*, et al.* (2016). Complement and microglia mediate early synapse loss in Alzheimer mouse models. Science *352*, 712-716.
Honkura, N., Matsuzaki, M., Noguchi, J., Ellis-Davies, G.C., and Kasai, H. (2008). The subspine organization of actin fibers regulates the structure and plasticity of dendritic spines. Neuron *57*, 719-729.
Horning, S.M., Melrose, R., and Sultzer, D. (2014). Insight in Alzheimer's disease and its relation to psychiatric and behavioral disturbances. Int J Geriatr Psychiatry *29*, 77-84.
Horvath, A., Andersen, I., Junker, K., Lyck Fogh-Schultz, B., Holm Nielsen, E., Gizurarson, S., Andersen, O., Karman, J., Rajnavolgyi, E., Erdei, A.*, et al.* (2001). Serum amyloid P component inhibits influenza A virus infections: in vitro and in vivo studies. Antiviral Res *52*, 43-53.
Howlett, D.R., Richardson, J.C., Austin, A., Parsons, A.A., Bate, S.T., Davies, D.C., and Gonzalez, M.I. (2004). Cognitive correlates of Abeta deposition in male and female mice bearing amyloid precursor protein and presenilin-1 mutant transgenes. Brain Res *1017*, 130-136.
Hutchinson, W.L., Hohenester, E., and Pepys, M.B. (2000). Human serum amyloid P component is a single uncomplexed pentamer in whole serum. Mol Med *6*, 482-493.

Hyman, B.T., Phelps, C.H., Beach, T.G., Bigio, E.H., Cairns, N.J., Carrillo, M.C., Dickson, D.W., Duyckaerts, C., Frosch, M.P., Masliah, E.*, et al.* (2012). National Institute on Aging-Alzheimer's Association guidelines for the neuropathologic assessment of Alzheimer's disease. Alzheimers Dement *8*, 1-13.
Iadecola, C., and Nedergaard, M. (2007). Glial regulation of the cerebral microvasculature. Nat Neurosci *10*, 1369-1376.
Iseki, E., Amano, N., Matsuishi, T., Yokoi, S., Arai, N., and Yagishita, S. (1988). A case of familial, atypical Alzheimer's disease: immunohistochemical study of amyloid P-component. Neuropathol Appl Neurobiol *14*, 169-174.
Isokawa, M., and Levesque, M.F. (1991). Increased NMDA responses and dendritic degeneration in human epileptic hippocampal neurons in slices. Neurosci Lett *132*, 212-216.
Iwanaga, T., Wakasugi, S., Inomoto, T., Uehira, M., Ohnishi, S., Nishiguchi, S., Araki, K., Uno, M., Miyazaki, J., Maeda, S.*, et al.* (1989). Liver-specific and high-level expression of human serum amyloid P component gene in transgenic mice. Dev Genet *10*, 365-371.
Jacobsen, J.S., Wu, C.C., Redwine, J.M., Comery, T.A., Arias, R., Bowlby, M., Martone, R., Morrison, J.H., Pangalos, M.N., Reinhart, P.H.*, et al.* (2006). Early-onset behavioral and synaptic deficits in a mouse model of Alzheimer's disease. Proc Natl Acad Sci U S A *103*, 5161-5166.
Jankowsky, J.L., Fadale, D.J., Anderson, J., Xu, G.M., Gonzales, V., Jenkins, N.A., Copeland, N.G., Lee, M.K., Younkin, L.H., Wagner, S.L.*, et al.* (2004). Mutant presenilins specifically elevate the levels of the 42 residue beta-amyloid peptide in vivo: evidence for augmentation of a 42-specific gamma secretase. Hum Mol Genet *13*, 159-170.
Jaroniec, C.P., MacPhee, C.E., Bajaj, V.S., McMahon, M.T., Dobson, C.M., and Griffin, R.G. (2004). High-resolution molecular structure of a peptide in an amyloid fibril determined by magic angle spinning NMR spectroscopy. Proc Natl Acad Sci U S A *101*, 711-716.
Jellinger, K.A., and Attems, J. (2013). Neuropathological approaches to cerebral aging and neuroplasticity. Dialogues Clin Neurosci *15*, 29-43.
Job, E.R., Bottazzi, B., Gilbertson, B., Edenborough, K.M., Brown, L.E., Mantovani, A., Brooks, A.G., and Reading, P.C. (2013). Serum amyloid P is a sialylated glycoprotein inhibitor of influenza A viruses. PLoS One *8*, e59623.
Kalaria, R.N. (1996). Cerebral vessels in ageing and Alzheimer's disease. Pharmacol Ther *72*, 193-214.
Kalaria, R.N., Galloway, P.G., and Perry, G. (1991a). Widespread serum amyloid P immunoreactivity in cortical amyloid deposits and the neurofibrillary pathology of Alzheimer's disease and other degenerative disorders. Neuropathol Appl Neurobiol *17*, 189-201.
Kalaria, R.N., Golde, T.E., Cohen, M.L., and Younkin, S.G. (1991b). Serum amyloid P in Alzheimer's disease. Implications for dysfunction of the blood-brain barrier. AnnNYAcadSci *640*, 145-148.
Kalaria, R.N., Golde, T.E., Cohen, M.L., and Younkin, S.G. (1991c). Serum amyloid P in Alzheimer's disease. Implications for dysfunction of the blood-brain barrier. Ann N Y Acad Sci *640*, 145-148.
Kalaria, R.N., and Grahovac, I. (1990). Serum amyloid P immunoreactivity in hippocampal tangles, plaques and vessels: implications for leakage across the blood-brain barrier in Alzheimer's disease. Brain Res *516*, 349-353.

Kalaria, R.N., and Kroon, S.N. (1992). Complement inhibitor C4-binding protein in amyloid deposits containing serum amyloid P in Alzheimer's disease. Biochem Biophys Res Commun *186*, 461-466.
Kalaria, R.N., and Perry, G. (1993). Amyloid P component and other acute-phase proteins associated with cerebellar A beta-deposits in Alzheimer's disease. Brain Res *631*, 151-155.
Kettenmann, H., Hanisch, U.K., Noda, M., and Verkhratsky, A. (2011). Physiology of microglia. Physiol Rev *91*, 461-553.
Kimura, M., Arai, H., Takahashi, T., and Iwamoto, N. (1994). Amyloid-P-component-like immunoreactivity in beta/A4-immunoreactive deposits in Alzheimer-type dementia brains. J Neurol *241*, 170-174.
Kinoshita, C.M., Ying, S.C., Hugli, T.E., Siegel, J.N., Potempa, L.A., Jiang, H., Houghten, R.A., and Gewurz, H. (1989). Elucidation of a protease-sensitive site involved in the binding of calcium to C-reactive protein. Biochemistry *28*, 9840-9848.
Kirkpatrick, L.L., Matzuk, M.M., Dodds, D.C., and Perin, M.S. (2000). Biochemical interactions of the neuronal pentraxins. Neuronal pentraxin (NP) receptor binds to taipoxin and taipoxin-associated calcium-binding protein 49 via NP1 and NP2. J Biol Chem *275*, 17786-17792.
Kisilevsky, R., and Fraser, P. (1996). Proteoglycans and amyloid fibrillogenesis. Ciba Found Symp *199*, 58-67; discussion 68-72, 90-103.
Knobloch, M., and Mansuy, I.M. (2008). Dendritic spine loss and synaptic alterations in Alzheimer's disease. Mol Neurobiol *37*, 73-82.
Koch, S.M., and Ullian, E.M. (2010). Neuronal pentraxins mediate silent synapse conversion in the developing visual system. J Neurosci *30*, 5404-5414.
Koenigsknecht, J., and Landreth, G. (2004). Microglial phagocytosis of fibrillar beta-amyloid through a beta1 integrin-dependent mechanism. J Neurosci *24*, 9838-9846.
Koenigsknecht-Talboo, J., and Landreth, G.E. (2005). Microglial phagocytosis induced by fibrillar beta-amyloid and IgGs are differentially regulated by proinflammatory cytokines. J Neurosci *25*, 8240-8249.
Koenigsknecht-Talboo, J., Meyer-Luehmann, M., Parsadanian, M., Garcia-Alloza, M., Finn, M.B., Hyman, B.T., Bacskai, B.J., and Holtzman, D.M. (2008). Rapid microglial response around amyloid pathology after systemic anti-Abeta antibody administration in PDAPP mice. J Neurosci *28*, 14156-14164.
Kolstoe, S., and Wood, S. (2010). Serum Amyloid P Component. In Protein Misfolding Diseases: Current and Emerging Principles and Therapies, M. Ramirez-Alvarado, J.W. Kelly, and C.M. Dobson, eds. (Hoboken, NJ, USA: John Wiley & Sons, Inc.), pp. 571-584.
Kolstoe, S.E., Ridha, B.H., Bellotti, V., Wang, N., Robinson, C.V., Crutch, S.J., Keir, G., Kukkastenvehmas, R., Gallimore, J.R., Hutchinson, W.L.*, et al.* (2009). Molecular dissection of Alzheimer's disease neuropathology by depletion of serum amyloid P component. Proc Natl Acad Sci U S A *106*, 7619-7623.
Korotzer, A.R., Pike, C.J., and Cotman, C.W. (1993). beta-Amyloid peptides induce degeneration of cultured rat microglia. Brain Res *624*, 121-125.
Kushner, I., and Kaplan, M.H. (1961). Studies of acute phase protein. I. An immunohistochemical method for the localization of Cx-reactive protein in rabbits. Association with necrosis in local inflammatory lesions. J Exp Med *114*, 961-974.
Lalonde, R., Dumont, M., Staufenbiel, M., Sturchler-Pierrat, C., and Strazielle, C. (2002). Spatial learning, exploration, anxiety, and motor coordination in female APP23 transgenic mice with the Swedish mutation. Brain Res *956*, 36-44.

Lanz, T.A., Carter, D.B., and Merchant, K.M. (2003). Dendritic spine loss in the hippocampus of young PDAPP and Tg2576 mice and its prevention by the ApoE2 genotype. Neurobiol Dis *13*, 246-253.
Lashley, T., Rohrer, J.D., Bandopadhyay, R., Fry, C., Ahmed, Z., Isaacs, A.M., Brelstaff, J.H., Borroni, B., Warren, J.D., Troakes, C.*, et al.* (2011). A comparative clinical, pathological, biochemical and genetic study of fused in sarcoma proteinopathies. Brain *134*, 2548-2564.
Le, P.T., Muller, M.T., and Mortensen, R.F. (1982). Acute phase reactants of mice. I. Isolation of serum amyloid P-component (SAP) and its induction by a monokine. J Immunol *129*, 665-672.
Lee, K.W., Lee, S.H., Kim, H., Song, J.S., Yang, S.D., Paik, S.G., and Han, P.L. (2004). Progressive cognitive impairment and anxiety induction in the absence of plaque deposition in C57BL/6 inbred mice expressing transgenic amyloid precursor protein. J Neurosci Res *76*, 572-580.
Lee, S.J., Wei, M., Zhang, C., Maxeiner, S., Pak, C., Calado Botelho, S., Trotter, J., Sterky, F.H., and Sudhof, T.C. (2017). Presynaptic Neuronal Pentraxin Receptor Organizes Excitatory and Inhibitory Synapses. J Neurosci *37*, 1062-1080.
Li, L., Gervasi, N., and Girault, J.A. (2015). Dendritic geometry shapes neuronal cAMP signalling to the nucleus. Nat Commun *6*, 6319.
Li, Y., Tan, M.S., Jiang, T., and Tan, L. (2014). Microglia in Alzheimer's disease. Biomed Res Int *2014*, 437483.
Lu, J., Marnell, L.L., Marjon, K.D., Mold, C., Du Clos, T.W., and Sun, P.D. (2008). Structural recognition and functional activation of FcgammaR by innate pentraxins. Nature *456*, 989-992.
Majno, G., Palade, G.E., and Schoefl, G.I. (1961). Studies on inflammation. II. The site of action of histamine and serotonin along the vascular tree: a topographic study. J Biophys Biochem Cytol *11*, 607-626.
Mandrekar, S., Jiang, Q., Lee, C.Y., Koenigsknecht-Talboo, J., Holtzman, D.M., and Landreth, G.E. (2009). Microglia mediate the clearance of soluble Abeta through fluid phase macropinocytosis. J Neurosci *29*, 4252-4262.
Manepalli, J., Grossberg, G.T., and Mueller, C. (1990). Prevalence of delirium and urinary tract infection in a psychogeriatric unit. J Geriatr Psychiatry Neurol *3*, 198-202.
Matarin, M., Salih, D.A., Yasvoina, M., Cummings, D.M., Guelfi, S., Liu, W., Nahaboo Solim, M.A., Moens, T.G., Paublete, R.M., Ali, S.S.*, et al.* (2015). A genome-wide gene-expression analysis and database in transgenic mice during development of amyloid or tau pathology. Cell Rep *10*, 633-644.
Matsuzaki, M., Ellis-Davies, G.C., Nemoto, T., Miyashita, Y., Iino, M., and Kasai, H. (2001). Dendritic spine geometry is critical for AMPA receptor expression in hippocampal CA1 pyramidal neurons. Nat Neurosci *4*, 1086-1092.
Matsuzaki, M., Honkura, N., Ellis-Davies, G.C., and Kasai, H. (2004). Structural basis of long-term potentiation in single dendritic spines. Nature *429*, 761-766.
McDermott, C., and Kelly, J.P. (2008). Comparison of the behavioural pharmacology of the Lister-Hooded with 2 commonly utilised albino rat strains. Prog Neuropsychopharmacol Biol Psychiatry *32*, 1816-1823.
Minami, T., Okazaki, J., Kawabata, A., Kuroda, R., and Okazaki, Y. (1998). Penetration of cisplatin into mouse brain by lipopolysaccharide. Toxicology *130*, 107-113.
Miskimon, M., Han, S., Lee, J.J., Ringkamp, M., Wilson, M.A., Petralia, R.S., Dong, X., Worley, P.F., Baraban, J.M., and Reti, I.M. (2014). Selective expression of Narp

in primary nociceptive neurons: role in microglia/macrophage activation following nerve injury. J Neuroimmunol *274*, 86-95.
Mold, C., Gresham, H.D., and Du Clos, T.W. (2001). Serum amyloid P component and C-reactive protein mediate phagocytosis through murine Fc gamma Rs. J Immunol *166*, 1200-1205.
Mold, M., Shrive, A.K., and Exley, C. (2012). Serum amyloid P component accelerates the formation and enhances the stability of amyloid fibrils in a physiologically significant under-saturated solution of amyloid-beta42. J Alzheimers Dis *29*, 875-881.
Montagne, A., Barnes, S.R., Sweeney, M.D., Halliday, M.R., Sagare, A.P., Zhao, Z., Toga, A.W., Jacobs, R.E., Liu, C.Y., Amezcua, L.*, et al.* (2015). Blood-brain barrier breakdown in the aging human hippocampus. Neuron *85*, 296-302.
Mosher, K.I., and Wyss-Coray, T. (2014). Microglial dysfunction in brain aging and Alzheimer's disease. Biochem Pharmacol *88*, 594-604.
Mostany, R., Anstey, J.E., Crump, K.L., Maco, B., Knott, G., and Portera-Cailliau, C. (2013). Altered synaptic dynamics during normal brain aging. J Neurosci *33*, 4094-4104.
Mu, Y., and Gage, F.H. (2011). Adult hippocampal neurogenesis and its role in Alzheimer's disease. Mol Neurodegener *6*, 85.
Mulder, S.D., Hack, C.E., van der Flier, W.M., Scheltens, P., Blankenstein, M.A., and Veerhuis, R. (2010). Evaluation of intrathecal serum amyloid P (SAP) and C-reactive protein (CRP) synthesis in Alzheimer's disease with the use of index values. J Alzheimers Dis *22*, 1073-1079.
Mulder, S.D., Veerhuis, R., Blankenstein, M.A., and Nielsen, H.M. (2012). The effect of amyloid associated proteins on the expression of genes involved in amyloid-beta clearance by adult human astrocytes. Experimental Neurology *233*, 373-379.
Negash, S., Wilson, R.S., Leurgans, S.E., Wolk, D.A., Schneider, J.A., Buchman, A.S., Bennett, D.A., and Arnold, S.E. (2013). Resilient brain aging: characterization of discordance between Alzheimer's disease pathology and cognition. Current Alzheimer research *10*, 844-851.
Nelson, S.R., Lyon, M., Gallagher, J.T., Johnson, E.A., and Pepys, M.B. (1991a). Isolation and characterization of the integral glycosaminoglycan constituents of human amyloid A and monoclonal light-chain amyloid fibrils. Biochem J *275 (Pt 1)*, 67-73.
Nelson, S.R., Tennent, G.A., Sethi, D., Gower, P.E., Ballardie, F.W., Amatayakul-Chantler, S., and Pepys, M.B. (1991b). Serum amyloid P component in chronic renal failure and dialysis. Clin Chim Acta *200*, 191-199.
Nimmerjahn, A., Kirchhoff, F., and Helmchen, F. (2005). Resting microglial cells are highly dynamic surveillants of brain parenchyma in vivo. Science *308*, 1314-1318.
Nimmerjahn, F., and Ravetch, J.V. (2008). Fcgamma receptors as regulators of immune responses. Nat Rev Immunol *8*, 34-47.
Njie, E.G., Boelen, E., Stassen, F.R., Steinbusch, H.W., Borchelt, D.R., and Streit, W.J. (2012). Ex vivo cultures of microglia from young and aged rodent brain reveal age-related changes in microglial function. Neurobiol Aging *33*, 195 e191-112.
Noursadeghi, M., Bickerstaff, M.C., Gallimore, J.R., Herbert, J., Cohen, J., and Pepys, M.B. (2000). Role of serum amyloid P component in bacterial infection: protection of the host or protection of the pathogen. Proc Natl Acad Sci U S A *97*, 14584-14589.

Nunomura, A., Perry, G., Pappolla, M.A., Wade, R., Hirai, K., Chiba, S., and Smith, M.A. (1999). RNA oxidation is a prominent feature of vulnerable neurons in Alzheimer's disease. J Neurosci *19*, 1959-1964.
O'Brien, R.J., Xu, D., Petralia, R.S., Steward, O., Huganir, R.L., and Worley, P. (1999). Synaptic clustering of AMPA receptors by the extracellular immediate-early gene product Narp. Neuron *23*, 309-323.
O'Keefe, J., and Nadel, L. (1978). The hippocampus as a cognitive map (Oxford: Oxford Univ. Press).
Oddo, S., Caccamo, A., Shepherd, J.D., Murphy, M.P., Golde, T.E., Kayed, R., Metherate, R., Mattson, M.P., Akbari, Y., and LaFerla, F.M. (2003). Triple-transgenic model of Alzheimer's disease with plaques and tangles: intracellular Abeta and synaptic dysfunction. Neuron *39*, 409-421.
Ogeng'o, J.A., Cohen, D.L., Sayi, J.G., Matuja, W.B., Chande, H.M., Kitinya, J.N., Kimani, J.K., Friedland, R.P., Mori, H., and Kalaria, R.N. (1996). Cerebral amyloid beta protein deposits and other Alzheimer lesions in non-demented elderly east Africans. Brain Pathol *6*, 101-107.
Ognibene, E., Middei, S., Daniele, S., Adriani, W., Ghirardi, O., Caprioli, A., and Laviola, G. (2005). Aspects of spatial memory and behavioral disinhibition in Tg2576 transgenic mice as a model of Alzheimer's disease. Behav Brain Res *156*, 225-232.
Ohl, F. (2005). Animal models of anxiety. Handb Exp Pharmacol, 35-69.
Orre, M., Kamphuis, W., Osborn, L.M., Melief, J., Kooijman, L., Huitinga, I., Klooster, J., Bossers, K., and Hol, E.M. (2014). Acute isolation and transcriptome characterization of cortical astrocytes and microglia from young and aged mice. Neurobiol Aging *35*, 1-14.
Osera, C., Pascale, A., Amadio, M., Venturini, L., Govoni, S., and Ricevuti, G. (2012). Pentraxins and Alzheimer's disease: at the interface between biomarkers and pharmacological targets. Ageing Res Rev *11*, 189-198.
Osmand, A.P., Friedenson, B., Gewurz, H., Painter, R.H., Hofmann, T., and Shelton, E. (1977). Characterization of C-reactive protein and the complement subcomponent C1t as homologous proteins displaying cyclic pentameric symmetry (pentraxins). Proc Natl Acad Sci U S A *74*, 739-743.
Paolicelli, R.C., Bolasco, G., Pagani, F., Maggi, L., Scianni, M., Panzanelli, P., Giustetto, M., Ferreira, T.A., Guiducci, E., Dumas, L.*, et al.* (2011). Synaptic pruning by microglia is necessary for normal brain development. Science *333*, 1456-1458.
Paolicelli, R.C., and Gross, C.T. (2011). Microglia in development: linking brain wiring to brain environment. Neuron Glia Biol *7*, 77-83.
Pardon, M.C., Sarmad, S., Rattray, I., Bates, T.E., Scullion, G.A., Marsden, C.A., Barrett, D.A., Lowe, J., and Kendall, D.A. (2009). Repeated novel cage exposure-induced improvement of early Alzheimer's-like cognitive and amyloid changes in TASTPM mice is unrelated to changes in brain endocannabinoids levels. Neurobiol Aging *30*, 1099-1113.
Parsley, S.L., Pilgram, S.M., Soto, F., Giese, K.P., and Edwards, F.A. (2007). Enriching the environment of alphaCaMKIIT286A mutant mice reveals that LTD occurs in memory processing but must be subsequently reversed by LTP. Learn Mem *14*, 75-83.
Paulin, J.J., Haslehurst, P., Fellows, A.D., Liu, W., Jackson, J.D., Joel, Z., Cummings, D.M., and Edwards, F.A. (2016). Large and Small Dendritic Spines Serve Different Interacting Functions in Hippocampal Synaptic Plasticity and Homeostasis. Neural Plast *2016*, 6170509.

Pellow, S., Chopin, P., File, S.E., and Briley, M. (1985). Validation of open:closed arm entries in an elevated plus-maze as a measure of anxiety in the rat. J Neurosci Methods *14*, 149-167.
Penzes, P., Cahill, M.E., Jones, K.A., VanLeeuwen, J.E., and Woolfrey, K.M. (2011). Dendritic spine pathology in neuropsychiatric disorders. Nat Neurosci *14*, 285-293.
Pepys, M.B. (1992). Amyloid P component and the diagnosis of amyloidosis. J Intern Med *232*, 519-521.
Pepys, M.B. (2006). Amyloidosis. Annu Rev Med *57*, 223-241.
Pepys, M.B., Baltz, M., Gomer, K., Davies, A.J., and Doenhoff, M. (1979). Serum amyloid P-component is an acute-phase reactant in the mouse. Nature *278*, 259-261.
Pepys, M.B., Booth, D.R., Hutchinson, W.L., Gallimore, J.R., Collins, P.M., and Hohenester, E. (1997). Amyloid P component. A critical review. Amyloid: International Journal of Experimental Clinical Investigation *4*, 274-295.
Pepys, M.B., Booth, S.E., Tennent, G.A., Butler, P.J., and Williams, D.G. (1994a). Binding of pentraxins to different nuclear structures: C-reactive protein binds to small nuclear ribonucleoprotein particles, serum amyloid P component binds to chromatin and nucleoli. Clin Exp Immunol *97*, 152-157.
Pepys, M.B., and Butler, P.J. (1987). Serum amyloid P component is the major calcium-dependent specific DNA binding protein of the serum. Biochem Biophys Res Commun *148*, 308-313.
Pepys, M.B., Dash, A.C., Markham, R.E., Thomas, H.C., Williams, B.D., and Petrie, A. (1978). Comparative clinical study of protein SAP (amyloid P component) and C-reactive protein in serum. Clin Exp Immunol *32*, 119-124.
Pepys, M.B., Herbert, J., Hutchinson, W.L., Tennent, G.A., Lachmann, H.J., Gallimore, J.R., Lovat, L.B., Bartfai, T., Alanine, A., Hertel, C.*, et al.* (2002). Targeted pharmacological depletion of serum amyloid P component for treatment of human amyloidosis. Nature *417*, 254-259.
Pepys, M.B., and Hirschfield, G.M. (2003). C-reactive protein: a critical update. J Clin Invest *111*, 1805-1812.
Pepys, M.B., Rademacher, T.W., Amatayakul-Chantler, S., Williams, P., Noble, G.E., Hutchinson, W.L., Hawkins, P.N., Nelson, S.R., Gallimore, J.R., Herbert, J.*, et al.* (1994b). Human serum amyloid P component is an invariant constituent of amyloid deposits and has a uniquely homogeneous glycostructure. Proc Natl Acad Sci U S A *91*, 5602-5606.
Pereira, G.K., Venturini, A.B., Silvestri, T., Dapieve, K.S., Montagner, A.F., Soares, F.Z., and Valandro, L.F. (2015). Low-temperature degradation of Y-TZP ceramics: A systematic review and meta-analysis. J Mech Behav Biomed Mater *55*, 151-163.
Perlmutter, L.S., Barron, E., Myers, M., Saperia, D., and Chui, H.C. (1995). Localization of amyloid P component in human brain: vascular staining patterns and association with Alzheimer's disease lesions. J Comp Neurol *352*, 92-105.
Perlmutter, L.S., Myers, M.A., and Barron, E. (1994). Vascular basement membrane components and the lesions of Alzheimer's disease: light and electron microscopic analyses. Microsc Res Tech *28*, 204-215.
Perry, V.H., Matyszak, M.K., and Fearn, S. (1993). Altered antigen expression of microglia in the aged rodent CNS. Glia *7*, 60-67.
Persidsky, Y., Stins, M., Way, D., Witte, M.H., Weinand, M., Kim, K.S., Bock, P., Gendelman, H.E., and Fiala, M. (1997). A model for monocyte migration through the blood-brain barrier during HIV-1 encephalitis. J Immunol *158*, 3499-3510.
Peters, A., Sethares, C., and Moss, M.B. (1998). The effects of aging on layer 1 in area 46 of prefrontal cortex in the rhesus monkey. Cereb Cortex *8*, 671-684.

Pilling, D., and Gomer, R.H. (2012). Differentiation of circulating monocytes into fibroblast-like cells. Methods Mol Biol *904*, 191-206.
Pisalyaput, K., and Tenner, A.J. (2008). Complement component C1q inhibits beta-amyloid- and serum amyloid P-induced neurotoxicity via caspase- and calpain-independent mechanisms. J Neurochem *104*, 696-707.
Price, J.L., McKeel, D.W., Jr., Buckles, V.D., Roe, C.M., Xiong, C., Grundman, M., Hansen, L.A., Petersen, R.C., Parisi, J.E., Dickson, D.W.*, et al.* (2009). Neuropathology of nondemented aging: presumptive evidence for preclinical Alzheimer disease. Neurobiol Aging *30*, 1026-1036.
Prut, L., and Belzung, C. (2003). The open field as a paradigm to measure the effects of drugs on anxiety-like behaviors: a review. Eur J Pharmacol *463*, 3-33.
Pugh, P.L., Richardson, J.C., Bate, S.T., Upton, N., and Sunter, D. (2007a). Non-cognitive behaviours in an APP/PS1 transgenic model of Alzheimer's disease. Behav Brain Res *178*, 18-28.
Pugh, P.L., Richardson, J.C., Bate, S.T., Upton, N., and Sunter, D. (2007b). Non-cognitive behaviours in an APP/PS1 transgenic model of Alzheimer's disease. Behavioural Brain Research *178*, 18-28.
Raisova, M., Hossini, A.M., Eberle, J., Riebeling, C., Wieder, T., Sturm, I., Daniel, P.T., Orfanos, C.E., and Geilen, C.C. (2001). The Bax/Bcl-2 ratio determines the susceptibility of human melanoma cells to CD95/Fas-mediated apoptosis. J Invest Dermatol *117*, 333-340.
Rassouli, M., Sambasivam, H., Azadi, P., Dell, A., Morris, H.R., Nagpurkar, A., Mookerjea, S., and Murray, R.K. (1992). Derivation of the amino acid sequence of rat C-reactive protein from cDNA cloning with additional studies on the nature of its dimeric component. J Biol Chem *267*, 2947-2954.
Rattray, I., Scullion, G.A., Soulby, A., Kendall, D.A., and Pardon, M.C. (2009). The occurrence of a deficit in contextual fear extinction in adult amyloid-over-expressing TASTPM mice is independent of the strength of conditioning but can be prevented by mild novel cage stress. Behav Brain Res *200*, 83-90.
Reinhold, A.K., and Rittner, H.L. (2017). Barrier function in the peripheral and central nervous system-a review. Pflugers Arch *469*, 123-134.
Ricklin, D., Hajishengallis, G., Yang, K., and Lambris, J.D. (2010). Complement: a key system for immune surveillance and homeostasis. Nat Immunol *11*, 785-797.
Ritchie, K., Carriere, I., Su, L., O'Brien, J.T., Lovestone, S., Wells, K., and Ritchie, C.W. (2017). The midlife cognitive profiles of adults at high risk of late-onset Alzheimer's disease: The PREVENT study. Alzheimers Dement.
Robey, F.A., and Liu, T.Y. (1981). Limulin: a C-reactive protein from Limulus polyphemus. J Biol Chem *256*, 969-975.
Rosenberg, G.A. (2014). Blood-Brain Barrier Permeability in Aging and Alzheimer's Disease. J Prev Alzheimers Dis *1*, 138-139.
Rosenberg, G.A., Bjerke, M., and Wallin, A. (2014). Multimodal markers of inflammation in the subcortical ischemic vascular disease type of vascular cognitive impairment. Stroke *45*, 1531-1538.
Rossner, W., and Tempel, K. (1966). [Quantitative determination of the permeability of the so-called blood-brain barrier of Evans blue (T 1824)]. Med Pharmacol Exp Int J Exp Med *14*, 169-182.
Roumenina, L.T., Ruseva, M.M., Zlatarova, A., Ghai, R., Kolev, M., Olova, N., Gadjeva, M., Agrawal, A., Bottazzi, B., Mantovani, A.*, et al.* (2006). Interaction of C1q with IgG1, C-reactive protein and pentraxin 3: mutational studies using

recombinant globular head modules of human C1q A, B, and C chains. Biochemistry *45*, 4093-4104.
Rovelet-Lecrux, A., Hannequin, D., Raux, G., Le Meur, N., Laquerriere, A., Vital, A., Dumanchin, C., Feuillette, S., Brice, A., Vercelletto, M.*, et al.* (2006). APP locus duplication causes autosomal dominant early-onset Alzheimer disease with cerebral amyloid angiopathy. Nat Genet *38*, 24-26.
Rozemuller, J.M., Stam, F.C., and Eikelenboom, P. (1990). Acute phase proteins are present in amorphous plaques in the cerebral but not in the cerebellar cortex of patients with Alzheimer's disease. Neurosci Lett *119*, 75-78.
Rubio-Perez, J.M., and Morillas-Ruiz, J.M. (2012). A review: inflammatory process in Alzheimer's disease, role of cytokines. TheScientificWorldJournal *2012*, 756357.
Salih, D.A., Rashid, A.J., Colas, D., de la Torre-Ubieta, L., Zhu, R.P., Morgan, A.A., Santo, E.E., Ucar, D., Devarajan, K., Cole, C.J.*, et al.* (2012). FoxO6 regulates memory consolidation and synaptic function. Genes Dev *26*, 2780-2801.
Salmon, D.P. (2012). Neuropsychological features of mild cognitive impairment and preclinical Alzheimer's disease. Curr Top Behav Neurosci *10*, 187-212.
Scahill, R.I., Schott, J.M., Stevens, J.M., Rossor, M.N., and Fox, N.C. (2002). Mapping the evolution of regional atrophy in Alzheimer's disease: unbiased analysis of fluid-registered serial MRI. Proc Natl Acad Sci U S A *99*, 4703-4707.
Schafer, D.P., Lehrman, E.K., Kautzman, A.G., Koyama, R., Mardinly, A.R., Yamasaki, R., Ransohoff, R.M., Greenberg, M.E., Barres, B.A., and Stevens, B. (2012). Microglia sculpt postnatal neural circuits in an activity and complement-dependent manner. Neuron *74*, 691-705.
Scheff, S.W., Price, D.A., Schmitt, F.A., and Mufson, E.J. (2006). Hippocampal synaptic loss in early Alzheimer's disease and mild cognitive impairment. Neurobiol Aging *27*, 1372-1384.
Scheibel, M.E., Crandall, P.H., and Scheibel, A.B. (1974). The hippocampal-dentate complex in temporal lobe epilepsy. A Golgi study. Epilepsia *15*, 55-80.
Schlageter, N.L., Carson, R.E., and Rapoport, S.I. (1987). Examination of blood-brain barrier permeability in dementia of the Alzheimer type with [68Ga]EDTA and positron emission tomography. J Cereb Blood Flow Metab *7*, 1-8.
Schlimgen, A.K., Helms, J.A., Vogel, H., and Perin, M.S. (1995). Neuronal pentraxin, a secreted protein with homology to acute phase proteins of the immune system. Neuron *14*, 519-526.
Scoville, W.B., and Milner, B. (1957). Loss of recent memory after bilateral hippocampal lesions. J Neurol Neurosurg Psychiatry *20*, 11-21.
Scullion, G.A., Kendall, D.A., Marsden, C.A., Sunter, D., and Pardon, M.C. (2011). Chronic treatment with the alpha(2)-adrenoceptor antagonist fluparoxan prevents age-related deficits in spatial working memory in APPxPS1 transgenic mice without altering beta-amyloid plaque load or astrocytosis. Neuropharmacology *60*, 223-234.
Segal, M. (2005). Dendritic spines and long-term plasticity. Nat Rev Neurosci *6*, 277-284.
Selkoe, D.J. (1989). Amyloid beta protein precursor and the pathogenesis of Alzheimer's disease. Cell *58*, 611-612.
Selkoe, D.J. (2001). Alzheimer's disease: genes, proteins, and therapy. Physiol Rev *81*, 741-766.
Selkoe, D.J. (2002). Alzheimer's disease is a synaptic failure. Science *298*, 789-791.
Seubert, P., Vigo-Pelfrey, C., Esch, F., Lee, M., Dovey, H., Davis, D., Sinha, S., Schlossmacher, M., Whaley, J., Swindlehurst, C.*, et al.* (1992). Isolation and

quantification of soluble Alzheimer's beta-peptide from biological fluids. Nature *359*, 325-327.
Shankar, G.M., Li, S., Mehta, T.H., Garcia-Munoz, A., Shepardson, N.E., Smith, I., Brett, F.M., Farrell, M.A., Rowan, M.J., Lemere, C.A.*, et al.* (2008). Amyloid-beta protein dimers isolated directly from Alzheimer's brains impair synaptic plasticity and memory. Nat Med *14*, 837-842.
Shi, J., Perry, G., Aliev, G., Smith, M.A., Ashe, K.H., and Friedland, R.P. (1999). Serum amyloid P is not present in amyloid beta deposits of a transgenic animal model. Neuroreport *10*, 3229-3232.
Sia, G.M., Beique, J.C., Rumbaugh, G., Cho, R., Worley, P.F., and Huganir, R.L. (2007). Interaction of the N-terminal domain of the AMPA receptor GluR4 subunit with the neuronal pentraxin NP1 mediates GluR4 synaptic recruitment. Neuron *55*, 87-102.
Sierra, A., Gottfried-Blackmore, A.C., McEwen, B.S., and Bulloch, K. (2007). Microglia derived from aging mice exhibit an altered inflammatory profile. Glia *55*, 412-424.
Singh, A. (2011). Negative feedback through mRNA provides the best control of gene-expression noise. IEEE Trans Nanobioscience *10*, 194-200.
Singh, A., and Hespanha, J.P. (2009). Optimal feedback strength for noise suppression in autoregulatory gene networks. Biophys J *96*, 4013-4023.
Siskova, Z., Justus, D., Kaneko, H., Friedrichs, D., Henneberg, N., Beutel, T., Pitsch, J., Schoch, S., Becker, A., von der Kammer, H.*, et al.* (2014). Dendritic structural degeneration is functionally linked to cellular hyperexcitability in a mouse model of Alzheimer's disease. Neuron *84*, 1023-1033.
Soininen, H., West, C., Robbins, J., and Niculescu, L. (2007). Long-term efficacy and safety of celecoxib in Alzheimer's disease. Dement Geriatr Cogn Disord *23*, 8-21.
Sonnen, J.A., Santa Cruz, K., Hemmy, L.S., Woltjer, R., Leverenz, J.B., Montine, K.S., Jack, C.R., Kaye, J., Lim, K., Larson, E.B.*, et al.* (2011). Ecology of the aging human brain. Arch Neurol *68*, 1049-1056.
Spires-Jones, T.L., Attems, J., and Thal, D.R. (2017). Interactions of pathological proteins in neurodegenerative diseases. Acta Neuropathol.
Squire, L.R. (1992). Memory and the hippocampus: a synthesis from findings with rats, monkeys, and humans. Psychol Rev *99*, 195-231.
Srinivasan, N., White, H.E., Emsley, J., Wood, S.P., Pepys, M.B., and Blundell, T.L. (1994a). Comparative analyses of pentraxins: implications for protomer assembly and ligand binding. Structure *2*, 1017-1027.
Srinivasan, N., White, H.E., Emsley, J., Wood, S.P., Pepys, M.B., and Blundell, T.L. (1994b). Comparative analyses of pentraxins: implications for protomer assembly and ligand binding. Structure *2*, 1017-1027.
Stargardt, A., Swaab, D.F., and Bossers, K. (2015). Storm before the quiet: neuronal hyperactivity and Abeta in the presymptomatic stages of Alzheimer's disease. Neurobiol Aging *36*, 1-11.
Starr, J.M., Farrall, A.J., Armitage, P., McGurn, B., and Wardlaw, J. (2009). Blood-brain barrier permeability in Alzheimer's disease: a case-control MRI study. Psychiatry Res *171*, 232-241.
Stevens, B., Allen, N.J., Vazquez, L.E., Howell, G.R., Christopherson, K.S., Nouri, N., Micheva, K.D., Mehalow, A.K., Huberman, A.D., Stafford, B.*, et al.* (2007). The classical complement cascade mediates CNS synapse elimination. Cell *131*, 1164-1178.

Stewart, S., Cacucci, F., and Lever, C. (2011). Which memory task for my mouse? A systematic review of spatial memory performance in the Tg2576 Alzheimer's mouse model. J Alzheimers Dis *26*, 105-126.
Stewart, W.C., Bobe, G., Vorachek, W.R., Pirelli, G.J., Mosher, W.D., Nichols, T., Van Saun, R.J., Forsberg, N.E., and Hall, J.A. (2012). Organic and inorganic selenium: II. Transfer efficiency from ewes to lambs. J Anim Sci *90*, 577-584.
Streit, W.J. (2006). Microglial senescence: does the brain's immune system have an expiration date? Trends Neurosci *29*, 506-510.
Streit, W.J., Braak, H., Xue, Q.S., and Bechmann, I. (2009). Dystrophic (senescent) rather than activated microglial cells are associated with tau pathology and likely precede neurodegeneration in Alzheimer's disease. Acta Neuropathol *118*, 475-485.
Sturchler-Pierrat, C., Abramowski, D., Duke, M., Wiederhold, K.H., Mistl, C., Rothacher, S., Ledermann, B., Burki, K., Frey, P., Paganetti, P.A.*, et al.* (1997). Two amyloid precursor protein transgenic mouse models with Alzheimer disease-like pathology. Proc Natl Acad Sci U S A *94*, 13287-13292.
Sunde, M., Serpell, L.C., Bartlam, M., Fraser, P.E., Pepys, M.B., and Blake, C.C. (1997). Common core structure of amyloid fibrils by synchrotron X-ray diffraction. J Mol Biol *273*, 729-739.
Sunyer, J.O., Zarkadis, I.K., and Lambris, J.D. (1998). Complement diversity: a mechanism for generating immune diversity? Immunol Today *19*, 519-523.
Swann, J.W., Al-Noori, S., Jiang, M., and Lee, C.L. (2000). Spine loss and other dendritic abnormalities in epilepsy. Hippocampus *10*, 617-625.
Taheri, S., Gasparovic, C., Huisa, B.N., Adair, J.C., Edmonds, E., Prestopnik, J., Grossetete, M., Shah, N.J., Wills, J., Qualls, C.*, et al.* (2011a). Blood-brain barrier permeability abnormalities in vascular cognitive impairment. Stroke *42*, 2158-2163.
Taheri, S., Gasparovic, C., Shah, N.J., and Rosenberg, G.A. (2011b). Quantitative measurement of blood-brain barrier permeability in human using dynamic contrast-enhanced MRI with fast T1 mapping. Magn Reson Med *65*, 1036-1042.
Taheri, S., Rosenberg, G.A., and Ford, C. (2013). Quantification of blood-to-brain transfer rate in multiple sclerosis. Mult Scler Relat Disord *2*, 124-132.
Taylor, S.C., Berkelman, T., Yadav, G., and Hammond, M. (2013). A defined methodology for reliable quantification of Western blot data. Mol Biotechnol *55*, 217-226.
Tennent, G.A., Lovat, L.B., and Pepys, M.B. (1995). Serum amyloid P component prevents proteolysis of the amyloid fibrils of Alzheimer disease and systemic amyloidosis. Proc Natl Acad Sci U S A *92*, 4299-4303.
Terry, R.D., Masliah, E., Salmon, D.P., Butters, N., DeTeresa, R., Hill, R., Hansen, L.A., and Katzman, R. (1991). Physical basis of cognitive alterations in Alzheimer's disease: synapse loss is the major correlate of cognitive impairment. Ann Neurol *30*, 572-580.
Terwel, D., Lasrado, R., Snauwaert, J., Vandeweert, E., Van Haesendonck, C., Borghgraef, P., and Van Leuven, F. (2005). Changed conformation of mutant Tau-P301L underlies the moribund tauopathy, absent in progressive, nonlethal axonopathy of Tau-4R/2N transgenic mice. J Biol Chem *280*, 3963-3973.
Thal, L.J., Ferris, S.H., Kirby, L., Block, G.A., Lines, C.R., Yuen, E., Assaid, C., Nessly, M.L., Norman, B.A., Baranak, C.C.*, et al.* (2005). A randomized, double-blind, study of rofecoxib in patients with mild cognitive impairment. Neuropsychopharmacology *30*, 1204-1215.
Thattai, M., and van Oudenaarden, A. (2001). Intrinsic noise in gene regulatory networks. Proc Natl Acad Sci U S A *98*, 8614-8619.

Tillett, W.S., and Francis, T. (1930). Serological Reactions in Pneumonia with a Non-Protein Somatic Fraction of Pneumococcus. J Exp Med *52*, 561-571.
Togashi, S., Lim, S.K., Kawano, H., Ito, S., Ishihara, T., Okada, Y., Nakano, S., Kinoshita, T., Horie, K., Episkopou, V.*, et al.* (1997). Serum amyloid P component enhances induction of murine amyloidosis. Lab Invest *77*, 525-531.
Town, T., Nikolic, V., and Tan, J. (2005). The microglial "activation" continuum: from innate to adaptive responses. J Neuroinflammation *2*, 24.
Tozzi, A., Sclip, A., Tantucci, M., de Iure, A., Ghiglieri, V., Costa, C., Di Filippo, M., Borsello, T., and Calabresi, P. (2015). Region- and age-dependent reductions of hippocampal long-term potentiation and NMDA to AMPA ratio in a genetic model of Alzheimer's disease. Neurobiol Aging *36*, 123-133.
Tsui, C.C., Copeland, N.G., Gilbert, D.J., Jenkins, N.A., Barnes, C., and Worley, P.F. (1996). Narp, a novel member of the pentraxin family, promotes neurite outgrowth and is dynamically regulated by neuronal activity. J Neurosci *16*, 2463-2478.
Twamley, E.W., Ropacki, S.A., and Bondi, M.W. (2006). Neuropsychological and neuroimaging changes in preclinical Alzheimer's disease. J Int Neuropsychol Soc *12*, 707-735.
Urbanyi, Z., Lakics, V., and Erdo, S.L. (1994). Serum amyloid P component-induced cell death in primary cultures of rat cerebral cortex. Eur J Pharmacol *270*, 375-378.
Urbanyi, Z., Laszlo, L., Tomasi, T.B., Toth, E., Mekes, E., Sass, M., and Pazmany, T. (2003). Serum amyloid P component induces neuronal apoptosis and beta-amyloid immunoreactivity. Brain Res *988*, 69-77.
Urbanyi, Z., Sass, M., Laszy, J., Takacs, V., Gyertyan, I., and Pazmany, T. (2007). Serum amyloid P component induces TUNEL-positive nuclei in rat brain after intrahippocampal administration. Brain Res *1145*, 221-226.
Vasek, M.J., Garber, C., Dorsey, D., Durrant, D.M., Bollman, B., Soung, A., Yu, J., Perez-Torres, C., Frouin, A., Wilton, D.K.*, et al.* (2016). A complement-microglial axis drives synapse loss during virus-induced memory impairment. Nature *534*, 538-543.
Verwey, N.A., Schuitemaker, A., van der Flier, W.M., Mulder, S.D., Mulder, C., Hack, C.E., Scheltens, P., Blankenstein, M.A., and Veerhuis, R. (2008). Serum amyloid p component as a biomarker in mild cognitive impairment and Alzheimer's disease. Dement Geriatr Cogn Disord *26*, 522-527.
Veszelka, S., Laszy, J., Pazmany, T., Nemeth, L., Obal, I., Fabian, L., Szabo, G., Abraham, C.S., Deli, M.A., and Urbanyi, Z. (2013). Efflux transport of serum amyloid P component at the blood-brain barrier. Eur J Microbiol Immunol (Bp) *3*, 281-289.
Vogel, C., and Marcotte, E.M. (2012). Insights into the regulation of protein abundance from proteomic and transcriptomic analyses. Nat Rev Genet *13*, 227-232.
Walsh, D.M., and Selkoe, D.J. (2004). Deciphering the molecular basis of memory failure in Alzheimer's disease. Neuron *44*, 181-193.
West, M.J., Coleman, P.D., Flood, D.G., and Troncoso, J.C. (1994). Differences in the pattern of hippocampal neuronal loss in normal ageing and Alzheimer's disease. Lancet *344*, 769-772.
Whicher, J.T., and Westacott, C.I. (1992). The acute phase response (London: Kluwer Academic).
Whitwell, J.L., Dickson, D.W., Murray, M.E., Weigand, S.D., Tosakulwong, N., Senjem, M.L., Knopman, D.S., Boeve, B.F., Parisi, J.E., Petersen, R.C.*, et al.* (2012). Neuroimaging correlates of pathologically defined subtypes of Alzheimer's disease: a case-control study. Lancet Neurol *11*, 868-877.

Winkler, D.T., Bondolfi, L., Herzig, M.C., Jann, L., Calhoun, M.E., Wiederhold, K.H., Tolnay, M., Staufenbiel, M., and Jucker, M. (2001). Spontaneous hemorrhagic stroke in a mouse model of cerebral amyloid angiopathy. J Neurosci *21*, 1619-1627.
Wood, J.H. (1980). Physiology, pharmacology, and the dynamics of cerebrospinal fluid. In Neurobiology of Cerebrospinal Fluid, J.H. Wood, ed. (New York: Plenum), pp. 1-16.
Wu, C.C., Chawla, F., Games, D., Rydel, R.E., Freedman, S., Schenk, D., Young, W.G., Morrison, J.H., and Bloom, F.E. (2004). Selective vulnerability of dentate granule cells prior to amyloid deposition in PDAPP mice: digital morphometric analyses. Proc Natl Acad Sci U S A *101*, 7141-7146.
Xaio, H., Banks, W.A., Niehoff, M.L., and Morley, J.E. (2001). Effect of LPS on the permeability of the blood-brain barrier to insulin. Brain Res *896*, 36-42.
Xu, D., Hopf, C., Reddy, R., Cho, R.W., Guo, L., Lanahan, A., Petralia, R.S., Wenthold, R.J., O'Brien, R.J., and Worley, P. (2003). Narp and NP1 form heterocomplexes that function in developmental and activity-dependent synaptic plasticity. Neuron *39*, 513-528.
Yasojima, K., Schwab, C., McGeer, E.G., and McGeer, P.L. (2000). Human neurons generate C-reactive protein and amyloid P: upregulation in Alzheimer's disease. Brain Res *887*, 80-89.
Ying, S.C., Jiang, H., Gewurz, A., and Gewurz, H. (1992a). Human serum amyloid P component (SAP) binds and activates the classical complement pathway via collagen-like region of Clq. FASEB J *6*, (Abstr.).
Ying, S.C., Marchalonis, J.J., Gewurz, A.T., Siegel, J.N., Jiang, H., Gewurz, B.E., and Gewurz, H. (1992b). Reactivity of anti-human C-reactive protein (CRP) and serum amyloid P component (SAP) monoclonal antibodies with limulin and pentraxins of other species. Immunology *76*, 324-330.
Yoshiyama, Y., Higuchi, M., Zhang, B., Huang, S.M., Iwata, N., Saido, T.C., Maeda, J., Suhara, T., Trojanowski, J.Q., and Lee, V.M. (2007). Synapse loss and microglial activation precede tangles in a P301S tauopathy mouse model. Neuron *53*, 337-351.
Zhang, R., Miller, R.G., Madison, C., Jin, X., Honrada, R., Harris, W., Katz, J., Forshew, D.A., and McGrath, M.S. (2013). Systemic immune system alterations in early stages of Alzheimer's disease. J Neuroimmunol *256*, 38-42.
Zhang, Y., Chen, K., Sloan, S.A., Bennett, M.L., Scholze, A.R., O'Keeffe, S., Phatnani, H.P., Guarnieri, P., Caneda, C., Ruderisch, N.*, et al.* (2014). An RNA-sequencing transcriptome and splicing database of glia, neurons, and vascular cells of the cerebral cortex. J Neurosci *34*, 11929-11947.
Zlokovic, B.V. (2008). The blood-brain barrier in health and chronic neurodegenerative disorders. Neuron *57*, 178-201.
Zlokovic, B.V. (2011). Neurovascular pathways to neurodegeneration in Alzheimer's disease and other disorders. Nat Rev Neurosci *12*, 723-738.
Zuo, Y., Lin, A., Chang, P., and Gan, W.B. (2005). Development of long-term dendritic spine stability in diverse regions of cerebral cortex. Neuron *46*, 181-189.